personal buildup for

Force Motors Ltd.

MTZ worldwide 2/2011, as epaper released on 13.01.2011
http://www.mtz-worldwide.com

content:

www.MTZonline.com

MTZ

WORLDWIDE

02 February 2011 | Volume 72

EXHAUST-GAS AFTERTREATMENT for Future Emission Requirements

ELECTROSTATIC Particulate Filter for Nanoparticle Reduction

HYBRID DRIVE with Mechanical Energy Storage

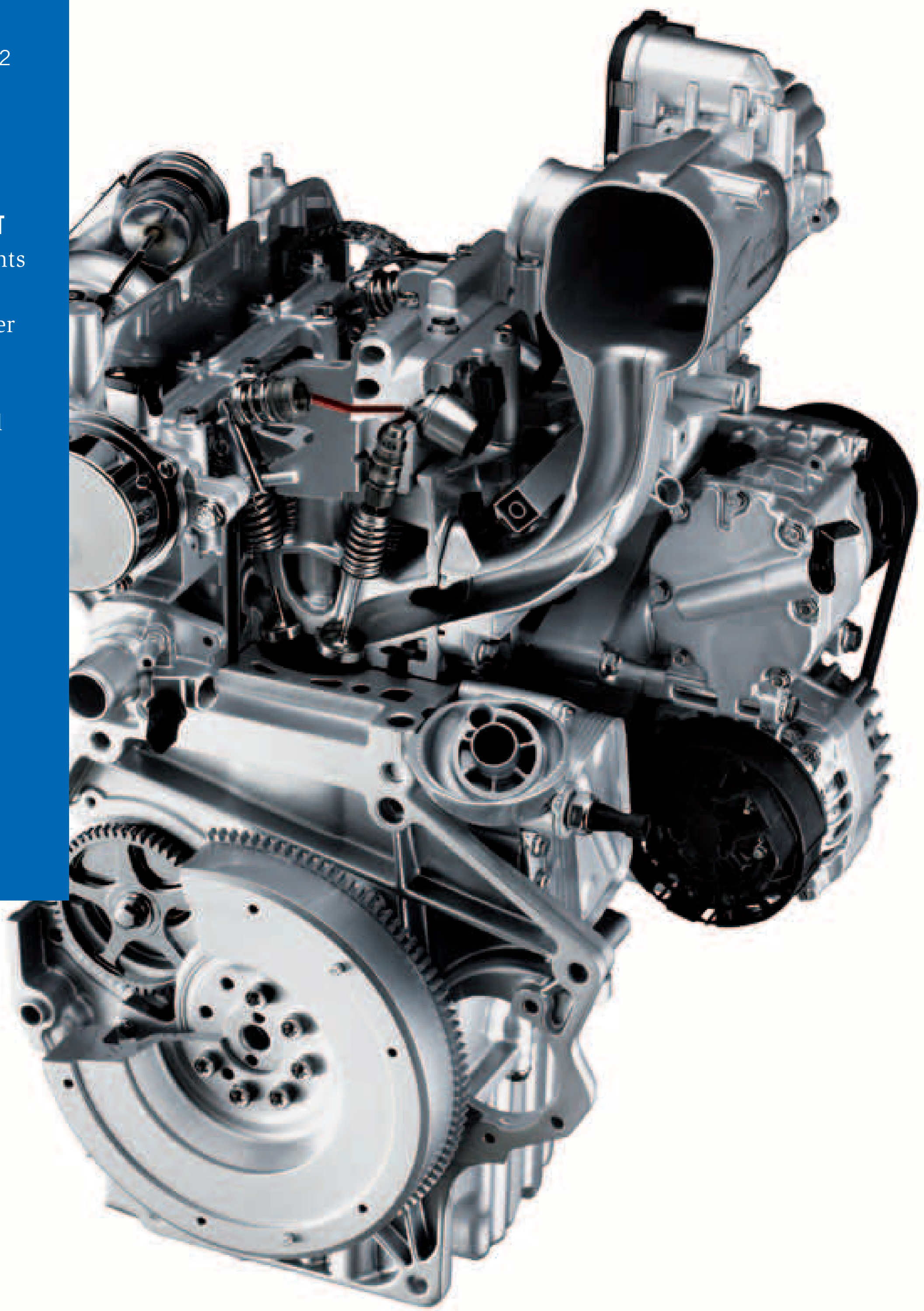

personal buildup for Force Motors Ltd.

THE CHALLENGES OF DOWNSIZING

CONTENTS

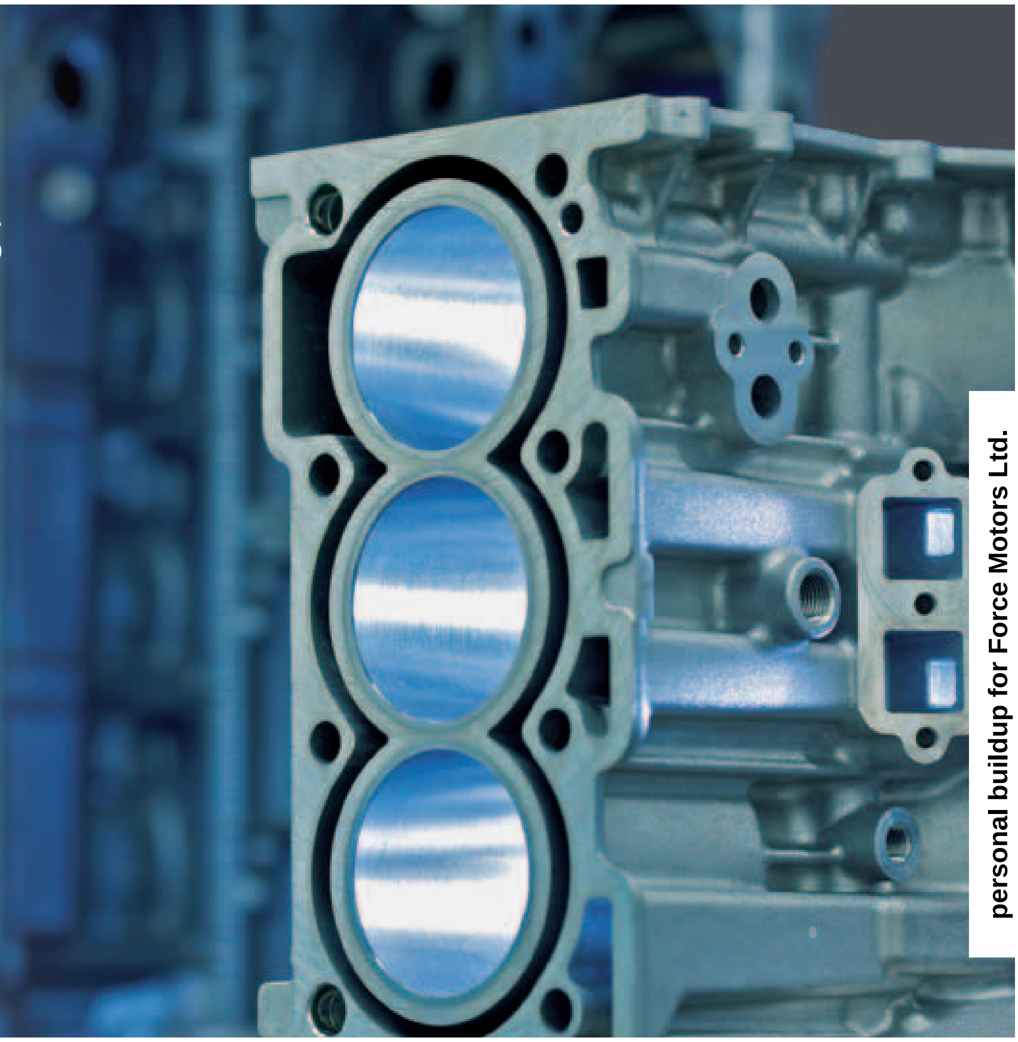

COVER STORY

THE CHALLENGES OF DOWNSIZING

4, 8 I Downsizing is increasingly becoming established as a key method of improving the efficiency of piston engines. The most striking example is without doubt the recently launched two-cylinder spark-ignition engine from Fiat, the development of which demonstrates not only the potential but also the special challenges of downsizing. These become even greater in diesel engines. Nevertheless, progress is being made here too, as shown by the example of Mercedes-Benz.

COVER FIGURE © Fiat **FIGURE ABOVE** © Kolbenschmidt

ON BOARD

Dear Reader,

In archaic societies, as anthropologists teach us, age is not seen as something negative. Of course, even among primitive peoples, a society of hunters is led by its younger members. But in difficult situations, they also turn to their elders for advice, as these have the invaluable benefit of greater knowledge and experience. The distribution of roles between the publisher and the editor-in-chief of a specialist magazine like ours is very similar. The editor-in-chief bears the responsibility for the publication – also legally – and produces it to the best of his ability together with his team. The publisher, on the other hand, has a supervisory role, ensuring that the view of what is essential and important in the long term does not get lost in everyday media business.

Against this background, I am pleased to inform you that we have succeeded in winning Dr. Johannes Liebl as our publisher from 1 March 2011. Together with our second publisher, Wolfgang Siebenpfeiffer, my predecessor, he will watch over the fortunes of ATZ, MTZ and their entire media family.

Dr. Liebl is no doubt familiar to most of you as BMW's "energy minister". In recent years, he has played a key role in shaping the brand's progress towards efficient dynamics and sustainability. In addition to energy management, his responsibilities also included issues such as aerodynamics, lightweight design, thermal management, driving performance and CO_2. MTZ readers will also remember him as an engine developer in the 1980s and 90s, when he initiated developments – such as the introduction of Valvetronic – that are still highly relevant today.

For all engineers involved in energy and transport technologies, sustainability in the sense of material cycles that are as closed as possible is the overriding objective for the coming decades. Our aim is to support this process with our magazines – and I am sure that Dr. Liebl will make a decisive contribution.

I look forward to 2011 and hope that you will find many exciting articles in our magazines and plenty of food for thought at our conferences.

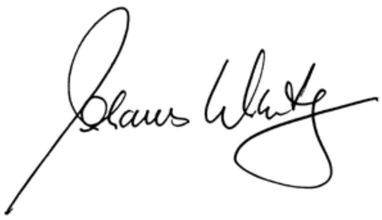

JOHANNES WINTERHAGEN, Editor-in-Chief
Wiesbaden, 20 December 2010

EXTREME DOWNSIZING BY THE TWO-CYLINDER GASOLINE ENGINE FROM FIAT

The new 0.9 l gasoline turbocharged two-cylinder engine represents a milestone in engine development at Fiat Powertrain Technologies. The so called Twinair engine is an excellent example of extreme downsizing: not only the overall displacement but also total number of cylinders are limited. Thanks to the turbocharging and the adoption of the Multiair technology excellent performances are reached, equalling those of 50 % larger displacement NA engines, while improving fuel economy by at least 25 %. Emission levels meet the current Euro 5 standards while the overall system is package-protected to reach the future Euro 6 standards. Thanks to the overall optimisations it was possible to set new standards for small engine NVH.

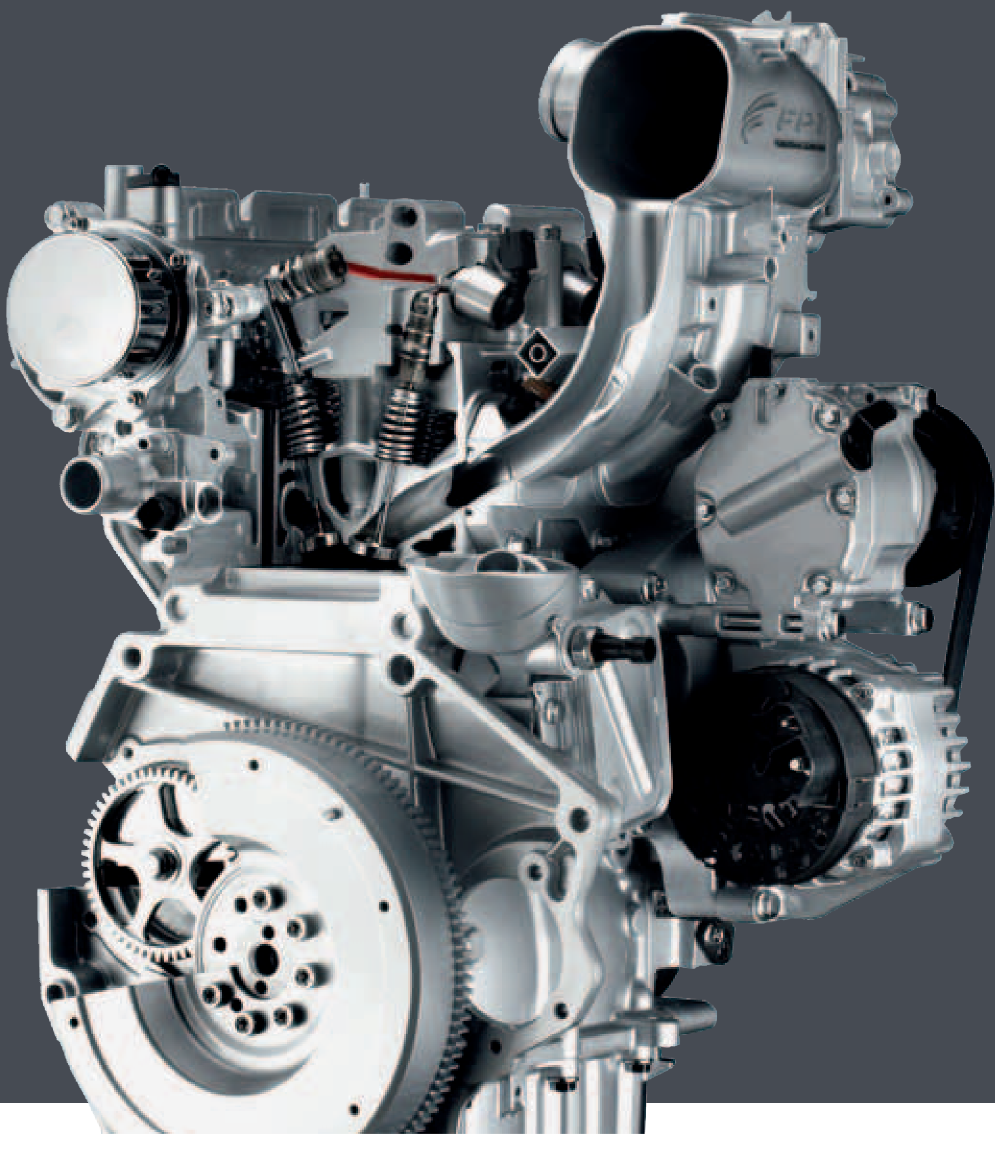

AUTHORS

GIOVANNI MASTRANGELO
is Platform Manager for the Twinair Engines Platform at Fiat Powertrain Technologies S.p.A. in Turin (Italy).

DAMIANO MICELLI
is Director for Mechanical Engineering and Gasoline Engine Research & Technology at Fiat Powertrain Technologies S.p.A. in Turin (Italy).

DARIO SACCO
is Vice President for Gasoline Engines Platforms at Fiat Powertrain Technologies S.p.A. in Turin (Italy).

LESS CONSUMPTION AND MORE FUN TO DRIVE DUE TO DOWNSIZING

Fiat has always been very strong in the A and B car segment. The key to this success is in the design and flexibility of these vehicles and in the reliability, performance and frugal fuel consumption of their engines. The increasing demand of fuel consumption reduction and more "fun to drive" can be satisfied with the downsizing concept as well as new more efficient engine architecture. Fiat Powertrain Technologies (FPT) decided to develop a new engine family to fully comply with the upcoming market demand [1]. This new engine family had to cover a power range from 48 to 77 kW focusing on urban cars, mainly A segment, with the possibility of use in B segment for high downsizing and premium fuel consumption. Three main configurations were identified: naturally aspirated, turbocharged (with 62.5 and 77 kW) and a CNG turbocharged version. All of these engines had to share the majority of the components in order to be as industrially efficient as possible.

ENGINE ARCHITECTURE

The optimal displacement choice was the first step of the new engine design. Performance and consumption simulation activity identified a displacement around 0.9 l as the best compromise. The second step design was the architectural definition of the engine (number of cylinder, bore, stroke, etc). Fuel consumption, cost, NVH and performance were the main drivers. Two-, three- and four-cylinder architectures were compared regarding thermodynamic efficiency and friction. As is shown in ❶, the two-cylinder configuration shows the best thermodynamic efficiency thanks to a convenient cylinder displacement. Two-cylinder architecture also offers longitudinal length and weight advantages; engine length advantage make the two-cylinder engine more suitable for hybridization. NVH behaviour of a two-cylinder configuration could be a potential issue: the use of a balance system for the first order free forces is a must; the remaining 2nd order free forces are even lower with respect to a four-cylinder engine, ❷. The twin configuration (0° to 360° crank design) was preferred to the 0° to 180° crankshaft layout mainly due to the equal spacing of the combustion that generates a first order dominant torque irregularity instead of the spurious half orders of the second architecture.

BASIC DESIGN

Main drivers of the basic design were friction reduction and components integration.

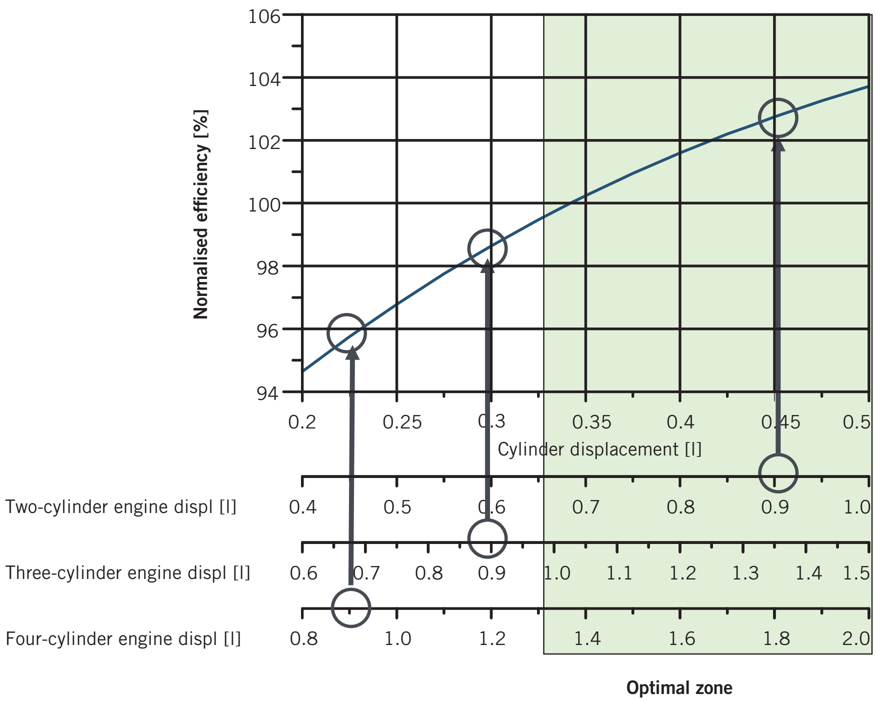

❶ Thermodynamic efficiency versus engine architecture

Engine architecture	Crankshaft layout	Free inertia forces 1st order	Free inertia forces 2nd order	Free inertia moments 1st order	Free inertia moments 2nd order	$Fa_1 = m_a \omega^2 r$ $Fa_2 = \lambda m_a \omega^2 r$ i = interbore distance ma = reciprocating mass r = crank radius ω = crank angular velocity λ = r / l, l = conrod length Firing spacing
Two-cylinder (with balance shaft)	1-2	0	2Fa2	0	0	1 2 1 0° 180° 360° 540° 720°
Two-cylinder (with balance shaft)	1 2	0	2Fa2	0	0	1 2 1 0° 180° 360° 540° 720°
Three-cylinder (without balance shaft)	1 2 3	0	0	√3(Fa1*i)	√3(Fa1*i)	1 2 3 1 0° 240° 360° 480° 720°
Four-cylinder (without balance shaft)	1-4 2-3	0	4Fa2	0	0	1 3 4 2 1 0° 180° 360° 540° 720°

❷ Free forces for different engine architectures

Journal diameters and piston weight were reduced to minimize cranktrain friction. The piston rings tension has been significantly reduced thanks to the adoption of a dummy head for cylinder honing (it decreases the 4th order bore deformation). Different balancing system layouts were designed and tested: final configuration consisted of a balance shaft installed into the crankcase driven by a couple of gears. Two roller bearings where preferred to plane supports to reduce impact on engine friction. The position of the balance shaft has been optimized to reduce the 1st order torque fluctuation on the crankcase. In fact, the balance shaft generates also a sinusoidal moment that has been tuned to be in opposition to the combustion torque reaction on the crankcase. The benefit is a reduction of vibration on the engine suspension bracket. The chain layout was optimised to gain low friction and the chain vane is closed by a frontal aluminium cover that ensures good ventilation within the engine. The water pump is integrated in the front cover and directly driven by the balance shaft with benefits on friction (no hub load from belts). This results in the front engine side being very compact and a chain drive system for life that requires no maintenance. For the engine block, cast iron was preferred to aluminium as the best compromise between costs, weight, robustness and NVH. Integration has been a driver for the design and all piping to oil filter and cooler and water bypass were integrated in the crankcase casting itself thus reducing piping costs, and eliminating fixations and leakage danger. The CNG version was taken into account from the beginning of the project. This is a bi-fuel engine (gasoline and CNG) with no performance reduction passing from gasoline to CNG fuel. The sharing of most of the components for all the engines of course has a positive impact on cost and investment. The drawback is that the design of

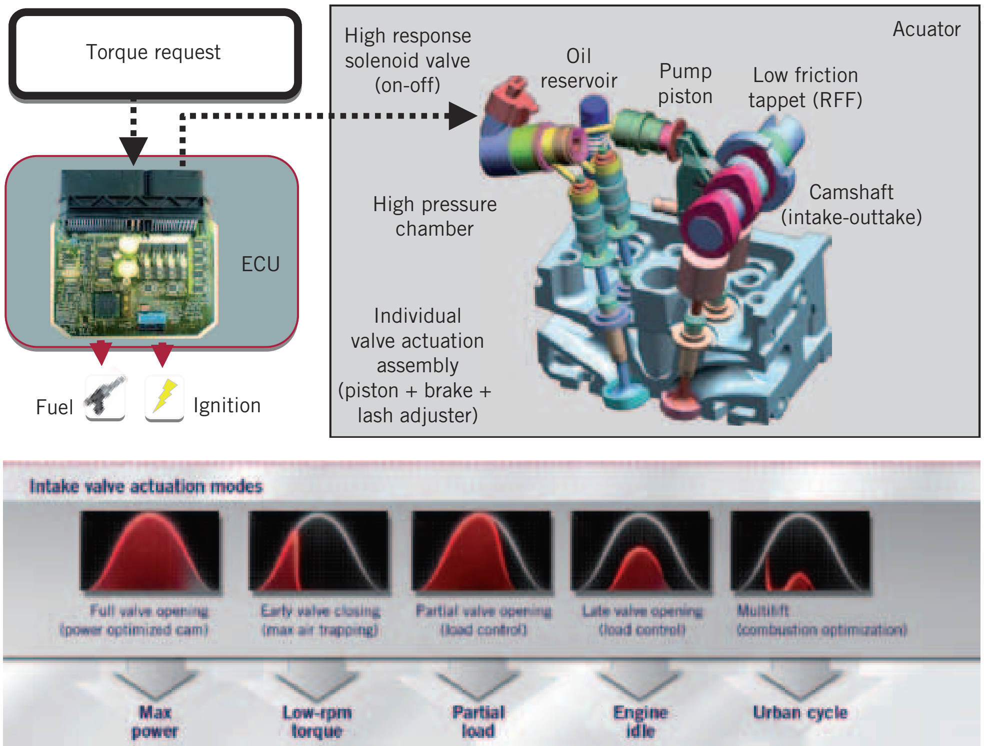

❸ Multiair Technology

each part (crankshaft, conrods, crankcase, cooling system, etc) has been done taking into account the envelope of the requirements of all the engines of the family.

FULLY VARIABLE VALVE SYSTEM

Multiair technology appeared on the market for the first time on the so called Fire engine in 2009 [2]. FPT invented and patented this technology: it is a fully variable control valve system that uses an electro-hydraulic actuator (so called Uniair actuator owned by INA Schaeffler) and a group of dedicated controls strategies to allow improved engine efficiency [3]. A new electronic control unit (developed by Magneti Marelli) integrates engine and Multiair module control. Multiair uses all capabilities offered by the Uniair actuator to manage the engine intake valves stroke-by-stroke and cylinder-by-cylinder. The main benefits arising from this full control are fuel consumption, thanks to pumping losses reduction, and performance thanks to volumetric efficiency optimization. Other benefits come from the quick response (stroke by stroke), internal EGR management, etc, ❸. For FPT it was clear from the beginning that the new two-cylinder engine should include Multiair technology to maximize the fuel consumption reduction and performance.

DEVELOPMENT TARGETS

For the first engine variant, the following targets were defined:

: 62.5 kW power @ 5500 rpm and 155 Nm torque @ 2000 rpm
: best in class fun to drive of all 0.9 to 1.4 l gasoline vehicles
: NVH which is equivalent to best four-cylinder in line engines
: < < 100 g CO_2/km on NEDC: benchmark in the class from 0.9 to 1.4 l gasoline vehicles
: durability of 200,000 km
: 24 months development time from project approval to engine SOP.

The main characteristics of the engine are given in ❹.

PERFORMANCE AND THROTTLE RESPONSE

To reach the required performance targets thorough calculations were computed to define cam timing, intake and exhaust port geometry and the combustion chamber layout including compression ratio. Two-cylinder specific fluid dynamics permitted the use of wide exhaust cams without the torque penalisations that can occur for example on a turbocharged four-cylinder inline engine. The intake ports were developed to obtain a high tumble air motion that is advantageous both for combustion stability and to reduce exhaust gas temperatures at WOT. Compression ratio was set at 10.0. This allowed reaching the required full load performances while offering an excellent base for good part-load fuel economy. The positive synergic effect of the Multiair system and the turbocharger on low end torque is shown in ❺. Compared to an engine with fixed valve timing the Multiair system allows almost 12 % increase in low-end torque and turbocharger speed. The optimisation of the volumetric efficiency by controlling the event of intake valve closure is very important in the low engine speed range and gives even more benefits than on NA type engines [4]. One of the most important issues in order to obtain the desired performance, especially regarding non-stationary engine operation, was the turbo matching. The strongly pulsating airflow of the two-cylinder engine leads typically to surging problems, especially on the compressor side. On a four-cylinder engine surging typically occurs in a continuous way while approaching the surge line on a two-cylinder engine the surging happens discontinuously and

NUMBER OF CYLINDERS		2
DISPLACEMENT	(l)	0.875
BORE	(mm)	80.5
STROKE	(mm)	86
STROKE/BORE RATIO		1.07
COMPRESSION RATIO		10
BORE PITCH	(mm)	88
MANI BEARING DIAM	(mm)	48
CONROD BIG EYE DIAM	(mm)	42
CONROD SMALL EYE DIAM	(mm)	21
CONROD LENGTH	(mm)	133.55
LAMBDA RATIO		0.322
INJECTION SYSTEM		PFI
INTAKE VALVE CONTROL		Multiair
CHARGING		Turbo
BALANCER SHAFT 1ST ORDER		Yes
MAX POWER		62.5 kW at 5500 rpm
MAX TORQUE		155 Nm at 2000 rpm
FUEL		95 RON

❹ Engine characteristics

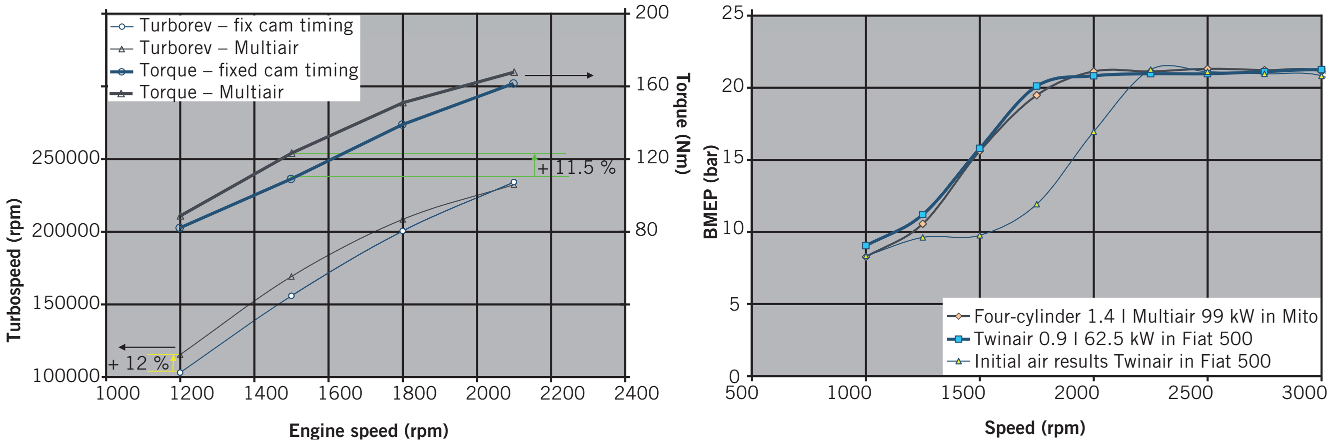

❺ Low end torque increase by Multiair (left) and transient performance in vehicle at full load in highest gear (right)

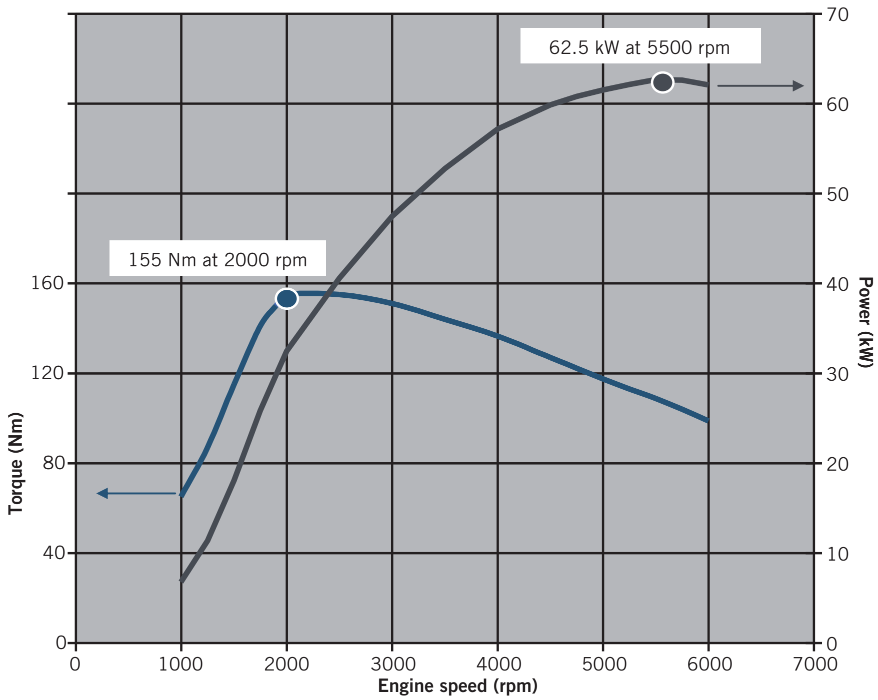

❻ Engine performance

also when the engine is operated at quite some distance from the surge line. Therefore, conventional compressor optimisations, done on stationary airflow benches, do not lead to satisfactory performance on a two-cylinder engine. As a result boosting such an engine with a centrifugal type compressor is generally considered not to be as effective as on three- or four-cylinder engines, which exhibit more stable air flows [5]. Dedicated research on this subject lead to the conclusion that a new compressor wheel had to be developed, sacrificing slightly the continuous flow performance at medium airflows while strongly improving it's capabilities in non-stationary low flow conditions. The final effect on dynamic engine performance is shown in ⑤. The starting point for the two-cylinder was not very promising but after the turbo optimisation and fine tuning of the calibration the dynamic performance of the two- and four-cylinder engines were found to be identical. The result of the performance optimisations is shown in ❻. The maximum power of 62.5 kW is reached at 5500 rpm and 155 Nm (22.2 bar BMEP, brake mean effective pressure) is delivered at 2000 rpm. The high torque at low speeds allows excellent fun to drive on small and mid size cars.

FUEL CONSUMPTION

To reach the best possible fuel economy massive efforts it was dedicated to reduce the frictional losses of the engine during the design and development phase. In addition the Multiair system itself was critically analysed to reduce the auxiliary losses. Compared to the first generation system, employed on the Fire engine, roller finger followers on the exhaust side were adopted and a significant reduction of overall cylinder head friction was obtained. Despite the low overall displacement the FMEP (friction mean effective pressure) values of the cylinder head are approaching those of best-in-class four-cylinder engines.

The combustion system of the engine was also subject to profound optimisation, employing CFD techniques and using engines with optical access to observe the real combustion process. To take the maximum benefit of the Multiair system a new combustion system was developed. Usually the early intake valve mode, due to the reduced maximum valve lift and deriving in-cylinder charge motion, leads to lower combustion efficiency, limiting so the benefit of the pumping losses reduction [6]. Thanks to the newly developed HTS (high tumble shrouded) combustion system, which increases the tumble ratio in partial valve lift conditions up to four

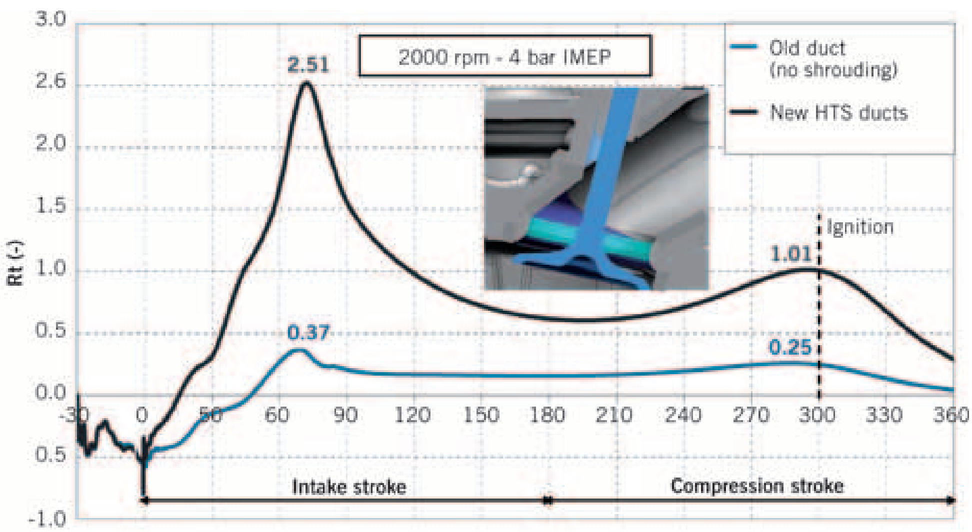

❼ Charge motion optimisation with HTS system

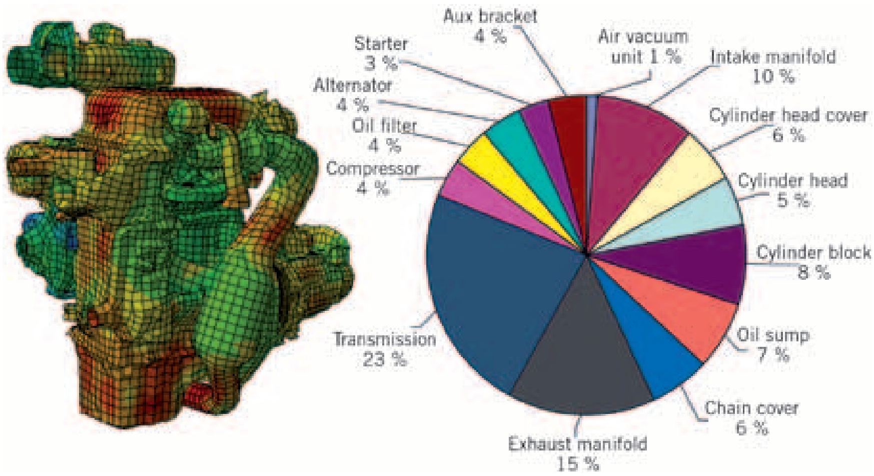

❽ Noise sources

times, it was possible to get excellent combustion efficiency also at part load, ❼. A further important advantage on a low displacement engine running often at high loads, is the possibility of controlling the effective compression ratio using the Multiair system. On a turbocharged engine above approximately 50 % of maximum load it is necessary to delay ignition timing with respect to the ideal (MBT, minimum spark advance for best torque) values due to knocking. The Multiair system, when used in the late closing mode, allows control of the effective compression ratio realising the Atkinson-Miller type cycle. Compared to cam phasing the advantage is that the start of the intake phase is maintained at the ideal moment. This is reflected by the BSFC values of 375 g/kWh at the 2000 rpm – 2 bar BMEP point and the minimum fuel consumption in the map of 242 g/kWh. Both values are benchmark for (turbo)charged engines below 1.4 l.

NVH OPTIMIZATION

The main task of the NVH engineering was to optimize the sound radiation in terms of level and quality. This NVH performance has been achieved by using state of the art CAE simulations which allowed an acoustical optimization of the single components installed on the engine. Therefore, a numerical FE Multibody and BEM methodology was applied with experimental support for the target definition, in order to predict the component normal modes that have most effect on the sound radiation and to give support to identify the modification's areas. In ❽ the calculated surface velocity and the acoustic power contribution of each engine part are shown. Such detailed analyses guided the choice of the components suitable for the acoustic optimization. In this way all the components, responsible for the noise radiation, have been improved, such as cylinder head cover, chain cover and oil pan, pulley, etc.

Based on the results of the tests the most important noise sources have been identified both at idle and during speed sweep wide open throttle (WOT). Parallel to numerical simulation, an experimental panel contribution (intensimetry technique) of the radiated noise in an anechoic chamber has been performed. Both activities allowed detecting and optimising all the radiation sources ensuring a good sound level and quality. Torque fluctuation is characterized mainly by 1st order, instead of the typical 2nd order of the four-cylinder engine, generating a different interaction with the transmission generating a shifting of the resonances at higher engine speeds. The typical speed ranges, on which gear rattle could be more critical, are then shifted at higher speeds letting this phenomena coming even less relevant respect to a four-cylinder engine. Further improvements were made to the exhaust system to control the noise level, enhancing the engine characteristic sound. Many tests were carried out in order to assess the number and the volume of silencers and the effect of resonators. The control of the right timing of valve opening and closing, trough the Multiair system, has been the key point. The result of the calculation and test activity has been one big centrally mounted silencer halfway the exhaust line and a resonator very close to the exit of the system.

During the NVH development, the Multiair technology played a particular role also in reducing the vibration of the powertrain in idle condition; in fact, thanks to the higher combustion stability obtained by this technology and the balance shaft, the powertrain vibration amplitude is very similar to a four-cylinder engine. The result of this activity made the Twinair a reference for this performance in his engine class.

ENGINE INTEGRATION ON CAR

The first application of the Twinair turbocharged engine is on the Fiat 500. This combination of a relatively powerful engine in a small car allows to reach very good in vehicle fuel economy. In the ❾ the CO_2 values obtained on the NEDC cycle are shown. A benchmark position is reached with respect to gasoline engine competitors while even few diesel engines can compete with the CO_2 value of 92 g/km (95 with the MT gearbox). To guarantee that the Fiat 500 Twinair car owner could reach best fuel economy also in normal driving conditions the car is equipped with an "ECO/NORMAL" button. In the "ECO" mode torque is limited to 100 Nm and the torque build up from 1000 to 2000 rpm is very soft. This allows relaxed city driving as practically the engine feels like a 1.1 l NA engine and no turbo lag is noticeable. In the "NORMAL" mode max torque is (due

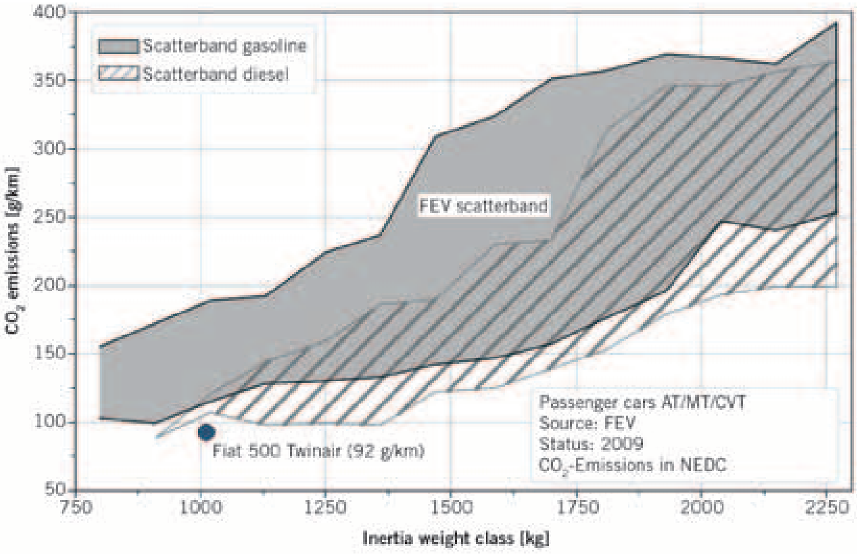

9 NEDC cycle CO_2 emission results

to the gearbox) limited to 145 Nm, which is reached at 1900 rpm. This NORMAL mode is recommended for highway driving where a maximum speed of 173 km/h is quickly reached and especially elasticity and fun to drive values are excellent. As an example, the 80 to 120 km/h acceleration time in last gear takes only 12.5 s, which is better than all its competitors up to 1.6 l displacement. The ECO mode allows fuel consumption reduction of approximately 13 %. In situ tests it was found out that the fuel economy in the ECO mode was also much less dependent on individual driver behaviour. The ECO mode button will thus help all users to get the best possible fuel economy from the vehicle.

CONCLUSIONS

The new Twinair engine is the most extreme example of downsizing of gasoline engines today. Thanks to the low overall displacement a high degree of downsizing is obtained while the relative large single cylinder volume allows to have excellent thermodynamic efficiency. Therefore in the displacement class below 1.0 l the two-cylinder engine is clearly the best choice for highest fuel efficiency and lowest CO_2 emissions, matched with an excellent fun to drive. In the development phase the two-cylinder typical characteristics (f. e. turbolag) were faced as challenges and successfully transformed into advantages compared to three-cylinder power units. The Multiair technology combined with turbocharging allowed to get excellent fuel economy and performances and permitted to elevate the two-cylinder NVH to a state of the art level. The industrialisation phase was mastered in an extremely short time and a new plant was designed and realised, where World Class Manufacturing practices are employed guaranteeing best in class engine quality. The compact FPT Twinair engine, which will cover the power range of 48 to 77 kW, ideally suited also for hybridisation, is therefore the best possible answer to the demand of lowest CO_2 emissions in small and mid-size cars for the coming decades.

REFERENCES

[1] Bernard, L.; Ferrero, P.E.: CO_2 solutions for Small Powertrains. 20th AVL Congress "Engine & Environment", Graz (Austria) 2008

[2] Bernard, L.; Ferrari, A.; Micelli, D.; Perotto, A.; Rinolfi, R.; Vattaneo, F.: Electro-hydraulic Valve Control with Multiair Technology. In: MTZ (70) 2009 No 12

[3] Borean, F.; Gustinetti, F.; Lucatello, M.; Venezia, C.: Model-based approach for Control and Calibration on Multiair Engine. 9th International Symposium on Internal Combustion Diagnostics, Baden Baden (Germany) 2010

[4] Andriesse, D.; Imarisio, R.; Rinolfi, R.; Vattaneo, F.: Variable Valve Timing Engines for High Performance SI Engines. ATA Congress "High Performance Engines and Cars, Como (Italy) 1998

[5] Weinowski, R.; Sehr, A.; Wedowski, S.; Heuer, S.; Hamm, T.; Tiemann, C.: Future Downsizing of S.I. engines – potentials and limits of 2- and 3-cylinder concepts. 30th International Vienna Motorsymposium, Vienna (Austria) 2009

[6] Andriesse, D.; Doria, V.: Pressure Indicating Analysis on a Spark Ignition Engine with Load Control by means of Early Intake Valve Closure. 3rd AVL International Indicating Symposium, Mainz (Germany) 1998

DOWNSIZING DIESEL ENGINES

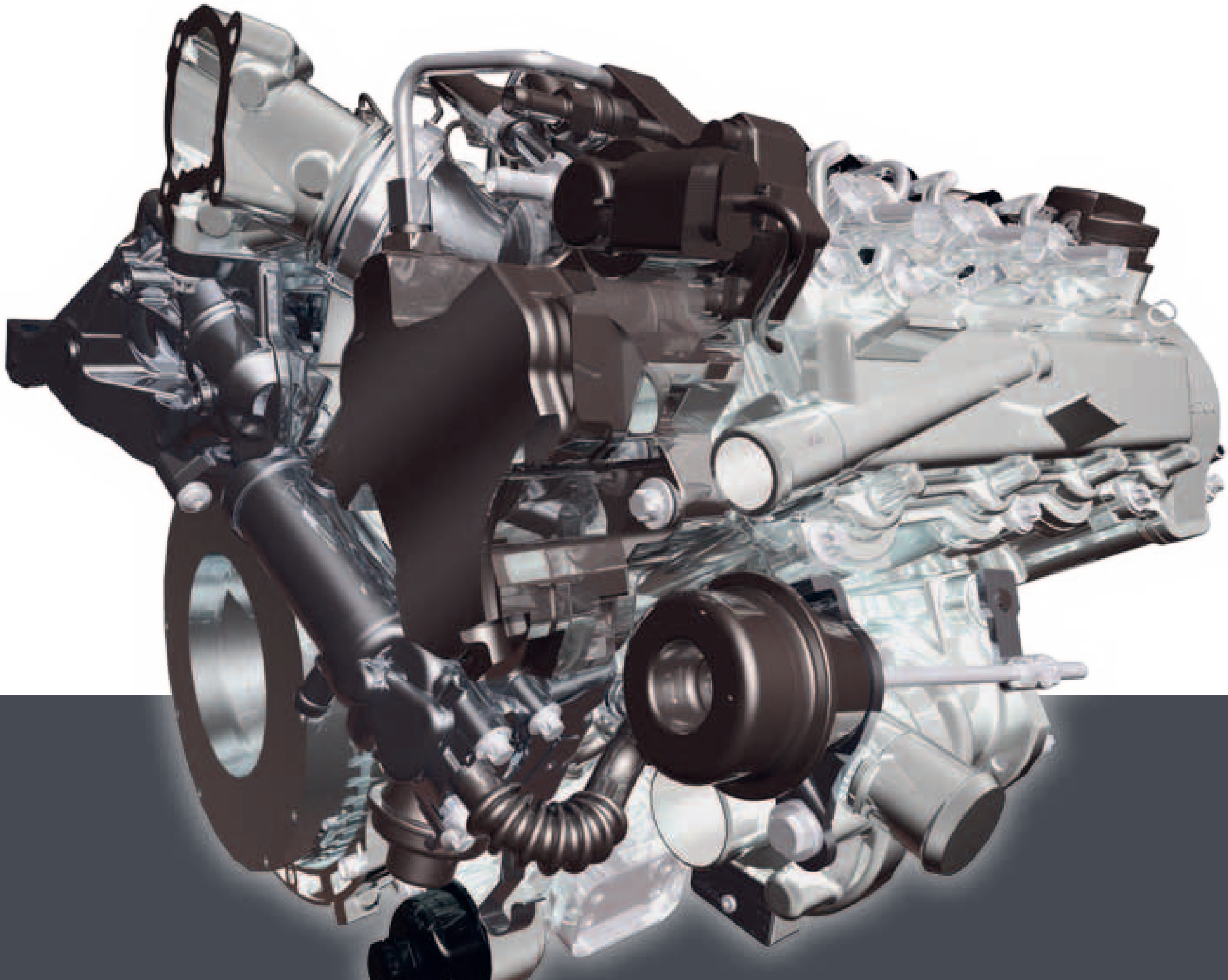

Downsizing is a trend that has already had a massive influence on spark-ignition engines. Diesel engine developers are now also taking their first steps in this direction, but they are facing a tougher conflict of objectives between reducing fuel consumption and emissions, which is proving to be a cost driver. Daimler illustrates both the opportunities and the challenges of downsizing diesel engines.

AUTHORS

DR.-ING. JOACHIM SCHOMMERS
is Director Development Passenger Car Diesel Engines at the Daimler AG in Stuttgart (Germany).

DR.-ING. RALPH WELLER
is Senior Manager Calculation Powertrain MBC at the Daimler AG in Stuttgart (Germany).

DIPL.-ING. MICHAEL BÖTTCHER
is Teamleader Gasdynamic in the Passenger Car Engine Development at the Daimler AG in Stuttgart (Germany).

DIPL.-ING. WILHELM RUISINGER
is Manager Thermodynamics Four-cylinder PC Diesel Engines at the Daimler AG in Stuttgart (Germany).

HISTORY AND REQUIREMENTS

Ever since Mercedes-Benz launched the world's first passenger car diesel engine in 1936, this engine concept has always been recognized for its low consumption due to outstanding efficiency. On top of this, the recent introduction of common-rail direct injection technology in 1997 and optimized turbocharging systems have improved performance and comfort to such an extent that diesel technology can now be successfully implemented in everything from Smart to S-Class vehicles and SUVs. Last century's relatively loud, sluggish and sometimes polluting but economical diesel engines have been transformed into this century's sporty, quiet, clean and even more economical engines.

As a result, the share of diesel engines on the European market for new vehicles has risen to more than 50 % – and more than 55 % for Mercedes-Benz passenger cars. This increase in the popularity of diesel engines has made an important contribution to the reduction of CO_2 emissions from passenger cars in Europe.

Against a background of discussions concerning CO_2, the anticipated depletion of crude oil reserves and the expected tightening of CO_2 legislation worldwide, fuel consumption is becoming an increasingly important factor in the design of new engines. The use of innovative technology means that conventional combustion engines still offer noteworthy fuel-saving potential. State-of-the-art direct injection technology ([1]) and downsizing ([2]), for example, have already led to a dramatic increase in the fuel economy of gasoline engines.

Despite the good economy today, Diesel engines are also subject to similar requirements to further reduce fuel consumption. In [3], the process and premises for implementing downspeeding and downsizing approaches were described in the context of innovative diesel engine concepts.

POTENTIALS OF DOWNSIZING

The benefit of downsizing may be classified into a thermodynamic and a mechanical part. From the thermodynamical point of view the operational range of the combustion engine will be moved to higher loads and so to better specific consumption values by the reduction of the displacement.

For mechanics the positive aspect for fuel consumption results from the lower friction of the piston unit (if no jump of cylinder occurs) respectively of the smaller number of cylinders. In addition for the downsized engine it will be possible to optimize especially at a given basic engine the cranktrain by a load level concept at lower ratings. The downsizing of diesel engines further allows a lower weight assembly by smaller dimensions as well as to provide as an enabler for advanced car measures like for example the use of hybrid technology.

The new four-cylinder concept outlined in [3] was implemented shortly afterward

❶ Downsizing effect using an example of the E-class in the new four-cylinder engine with the internal designation OM 651 ([4]). In the E-Class, this engine has enabled downsizing with a jump of cylinder number by replacing the V6 engine of equivalent performance. Instead of a displacement of 3 l only 2,2 l were necessary for the same performance thanks mainly to the two-stage turbocharger. This made it possible to utilize considerable potential for reducing consumption by shifting the operating point at equivalent performance levels. ❶ shows the benefits of this combination of downsizing and downspeeding with a 14 % reduction of fuel consumption.

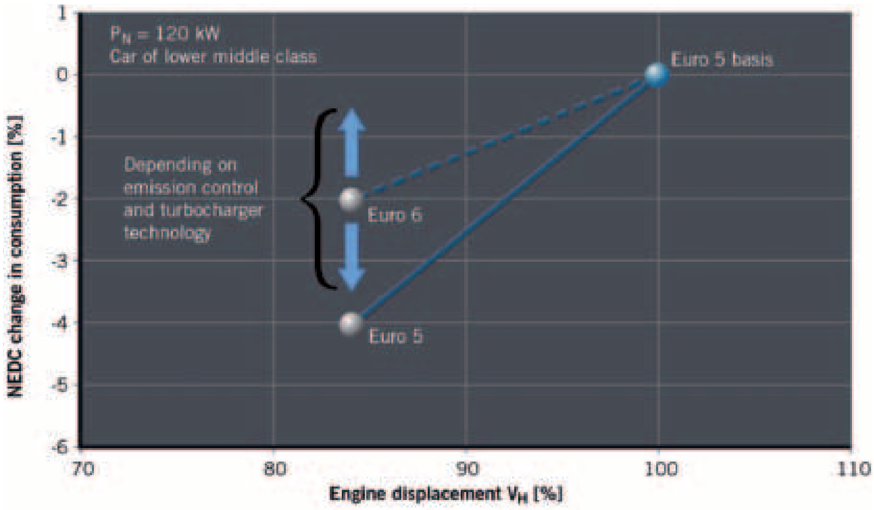

❷ Consumption potential through downsizing using the example of a four-cylinder engine with 120 kW

CHALLENGES FOR DOWNSIZING OF DIESEL ENGINES

Unlike in gasoline engines, the control of air/fuel ratio also cancels out any improvement in the engine process through dethrottling. This means that diesel engines generally offer less downsizing potential than gasoline engines.

In a vehicle of the lower middle-class, compliant with emissions level Euro 5, with a constant rated power of 120 kW and a variation in engine displacement up to -16 %, fuel savings of around 4 % can be achieved, ❷. Despite equivalent power it has to be considered that the engine with the smaller displacement will show some handicaps especially with starting and accelerating from low speed that have to be counteracted by appropriate measures.

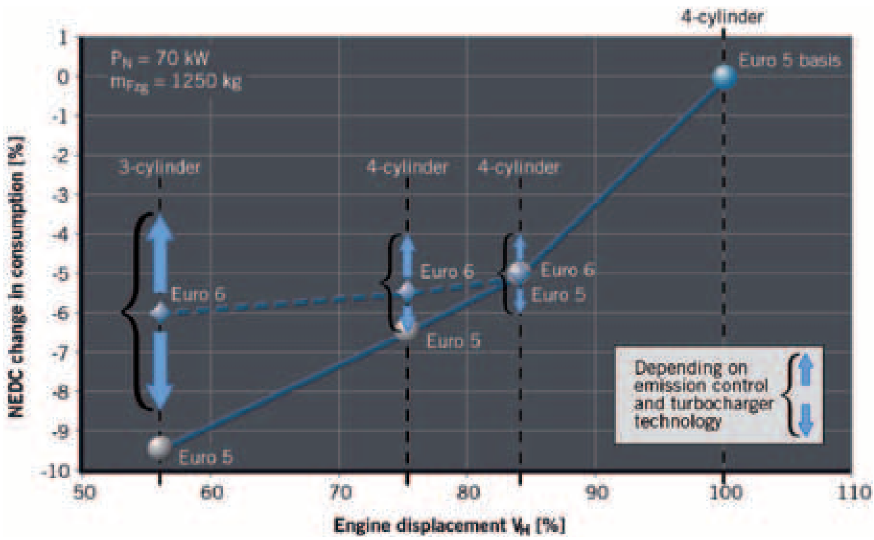

❸ Consumption potential through downsizing an I4 with 70 kW

Even today, compromises for the maximum potential fuel economy of diesel engines were made as this would affect compliance with emissions targets, particularly for NO_x. When the displacement is reduced, this conflict of objectives becomes even more evident because the charger size is primarily dependent on the required rated power. This means that with a smaller displacement, it becomes more difficult to obtain the high charge pressure necessary in the partial load range for achieving the required EGR rate.

Diesel engines can only achieve compliance with the more stringent emissions requirements of Euro 6 through the use of additional technology. Alongside in-engine improvements, the Bluetec packages at Mercedes-Benz encompass measures such as improved EGR systems, turbocharger technology as well as NO_x storage catalysts or SCR exhaust gas after-treatment systems. In conjunction with downsizing measures, this requires appreciable extra outlay. Depending on the technology used, consumption potential can be further changed, ②.

If the displacement is reduced in a vehicle that weighs less (1250 kg) and has a rated power of 70 kW, the same basic characteristics can be observed at Euro 5 level. Given that three-cylinder engines are possible in this performance class, the fuel consumption can be potentially improved by up to 9 %, ❸, although it should be pointed out that even in this vehicle class, a multi-channel EGR system or an active denox measure is required in three-cylinder engines to ensure compliance with Euro 5. The comfort and NVH characteristics of the three-cylinder engine may cause further problems. In addition such three-cylinders are normally derived from existing four-cylinder basic engines by significant modifications and so the cost position of such three-cylinder engines may be poor.

If compliance with Euro 6 limits is required, the reachable fuel efficiency may be reduced dependent from the sophisticated emission control technology, ③.

CHARGING

Since it is more difficult with smaller displacements and with a constant performance and vehicle weight to ensure compliance with requirements regarding NO_x

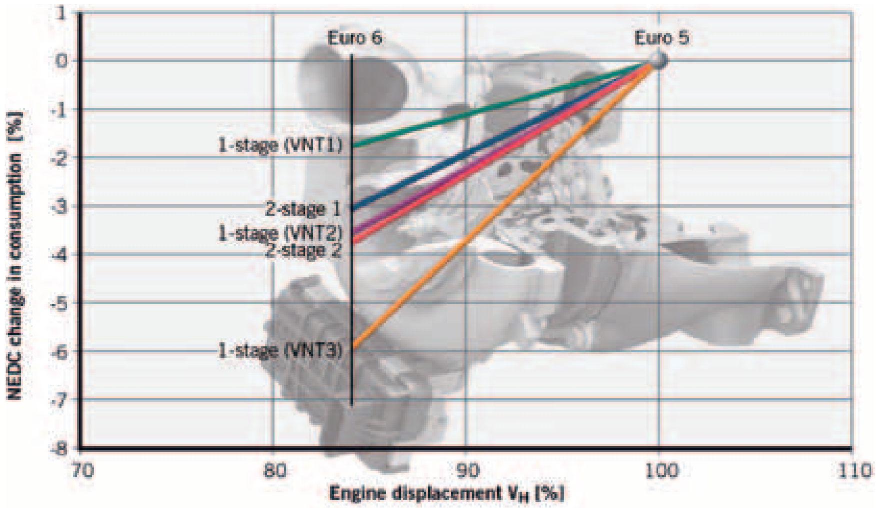

❹ Impact of the turbocharger unit on fuel consumption potential as part of downsizing

emissions, turbocharger technology plays an increasingly important role. ❹ shows the impact of three different VNT chargers and two two-stage turbocharger units on fuel consumption with a decrease in displacement. Starting point is an engine with an one-stage VNT charger in Euro 5. The emission category of the downsized charging variants is again Euro 6. It is clear that the potential of the downsizing is highly dependent on the grade of the turbocharger units. Hereby the influence of possible exhaust gas aftertreatment technologies to reach Euro 6 is not considered. ❺ shows the different starting behavior for these five turbochargers. It can be seen, that best driving performance (here: starting behavior) not necessary means poor fuel efficiency.

CUBIC CAPACITY

In more general terms, an improvement of the consumption can be reached by raising the load to more fuel-efficient characteristic map ranges, if starting with a relatively high cubic capacity, the engine displacement is reduced. This is possible up to the point at which any further reduction in displacement leads to a deterioration in fuel economy due to the in-engine measures required for ensuring compliance with NO_x limits. This impact will be superimposed by the necessary measures of exhaust gas aftertreatment dependent from the emission target.

Key factors influencing the potential for downsizing are therefore the engine- and exhaust-gas-related measures required for achieving the NO_x emissions targets, the desired driving performance in connection with the vehicle weight as well as any compromise in terms of comfort and NVH characteristics at a jump of cylinder number. The success of such a concept can be seen at the example of the smart cdi. With a three-cylinder diesel engine 3,3 l/100 km and a CO_2-emission of 86 g/km CO_2 is reached.

CONCLUSION

In addition to the technical dependencies outlined here, economic questions can also influence decisions regarding suitable engine sizes. This includes the question to the range of additional technologies to meet the emission limits as well as to guarantee an appropriate NVH behaviour. Moreover massive downsizing may cause the generation of completely new engines resp. engine-families combined with high capital costs. To sum up it can be stated that the downsizing of the diesel engine as well will become more important in the future.

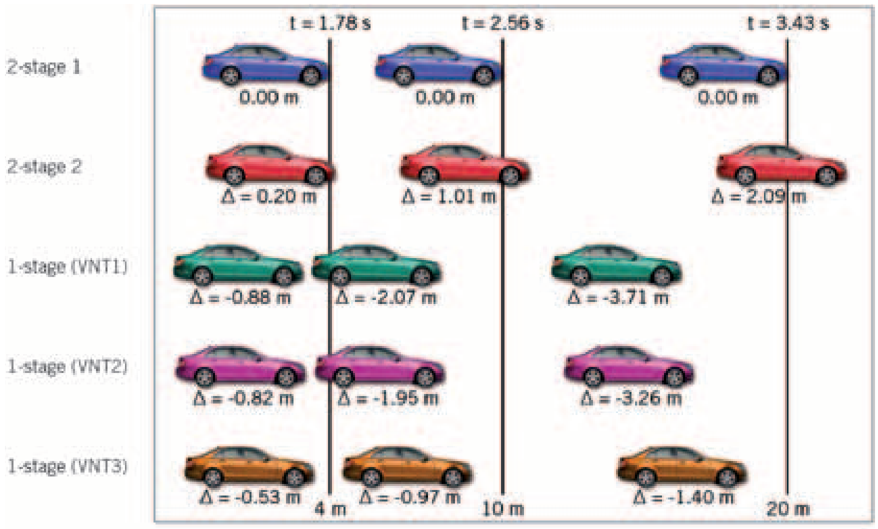

❺ Impact of the turbocharger unit on the starting behaviour: acceleration from stand still

REFERENCES

[1] Waltner, A.; Lückert, P.; Breitbach, H.; Doll, G.; Herwig, H.; Kemmler, R.; Weckenmann, H.: Der neue V6-Ottomotor mit Direkteinspritzung von Mercedes-Benz. In: 31. Int. Wiener Motorensymposium 2010

[2] Lückert, P.: CO_2-Reduzierung beim Ottomotor – die Summe der Lösungen ist entscheidend. In: 4. MTZ-Konferenz „Der Antrieb von morgen", 2008, München

[3] Schommers, J.; Lingens, A.; Breitbach, H., Betz, T.: Innovative Dieselmotorkonzepte – der Weg zur nachhaltigen CO_2-Absenkung. In: 29. Int. Wiener Motorensymposium 2008

[4] Schommers, J.; Leweux, J.; Betz, T.; Huter, J.; Jutz, B.; Knauel, P.; Renner, G.; Sass, H.: Der neue 4-Zylinder Pkw-Dieselmotor von Mercedes-Benz für weltweiten Einsatz. In: 17.Aachener Kolloquium Fahrzeug- und Motorentechnik 2008

THANKS

The authors would like to thank Dipl.-Ing. Christian Henrich and Dr. rer. nat. Walter Möhrmann for their effort on this article.

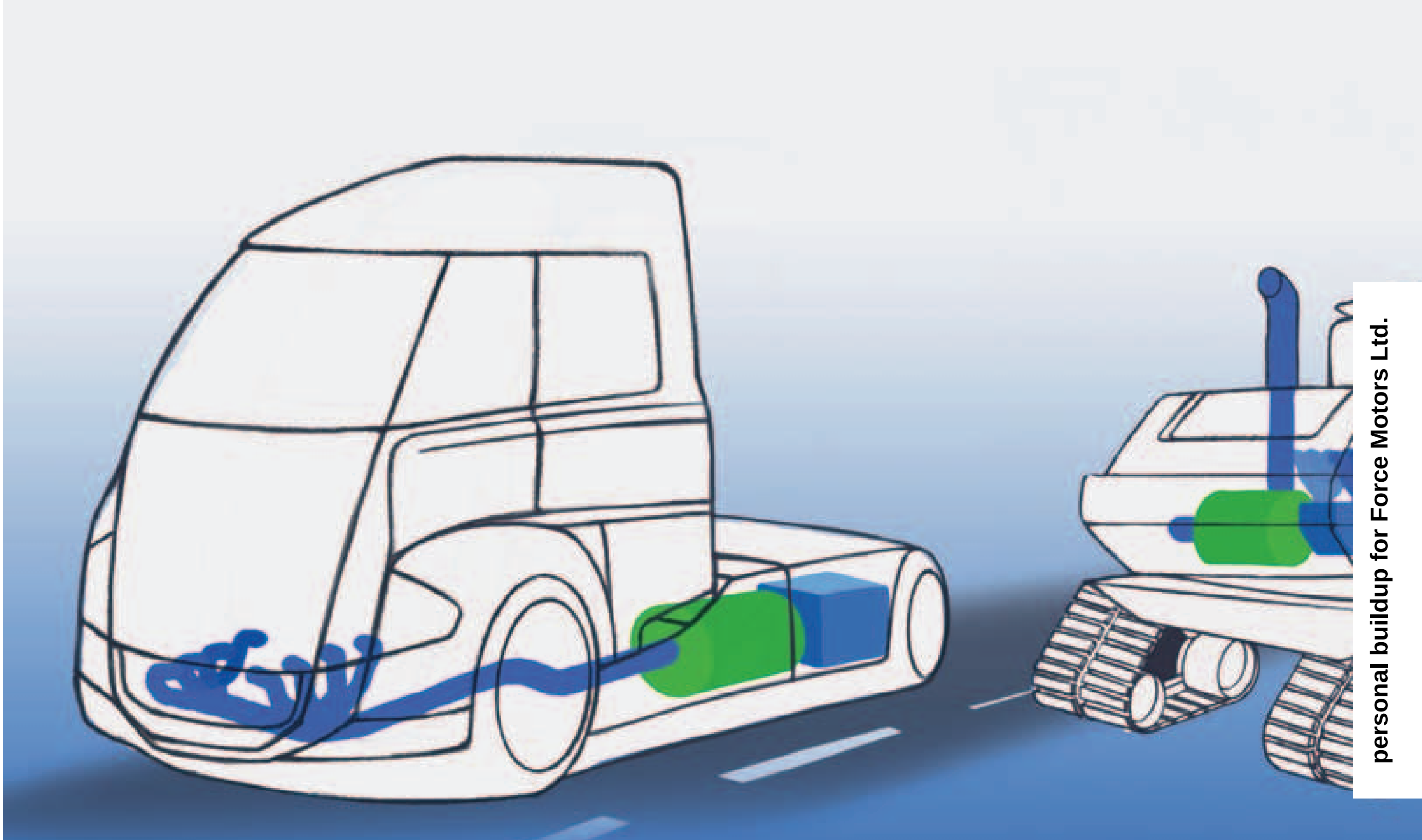

EXHAUST-GAS AFTERTREATMENT CONCEPTS FOR MEETING FUTURE EMISSION REQUIREMENTS

REQUIREMENTS FROM FUTURE TESTS

Ever since emission limits were introduced for combustion engines [1, 2], they have been continually tightened. In respect of exhaust-gas aftertreatment (EAT) meanwhile introduced in commercial-vehicle diesel engines, this means that alongside the diesel oxidation catalyst (DOC) it will also be necessary to use a diesel particulate filter (DPF) and a denoxing system – in commercial vehicles currently an SCR system with Adblue as reducing agent. In addition to defining mass-related emission limit values, a number-based limitation on particulate emissions is also being planned for future European on-highway legislation.

Over and above to the limit values themselves, the boundary conditions under which they must be met are changing too: In the on-highway segment, the World-Harmonized Stationary Cycle (WHSC) and World-Harmonized Transient Cycle (WHTC) will replace the ESC and ETC (European) in use to date once Euro VI is introduced. The off-road equivalents are the NRSC and NRTC (Non-Road), making it necessary for the first time to conduct a transient test in this segment when 97/68/EC, Stage III B, is introduced [3, 4]. Other conditions must also be met. Alongside satisfying the NTE values, these also include meeting the limit values in actual operation by conducting vehicle measurements [5].

Not only presenting the NO_x and PM limit values for on-highway and off-road applications ($P > 130$ kW), ❶ also shows the load points used in the engine map for realizing the various cycles. It becomes clear that the WHTC poses a major challenge for EAT as a result of low mean load, and associated low exhaust-gas temperatures, as well as a high overrun component in the driving profile. With a cold-started cycle making up a percentage of emission assessment beside the familiar warm-engine transient test cycles, the significance of the

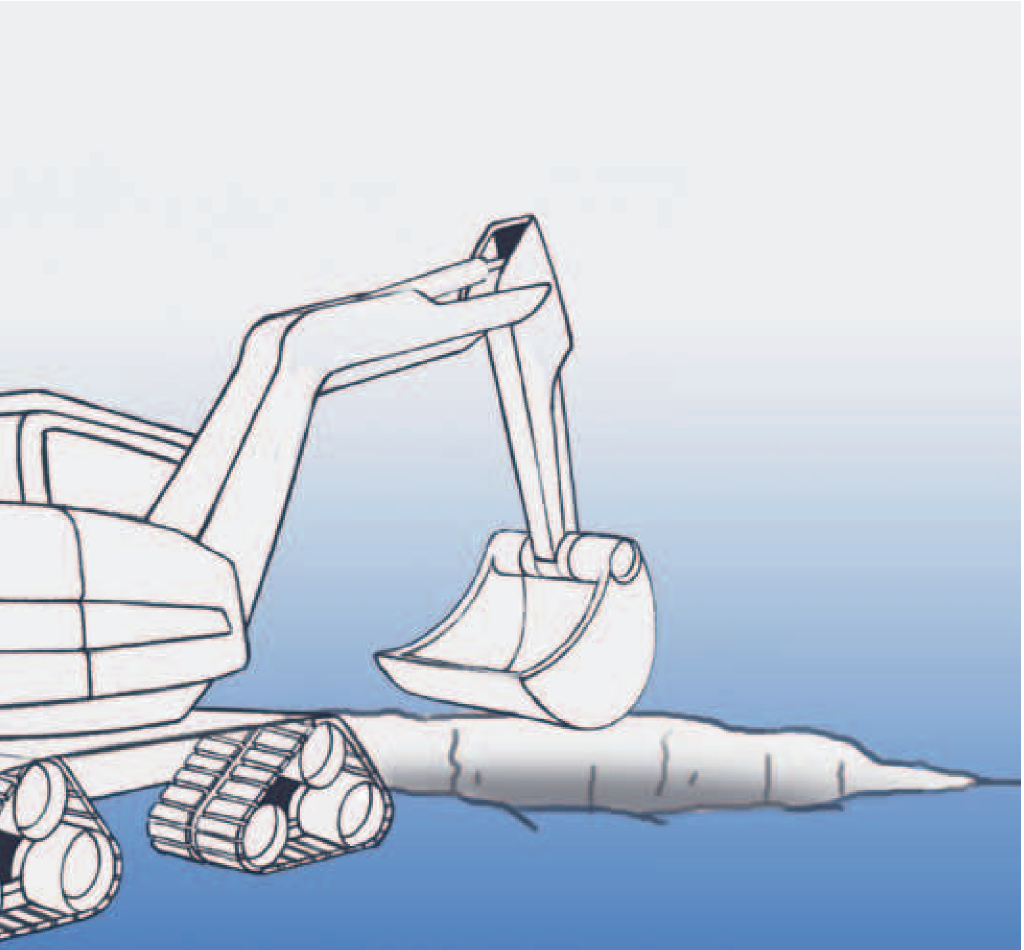

Proceeding from a modern two-stage supercharged commercial-vehicle engine employing measures inside the engine to satisfy the NO_x limit values for Euro V and EEV as well as a partial-flow particulate filter system for meeting the particulate limit values prescribed under Euro V and EEV, the IAV investigated potential approaches to complying with future emission standards in the on-road and off-road segments.

AUTHORS

TOBIAS TÖPFER
is a project engineer in the Commercial Vehicles division at IAV GmbH in Berlin (Germany).

DR.-ING. CHRISTIAN WEISKIRCH
is team manager for Calibration/ Exhaust-Gas Aftertreatment in the Commercial Vehicles Division at IAV GmbH in Gifhorn (Germany).

KAI BEHNK
is head of Commercial Vehicles in the Diesel Engines section at IAV GmbH in Gifhorn (Germany).

DR.-ING. RAIMUND MUELLER
is General Manager Technical Sales for the Heavy Duty Truck and Non-road Business at Emitec Gesellschaft fuer Emissionstechnologie, Lohmar (Germany).

EAT system's light-off behavior will grow considerably.

TEST ENVIRONMENT

❷ shows a schematic diagram of the test-bench set-up employed. The heavy-duty engine (six-cylinder, 13 l category) currently certified under Euro V/EEV has a two-stage supercharging system with intermediate cooling and cooled high-pressure EGR. This was run in its production state on a highly dynamic engine test bench with appropriate automation system. As the objective of this study did not center on meeting the next-higher emission stages, the engine's production-based calibration was not adjusted during these investigations. The exhaust-gas aftertreatment system provided was made up of a hot-end DOC and changeable canning as the basis for quickly changing individual components. The components listed in the table were installed to suit the focus of the particular test series. A Denoxtronic I (Bosch) was used for operation with Adblue. In addition to applying the usual standard measurement technology, the pollutant components were analyzed by means of two FTIR systems for assessing NO_x conversion, an MSS (Micro Soot Sensor), an EEPS 3090 from TSI, and an APC (AVL Particle Counter) to deter-

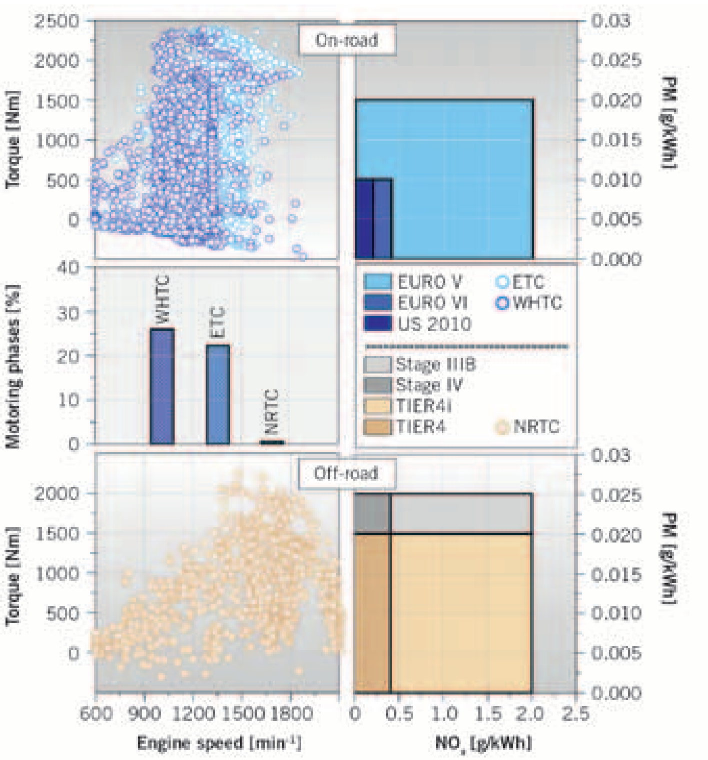

❶ Emission limit values, load-point spread in test cycles, overrun phases

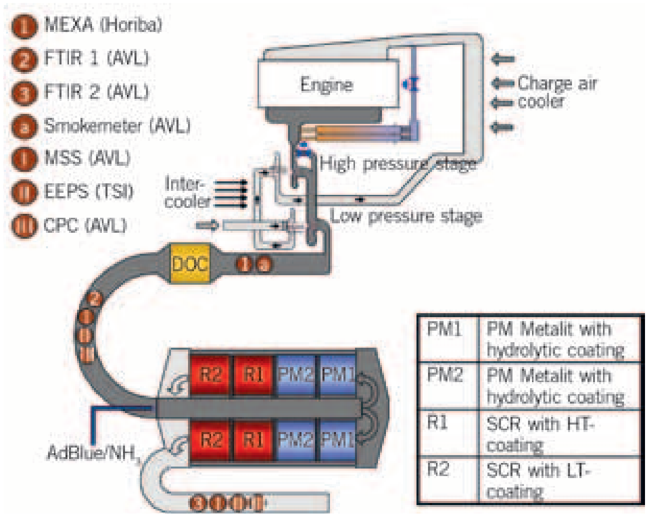

❷ Schematic test set-up with measurement system used and changeable canning

mine carbon concentration, particle-size distribution and particle number. Test-bench internal CAN communication formed the basis for metering the reducing agent and for providing control in the trailing-throttle state.

PARTICULATE EMISSIONS

The particulate-reducing capacity was evaluated in the different emission cycles using a VERT-certified DPF in addition to the reference PM Metalit available in the changeable canning. This provides the capability of performing a fundamental comparison of both filter techniques in relation to both particulate mass and particle number.

❸ shows the particulate reduction from both filter systems. The particulate reduction achieved (in relation to the untreated level downstream of the DOC) must be understood as a mean value from all six test cycles (WH-TC/SC, E-TC/SC- and NR-TC/SC). Comparing results from the various test cycles revealed that only marginal differences can be identified in specific particulate reduction capacity. The PM Metalit attained moderate degrees of filtration of 84 % in relation to particle number, and 67 % in relation to particulate mass. The levels of carbon concentration downstream of the VERT-certified DPF were measured at approximately 1 % of untreated emissions both in relation to particle number and also in relation to particulate mass. Fluctuations in the level of DPF efficiency accounted for less than one percent of the starting value. No active regeneration of the filter was initiated during the measurements.

As the engine used did not undergo any cycle-specific emission calibration, no benefit is gained from carrying out a direct comparison between the particle number achieved and the particulate limit value proposed by the legislator. Generally speaking, it is possible to formulate the following statement on all of the cycles under test: In its dimension and configuration used in the program, the particulate filter system (PM Metalit, generation two) was not able to meet the particle number limit demanded in future for Euro VI. The particle number downstream of the PM Metalit is still well above the limit value in specific cycles. The particle number measured downstream of the DPF remains below the limit value if a filter cake is formed through operation or conditioning. As a result of phases of active regeneration and aging effects, the distance from the limit value can be very small or lost completely for the wallflow DPF too. This is where the dynamic WHTC in particular, with its lower particle-number limit values, presents a major challenge for calibrating the engine's untreated emissions.

❹ shows the levels of filter efficiency in relation to particle-size distribution. It is clear to see that the optimum level of efficiency can be achieved in the range

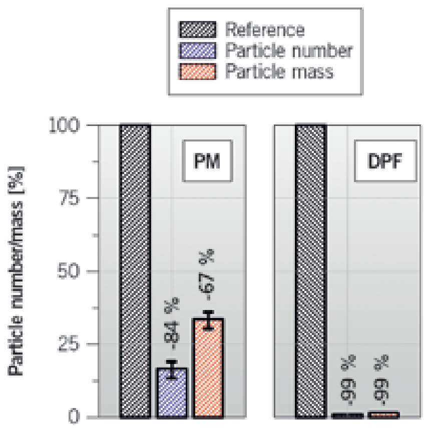

❸ Particulate-reducing capacity of the different filter systems

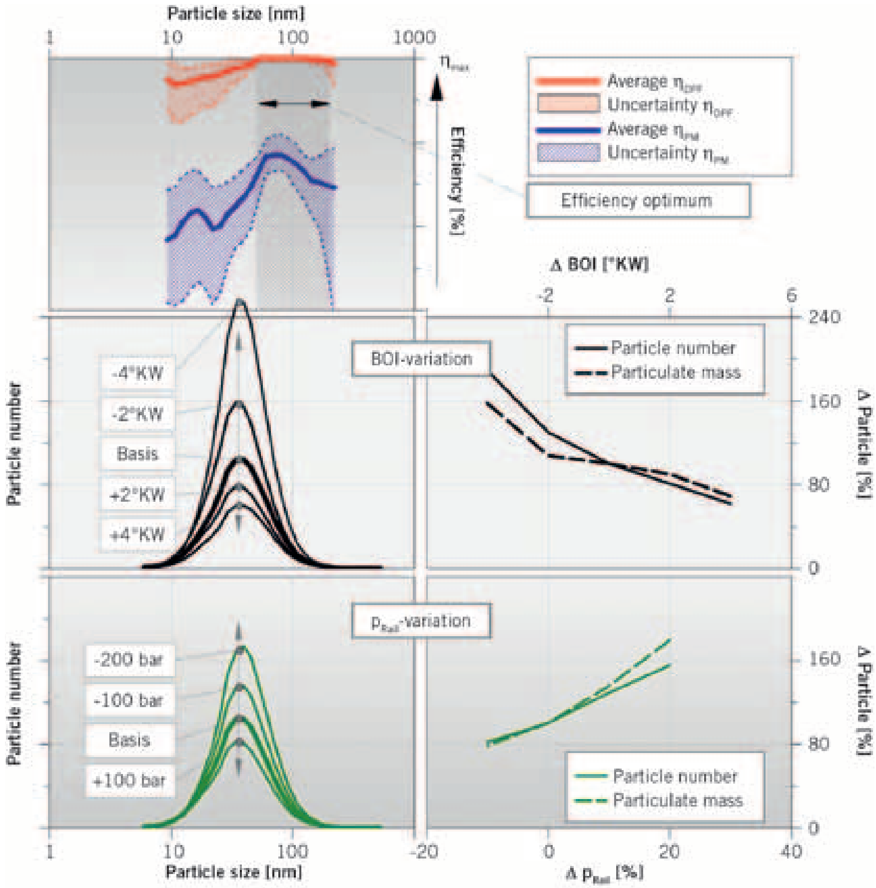

❹ Level of filter efficiency, particle distribution and correlation between particulate mass and number.

agent, e. g. based on solids, are conceivable in future.

The level of SCR efficiency is largely governed by nitrogen-oxide composition (NO, NO_2), operating temperature, the reducing agent (NH_3) and space velocity in the catalyst. As stated above, low average loads and proportional assessment based on cycles started with a cold engine represent a major challenge to EAT in relation of working temperature. This applies in particular to the SCR system. To complicate matters further, engines delivering a high specific power output use a multiple-stage supercharging group which, in turn, reduces exhaust-gas temperature upstream of the EAT system. If the temperature in the components of the SCR system drops below the critical operating temperature, their efficiency falls too. ❺ presents the different levels of SCR efficiency ascertained in the investigations carried out for the various test cycles. The efficiency differences are plain to see between ETC and WHTC. The main reason for this lies in significantly lower exhaust-gas temperatures and long overrun phases in the WHTC. Resulting from the absence of overrun phases and a high basic level of requested load, the amplitudes in SCR efficiency are much lower during the NRTC than they are in the WHTC or ETC.

Without appropriate exhaust-gas temperature management, long overrun phases at

between 50 to 200 nm. It also shows the change in particle-size distribution in response to adjusting calibration in various ways (varying rail pressure and start of injection). It can be seen that calibration measures are unable to influence particle-size distribution in untreated emissions to such an extent that would move it into the optimum range of filter efficiency [6]. This also makes it possible to explain why varying the injection parameter results in a more or less proportional change in particulate mass and particle number.

NO_x EMISSIONS

Active exhaust-emission denoxing appears unavoidable for the forthcoming emission stages. This is why SCR systems have become established and proven their worth in the commercial-vehicle segment over the last decade. The aqueous urea solution used in this context as an additive is finding acceptance above all in the field of on-highway use. In the off-highway domain as well as in niches of the on-highway segment, alternative processes for generating the reducing

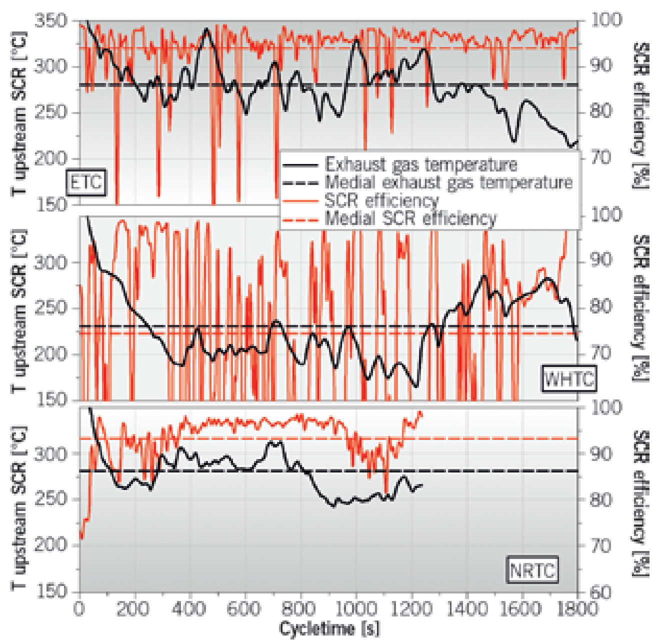

❺ NO_x conversion rates in different certification cycles.

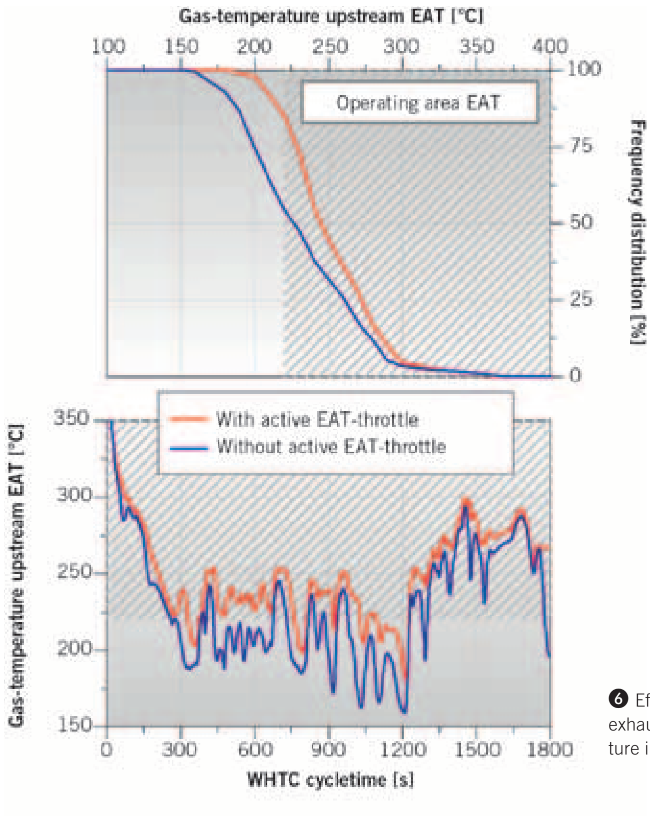

❻ Effects of managing exhaust-gas temperature in the WHTC

high engine speeds result in the EAT system quickly cooling down. One proven way in engine calibration of reducing this effect is to open the EGR path during overrun phases and additionally close the exhaust-gas flap while reducing the mass of exhaust-gas flowing through the EAT system. The effects of these measures in the WHTC are shown in ❻.

EAT COMPONENT AGING

A simulation tool developed in-house at IAV was used for obtaining a rough assessment of aging in SCR catalysts. The reaction model of the conditioned SCR catalyst was adapted here on the basis of measurements on the synthetic-gas test bench. A model of a catalyst having undergone moderate hydrothermal aging was derived from this on the basis of empirical values from the first model. ❼ shows the comparison between data measured and results computed for the catalyst conditioned in the NRTC. Although the model shows variations from the actual results measured over the transient cycle, the cumulated NO_x emissions downstream of the catalyst are predicted with an error of less than 1 % in relation to the final untreated-emission value, allowing the model to be regarded as sufficiently accurate for the rough assessment in hand.

❽ shows a comparison of NO_x emissions as computed with models for the conditioned and the aged catalyst. At 0.388 g/kWh, the aged catalyst is just about capable of meeting the limit value in the NRTC. This does, however, show that even merely

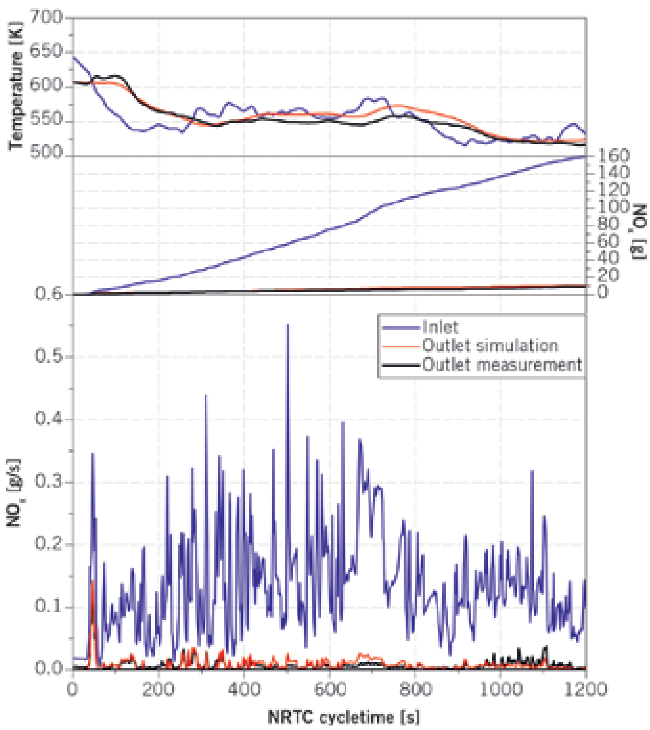

❼ Temperature curve and conversion rates in the NRTC

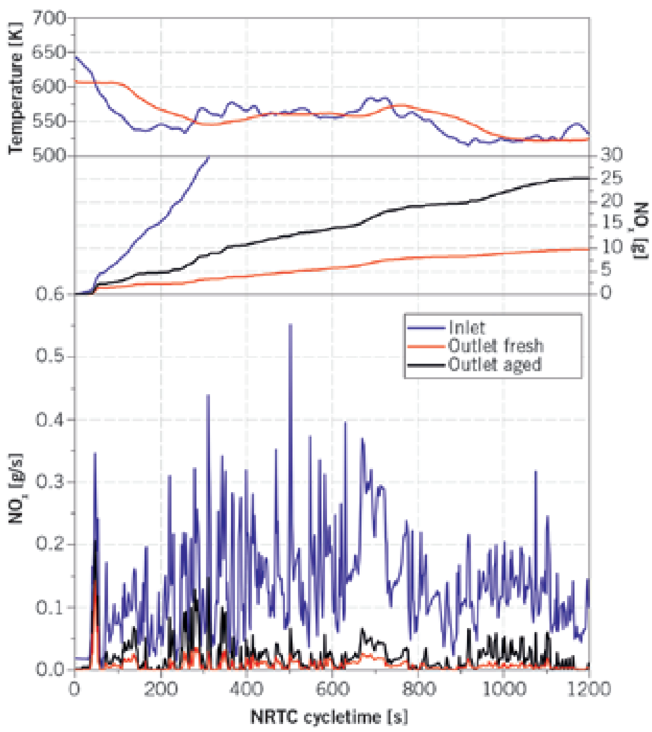

❽ Comparison of fresh and aged SCR system

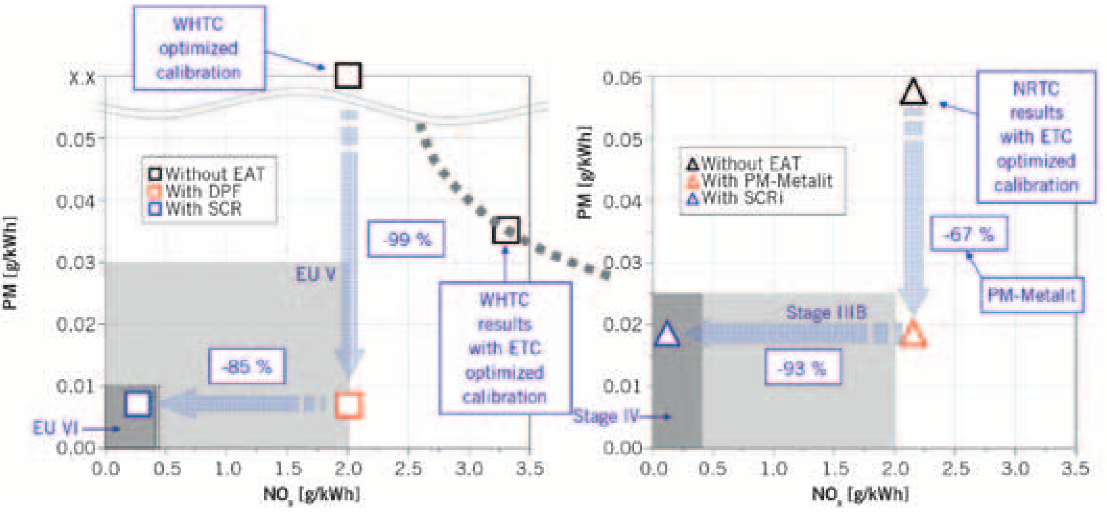

❾ Potential EAT concepts for Euro VI/ Stage IV

moderate aging can lead to significant deterioration in reducing nitrogen oxide. Aging of SCR catalysts can vary widely depending on type and version. In addition to this, oxidation catalyst aging will also have a strong influence on nitrogen-oxide reduction in the SCR system so that these effects must be closely monitored and compensated for at the configuration stage or by calibration measures.

SUMMARY AND OUTLOOK

The levels of efficiency provided by the exhaust-gas aftertreatment systems under study largely depend on engine operating behavior. Performance of the SCR in particular is extensively governed by exhaust-gas temperature. This being so, exhaust-gas temperature management would appear to be a major challenge in calibrating future on-highway engines. Modified testing conditions and the requisite verification of the actual engine performance in the various applications will add further stringency to future emission limits. In addition to conventional cold-running and warm-up strategies, supplementary measures must be implemented in order, for example, to prevent the EAT system from cooling down. Proceeding from consumption-optimized operation at higher untreated NO_x emission levels in long-distance driving (NO_x-bsfc trade-off), a significantly lower level of NO_x must be achieved inside the engine for the cold WHTC so as to take account of inactive EAT during the warm-up phase.

❾ presents the potential strategies for the off and on-road sector. In meeting the Stage IV/Tier4 limit values, there is not absolute need to achieve the necessary reduction in particulate emissions by means of a closed DPF. In addition to using closed filter systems, operating without DPF is even conceivable since the legislator has so far not made any provision for limiting the particle number, and the particulate mass limit value is easy to meet using engine-based means or with the PM Metalit filter. Local requirements, however, do exist (e. g., construction site vehicles in Switzerland) that demand the use of a particulate filter. Provided it is possible to dispense with a particulate filter, the possibility of an upstream configuration produces advantages for aftertreating NO_x emissions which will be necessary anyway. For this concept, downstream filter systems with burner then lend themselves to regional special-purpose applications as a way of satisfying additional requirements. Compared with a Euro V configuration with engine-internal NO_x reduction, engine hardware or engine calibration only requires minor modifications in the off-road- segment – the optimum must be found between consumption and possible NO_x conversion.

Greater efforts, in contrast, are required for Euro VI: From today's perspective, the closed particulate filter will be imperative, giving rise to the described problems particularly in the low-load operating conditions (distribution traffic, etc.). This is where different solutions must be provided for different application cases to achieving the best possible compromise. The close correlation between exhaust-gas temperature and SCR performance has already been described. The WHTC represents a particular challenge in this context. Based on measures for managing exhaust-gas temperature, SCR efficiency levels of at least 85 % should be the development target. Lower levels of efficiency would result in higher untreated particulate emissions (PM/NO_x trade-off) which, in turn, demands the need for frequent filter regeneration. This is counter-productive, especially in the light of fuel consumption.

As a result of cost pressure simultaneously rising on the operator side, it will be necessary in future to assess the merits of each vehicle concept on a case-to-case basis and decide which combination is ultimately the most favorable overall system for the consumer. Whereas optimizing wind resistance provides a major cost-reducing potential in long-distance traffic, these effects are extremely minor, for example, in urban distribution traffic. Consequently, greater importance will again be attached to the potential savings on the powertrain side. Legislation therefore continues to make powertrain development an exciting subject in the commercial-vehicle segment too.

REFERENCES

[1] http://eur-lex.europa.eu/LexUriServ/LexUriServ.do?uri=OJ:L:2004:225:0003:0107:EN:PDF
[2] http://www.epa.gov/otaq/highway-diesel/regs/2007-heavy-duty-highway.htm
[3] http://eur-lex.europa.eu/LexUriServ/LexUriServ.do?uri=OJ:L:2010:086:0029:0047:DE:PDF
[4] http://www.epa.gov/nonroad-diesel/regulations.htm
[5] http://ies.jrc.ec.europa.eu/eu-pems/links.html
[6] Raatz, T.: Untersuchungen zur homogenen Dieselverbrennung (Investigations into Homogeneous Diesel Combustion); Dissertation, Braunschweig University of Technology, 2002

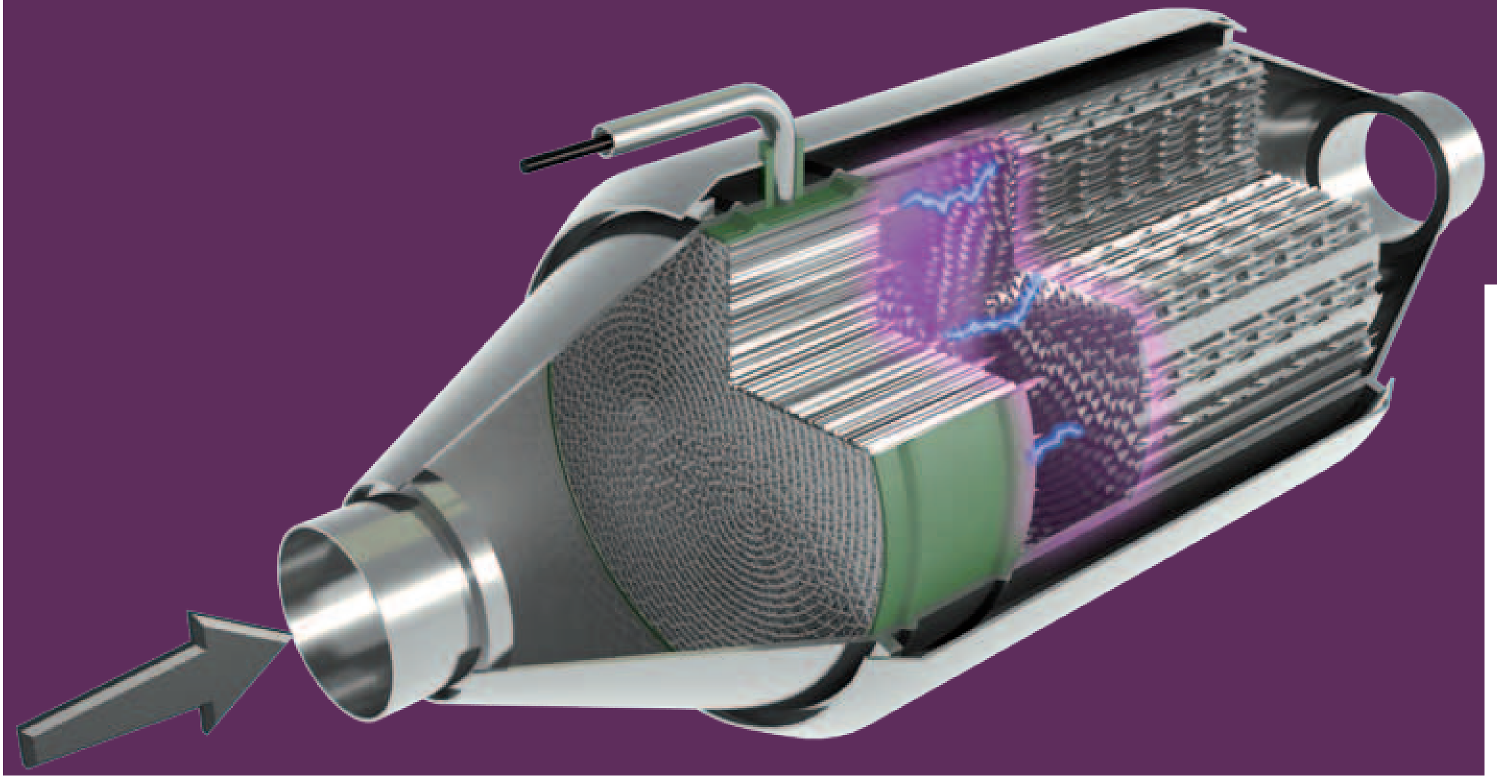

AUTHORS

DIPL.-ING. WOLFGANG MAUS
is Chairman of the Board of Management at the Emitec GmbH in Lohmar (Germany).

DIPL.-ING. ROLF BRÜCK
is Managing Director Research, Development and Application at the Emitec GmbH in Lohmar (Germany).

DIPL.-ING. JAN HODGSON
is Head of Research at the Emitec GmbH in Lohmar (Germany).

DIPL.-ING. CHRISTIAN VORSMANN
is Staff Member Research at the Emitec GmbH in Lohmar (Germany).

ANCILLARY CONDITIONS

Euro 6 legislation for passenger cars and Euro VI legislation for commercial vehicles for the first time also limit particle numbers in addition to gaseous emissions and particle mass. The main focus lies on the reduction of nanoparticles, which are considered harmful to health.

Particle number limits for commercial vehicles and for passenger cars with petrol engines are currently being discussed. The original approach to limiting particle numbers required the number limit to correlate with the mass limit and also to be determined by best available technology.

However, this poses the question as to which of today's particulate filter technologies represent the best available technology and whether it also represents the best technology to meet the requirements for particle number reduction.

The EU PMP project (Particle Measurement Programme, [1]) created a database for passenger cars and commercial vehicle engines. However, measurements and comparisons of particle mass and particle number did not distinguish between raw emissions and tailpipe emissions. In particular, the correlation of tailpipe emissions did not take account of the different filter rates during number and mass measurements.

For example, a mass limit of 10 mg/kWh relating to the raw emissions from a typical commercial vehicle diesel engine corresponds to a number limit of approximately 1×10^{13} particles per kWh [1]. By contrast, the heavy-duty limit of 6×10^{11} particles/kWh under discussion would correspond to a raw emission mass limit of less than 1 mg/kWh. As a result, particle number legislation stipulates a ten times more stringent mass limit.

Hastily introduced particle number limits will impede or even prevent further engine developments that could give European engine manufacturers a competitive edge over the rest of the world. These innovative engines are able to keep within the mass limit but still require a particulate filter to comply with the number limit, which increases fuel consumption and hence CO_2 emissions (because of greater pressure loss and the necessary active regeneration measures).

The aim must therefore be to comply with future limits with a minimum of pressure loss and without active regeneration measures. It goes without saying that

ELECTROSTATIC PARTICULATE FILTER FOR NANOPARTICLE REDUCTION

Future emission legislation for passenger cars (petrol and diesel) and heavy-duty vehicles will also require a reduction in particle numbers in addition to a reduction in particle mass. Conventional filters that combine current levels of porosity with new, low soot-emitting engines are unable to filter nanoparticles with sufficient effectiveness because of the lack of a soot filter cake. The necessary reduction in pore size would lead to greater pressure loss. The Electrostatic Particulate Filter PM-Metalit Advanced by Emitec represents a new generation of particulate filters for the automotive industry.

the potential costs of exhaust gas aftertreatment have to be substantially reduced at the same time.

FILTER TECHNOLOGIES

Particulate filters for automotive applications are subject to very high technical requirements because of high temperatures, rapid temperature changes and mechanical stress. The separation rate for particles in the 10 to 500 nm range should be significantly above 90 % with minimum pressure loss. ❶ shows the separation rate of technical filter systems as a function of particle diameter.

OPERATING PRINCIPLES OF PARTICULATE FILTERS (DEPTH FILTERS)

For small particle diameters the separation of particles is based on a combination of inertial separation (impaction), interception from a limiting particle path (interception) and separation as a result of Brownian particle motion (diffusion). ❷ shows the effective range of the filter mechanisms in relation to particle diameter.

The probability of a particle being separated depends on the filter structure, the pore size of the internal surface, the flow speed and the filter depth.

Deposited particles agglomerate on the surface of the filter and form a filter cake. This filter cake increases the internal surface and thus improves the separation rate. Pressure loss rises simultaneously. As soot deposits grow the depth filter becomes a surface filter with increasing efficiency. Partial-flow filters take this fact into consideration by directing only a part of the flow through the filter medium but repeating this process several times.

ELECTRIC FILTERS

Electric filters or electrostatic separators are systems that separate particles from

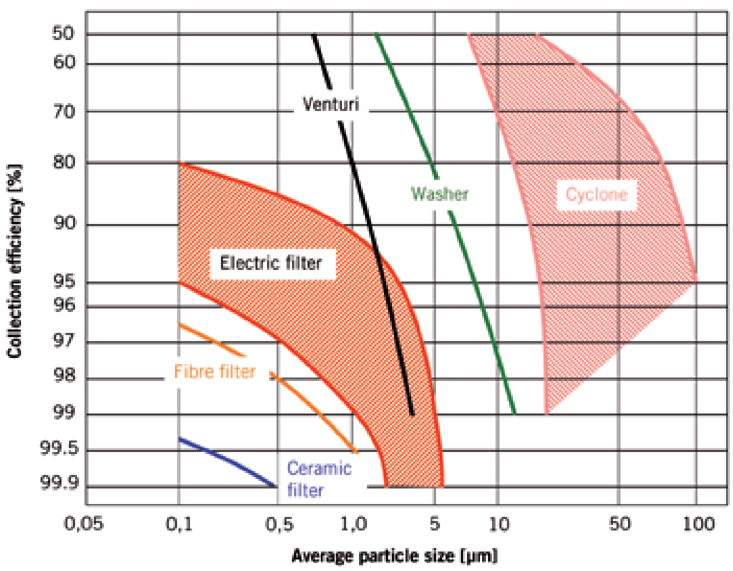

❶ Separation rate of technical filter systems as a function of particle diameter [2] gases on the basis of the electrostatic principle. Coulomb's law states that charges repel or attract each other. Separation in electric filters can be divided into five stages [4]:

: Generation of electric charges: Electric charges are generated by the application of a high voltage to two objects. The charges move along the lines of force of the electrical field created by the voltage.
: Charging of particles: A particle crossing this electrical field is charged by deposits of negative charges. Depending on their size particles are charged by field or diffusion charging.
: Transport of charged particles to the precipitation electrode: Stokes' law states that charged particles travel to the precipitation electrode where they adhere and discharge their energy.
: Particle adhesion to the collecting electrode: After the particles have discharged their energy they adhere because of the adhesive forces acting between the particles themselves and between the particles and the filter wall. Particles are considered to have been separated when the adhesive forces are stronger than the flow forces.
: Particle removal: Industrial electric filters are usually cleaned by brushing the particles from the collecting electrode. The removed particles fall into a bunker from where they can be disposed of. However, in automotive applications electric filters will have to be regenerated continuously.

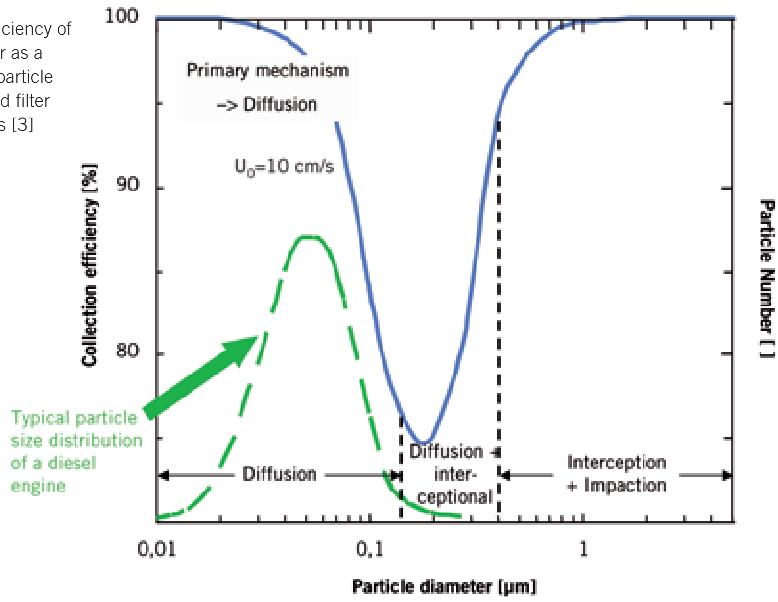

❷ Filter efficiency of a depth filter as a function of particle diameter and filter mechanisms [3]

ELECTRIC FILTERS FOR AUTOMOTIVE APPLICATIONS

Electric filter processes had already been used for the primary separation of soot particles in automotive applications in the past.

Soot deflectors separate particles in an electrostatic agglomerator where the particles agglomerate and are removed again by gas-dynamic forces after reaching a critical size. Due to their inertia the agglomerated particles can be separated into a clean and a particle-rich partial flow. The particle-rich flow can subsequently be filtered by a particulate filter in the conventional manner and regenerated discontinuously.

However, electric filters for mobile applications should operate on the basis of continuous regeneration. In diesel engines soot can be regenerated using the NO_2 contained in the exhaust gas. Large surfaces that guarantee interaction between the NO_2 and the particles are required to ensure that the reaction continues to the point of completion, particularly at low temperatures. This means that it is necessary to distribute the particles across the largest possible separation surface. In petrol engines, which have a higher temperature profile, the particles are additionally oxidised using the residual oxygen in the exhaust gas.

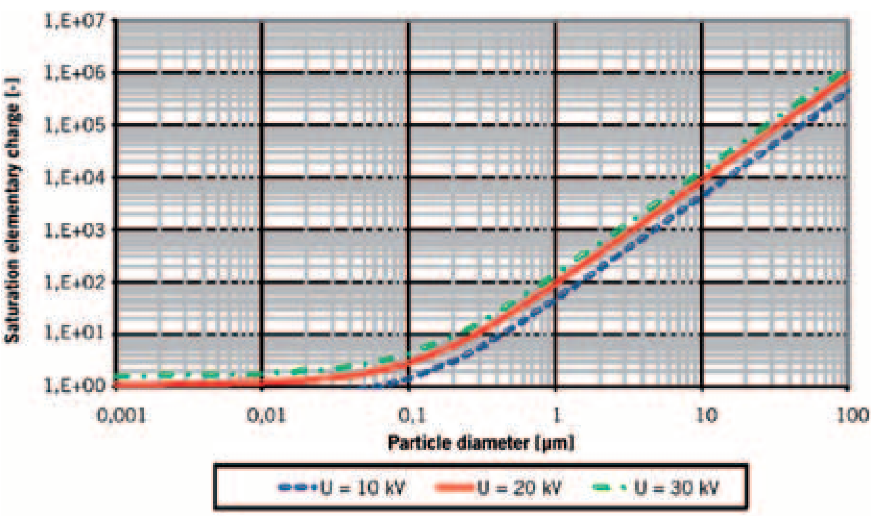

❸ Correlation between electric charge and particle diameter for different voltages

CALCULATION OF ELECTROSTATIC SOOT PARTICLE SEPARATION

An electric field is generated by the application of a high voltage to two objects [5, 6]. This consists of an active and a passive field. Electrons are released in the active field.

In the passive field particles are charged by negative ions. This process is based on two mechanisms. The first mechanism is field charging where the particles are charged by ions that move in the direction of the electric field. The maximum charge of the particles depends on the electric field strength. In diffusion charging particles are charged by random collisions with thermally moved charge carriers.

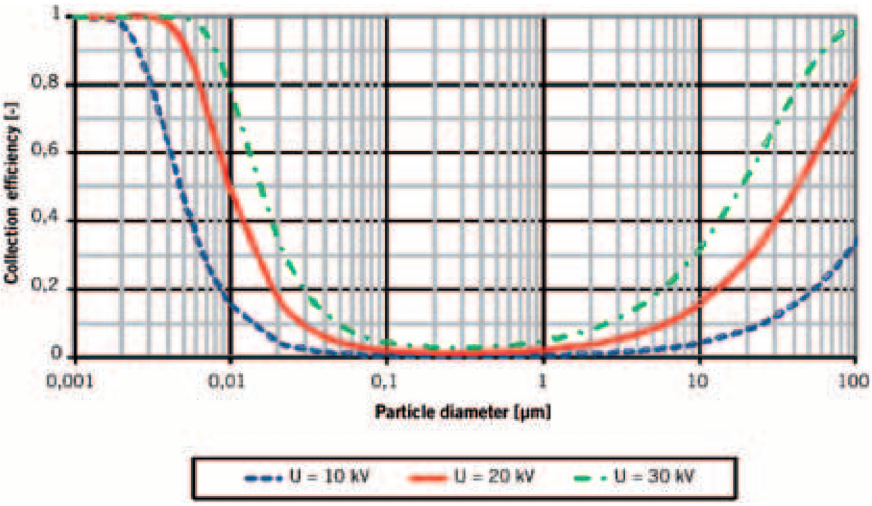

❹ Separation effectiveness in relation to particle diameter and electric field strength in turbulent flow

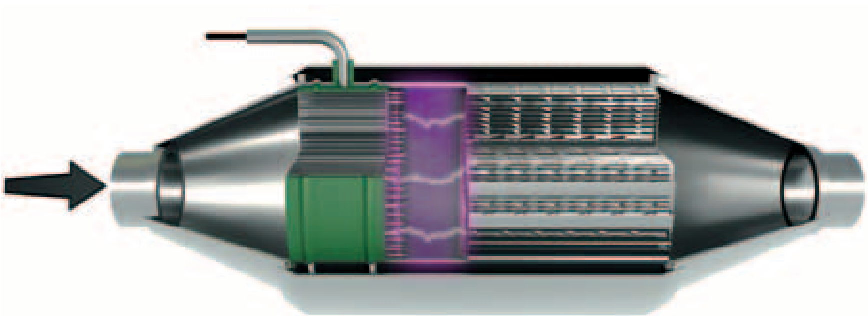

❺ PM-Metalit Advanced consisting of a current distribution substrate with soldered electrodes and a deposition substrate

The electric field strength for a wire/cylinder electric filter can be calculated on the basis of the voltage and the distance between the electrodes. Taking into consideration the two charging mechanisms the saturation charge of a particle can be determined by Cochet's equation while the number of charge carriers can be

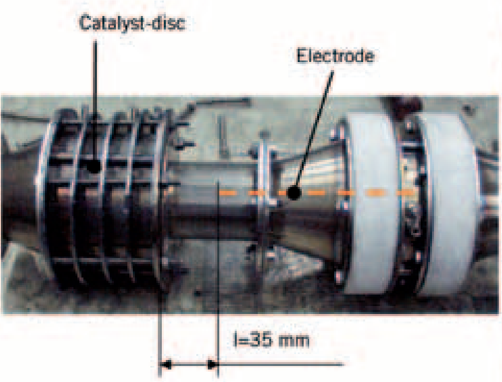

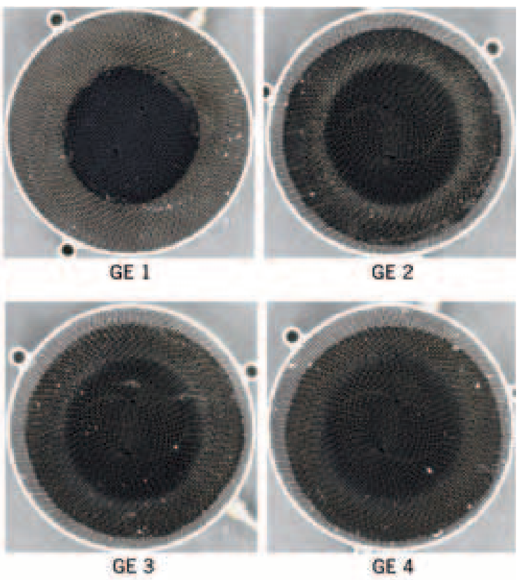

❻ Test setup: Deposition substrate in four discs with upstream single rod electrode

established on the basis of the elementary charge. ❸ shows how the charge depends on electric field strength and particle diameter.

A charged particle is subject to an electrostatic force and an opposing resisting force in the surrounding fluid. A speed component is added as soon as the electric force is greater than the resisting force. The migration speed acting on a charged particle and the resulting effectiveness of the separation can be calculated on the basis of this correlation. ❹ shows the separation effectiveness in relation to particle diameter and electric field strength in turbulent gas flow.

The electric field strength and the particle diameter can be seen to have a great effect on the saturation charge and the separation probability. The aim of the development of the PM-Metalit Advanced was to improve the low level of effectiveness in the 0.05 to 5 µm range.

PM-METALIT-ADVANCED

There have been several attempts at developing electric filters, electrostatic agglomerators and soot deflectors with cyclone separators over the past 25 years. However, due to the small amount of NO_2 in relation to soot these systems were unable to passively regenerate the soot and could only collect it.

Problems caused by high voltage generation and the electric feedthrough can now be prevented by dynamically controlled high voltage supplies. Modern diesel engines emit less soot so that the electric feedthrough is far less likely to become soiled, thus reducing the likelihood of short circuits.

As described the aim must be to oxidise the filtered soot by passive regeneration alone. This requires the soot to be distributed across a large surface to facilitate a reaction with the NO_2 contained in the exhaust gas.

Metal honeycombs have been used in catalytic converters of cars and two-wheelers for a long time and combine the advantages of mechanical/thermal durability, low pressure loss, large surfaces and electrical conductivity.

To this end, a metal honeycomb was developed that also functioned as a precipitation electrode. The design was based on the PM-Metalit partial-flow deep-bed

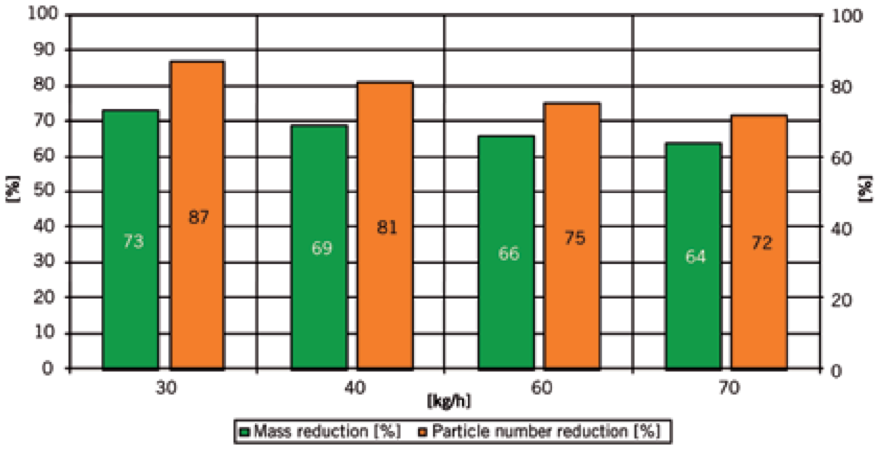

❼ Reduction of particle mass and particle number in relation to exhaust gas mass flow at a constant voltage

filter and was particularly effective at preventing deposited soot from being blown out during dynamic operations. The blades installed in the channels disrupt laminar flow and improve electrostatic separation. The PM-Metalit has already been put into large-scale production and proven itself in commercial vehicles and non-road applications for many years. For maximum effectiveness the electric field has to be built up over the entire cross-section of the honeycomb as uniformly as possible.

It is difficult to build up an electric field in large catalyst cross-sections with just one single discharge electrode. Several electrodes increase the complexity of the construction and would have to be electrically interconnected. Therefore a second metal honeycomb was designed to act as a current distributor. The electrodes are soldered into the honeycomb. The number and form of the electrodes can be adapted to the specific basic conditions.

The high voltage insulation and mounting extends across the circumference of the honeycomb. Specially developed deflecting structures are used to prevent impurities. The electric field builds up between the tips of the electrodes and the deposition substrate. Both the current distribution substrate and the deposition substrate can be catalytically coated and so ensure the effectiveness of the catalyst. ❺ shows the assembly and the electric field between the two metal substrates.

This construction charges the particles electrostatically and thus increases the efficiency of the PM-Metalit filter. The electrostatic forces intensify the diffusion separation by adding another force component. Since particles are separated in the channel structures efficiency is increased across the entire particle size range.

TEST RESULTS

The PM-Metalit Advanced is currently in the predevelopment phase. First trials were carried out on a dynamic test bench using an EU IV car diesel engine. The PM-Metalit Advanced was connected to a distributor capable of varying the mass flow supply independently of the engine operating point.

The aim of these tests was to determine whether soot was going to be deposited over the entire length of the deposition substrate or only on its front surface. To this end, a small metal substrate (70 mm) was eroded to form discs and fitted to the exhaust system with an air gap of 2 mm, ❻.

A single electrode was positioned at a distance of 35 mm in front of the separator. The electric field was supposed to build up only across part of the substrate diameter to make it possible to distinguish areas inside the electric field from adjacent areas.

Soot is clearly visible in the channels of the first disc. However, the deposits cover only the area inside the electric field (central section of catalyst). The transverse exchange in the gap between the individual discs resulted in a larger deposition zone for discs two to four. The fact that soot is visible also at the end of the last disc confirms the complete utilisation of the separation surface, which creates ideal conditions for passive regeneration.

The same test setup was used to measure particle mass reduction and particle number reduction at varying mass flows and constant voltage at a temperature of 270 °C, ❼. At a constant voltage of 16 kV particle mass was reduced by 60 to 70 % and particle number by 70 to 85 % depending on the exhaust gas mass flow. According to the theory separation decreases with increasing exhaust gas mass flow at a constant voltage. In real applications the voltage is adjusted according to the load point. This should be regarded as a positive result because the electric field builds up only across part of the cross-section of the precipitation substrate, as shown in ⑥.

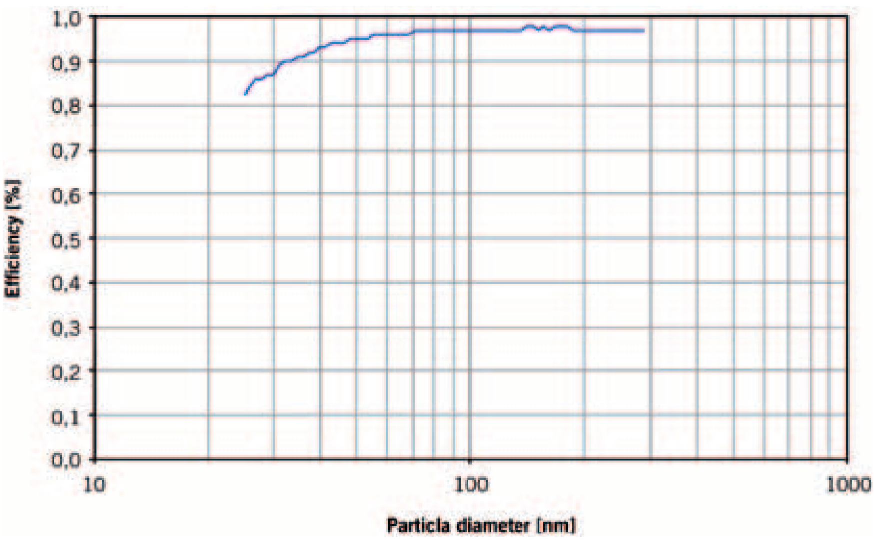

❽ Number effectiveness in relation to particle diameter

A system similar to the setup shown in ⑤ was measured in a further test. During these tests, particle mass and particle number were reduced by over 90 % in the NEDC. For clarification particle number effectiveness was determined by particle size at a medium load point. ❽ shows number effectiveness as a function of particle diameter.

According to the theory, number effectiveness depends on particle diameter and is over 90 % in the 50 to 300 nm range. The result makes it clear that the electrostatic separation of soot particles in the channels of honeycombs with guide blades works successfully across the entire particle size range.

SUMMARY AND OUTLOOK

The PM-Metalit Advanced electrostatic particulate filter for mobile applications represents a completely new development capable of complying with particle number limits while causing minimum pressure loss. Building on the proven partial-flow deep-bed concept, the separation of nanoparticles, in particular, is improved by the application of electrostatic forces, which act as a diffusion and adhesion booster. The system is able to separate well over 90 % of particles that have been charged in an electric field without the previously inevitable increase in backpressure.

First results indicate that the innovative use of metal substrates as current distributors and separators presents a new method of particulate filtration. When used as a separator, PM-Metalit substrates with small channels and guide blades achieve good separation rates for all particle sizes.

As a next step, both the power supply and the PM-Metalit Advanced will undergo further development with the aim of creating a durable solution for passenger car and commercial vehicle applications.

Apart from this development work, it is crucial that authorities restrict themselves to defining new limits and do not directly or indirectly express a preference for, or even prescribe, particular technologies. Such prescriptive legislation would put an end to innovation and place Europe at a disadvantage in international competition.

REFERENCES

[1] GRPE: PMP Particle Measurement Programme. Particulates Meeting, 30th March 2009
[2] Zievers: Lexikon Verbrennungsmotoren Partikel
[3] Brück, R.; Kaiser, F.-W.; Konieczny, R.: Der metallische Nebenstromfilter PM-Metalit: eine Lösung zur Partikelreduktion bei Pkw- und Nfz-Anwendungen. In: HdT-Tagung, Ismaning, 16.–17. Mai 2006
[4] Hinds, W. C.: Aerosol Technology. Second Edition
[5] Riehle, C.: Applied Electrostatic Precipitation. Edited by K. R. Parker
[6] Kukla, P.; Wright, J.: A Novel Electrostatic Method of Ultrafine PM Control Suitable for Low Exhaust Temperature Applications. SAE Paper 2003- 01-0771

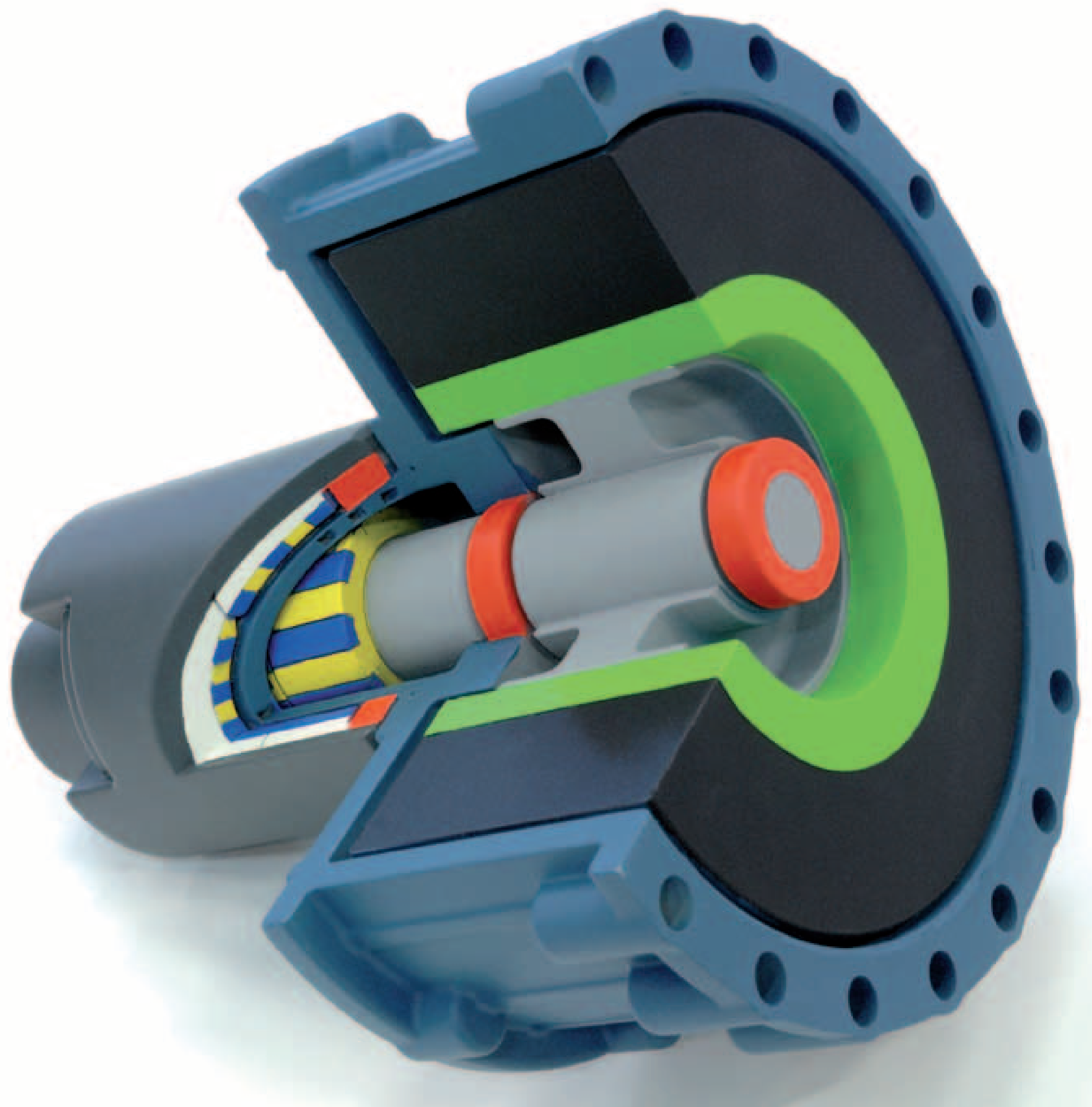

THE RICARDO MECHANICAL HYBRID DRIVE

Ricardo has developed a mechanical hybrid drive system in which kinetic energy is stored by a flywheel and supplied to the drive train via a continuously variable transmission. Studies carried out by Ricardo have shown that the system offers a reduction in fuel consumption of up to 25 % at a relatively low cost.

AUTHORS

DR. ANDREW ATKINS
is Chief Engineer of Innovation for Ricardo. As such he has, with other technologies such as cryogenic engines, directed the Kinergy Programme at the Technical Centre at Ricardo plc at Shoreham (United Kingdom).

PETER FEULNER
is Leader Research and Technology at the Ricardo Deutschland GmbH in Schwäbisch Gmünd (Germany).

ENERGY RECOVERY BY FLYWHEEL

Interest in kinetic energy recovery systems (Kers) was stimulated by Fédération Internationale de l'Automobile (FIA) rule changes for the Formula 1. Ricardo, as the technology partner for one of the major teams, developed a number of alternate solutions based on different technology platforms. One of these platforms was high speed flywheels. This work, and subsequent development undertaken by Ricardo, showed that KES (kinetic energy storage) systems based on flywheel technology are extremely well suited for optimization for high cycle, high power density applications (for example, motor sport, inner-city mass transit or special operations vehicles) because power and energy densities are defined by independently optimisable sub-systems. That is, the power capability is defined by the continuously variable transmission (CVT) and the energy capacity by the flywheel. As a consequence, the whole system can be highly tailored to any particular application. In addition, flywheel based KES systems are inherently more efficient than electrical energy storage systems because there are no energy conversions in the system. In electrical energy storage systems, torque is converted to chemical energy via electrical, reducing potential energy recovery. In addition, power density and energy density are cross-linked parameters, enshrined in a single entity, namely the battery or ultra-capacitor.

SYSTEM OVERVIEW

The mechanical hybrid drive, labelled Kinergy by Ricardo, is made up of three main sub-systems, ❶:

: the flywheel, scaled to the energy storage needs of the system
: the coupling, designed to transfer the torque into the vacuum space
: the CVT controls the power flow.

In the next part of the paper these three sub-systems will be reviewed independently.

FLYWHEEL FUNDAMENTALS AND DESIGN CHALLENGES

At the heart of a KES system is the flywheel. The energy, E, is stored therein through rotation, where $E = \frac{1}{2} I \omega^2$. As such, the key to a high energy density is high angular velocity and a high diameter. The limiting factors on this being the ultimate tensile strength of the material the flywheel is made from and the available packaging space. Further, major, factors to be considered during the design are: the ability to manage surface heating by maintaining an acceptable environment about the flywheel; the ability to design the shape of the flywheel such that the system dynamics are controlled to an acceptable level in the operating range; and the ability to specify bearings suitable for the speed and loading, ❷.

As part of Ricardo's development process the flywheel mass mapped for a matrix of diameters and energy stored at different maximum speeds. From this work it is possible to quote and estimate the energy density of flywheels using the current design methodology as approximately 200 kJ/kg. However, a large number of factors can affect this value. By example, ❸ illustrates the mapped design space for a maximum speed of 60.000 rpm. ③ uses example figures to illustrate the output of Ricardo's proprietary design tool for high speed flywheels. The tool includes the learning and design choices garnered during the development process. The right hand column of ③ illustrates how the final energy density for a given maximum speed is non-linear with diameter and is strongly determined by the available package diameter. By example a 0.5 kWh, 1.8 MJ flywheel at 280 mm (11") will weigh 12.88 kg. This flywheel is a disc, (where the diameter is greater than the axial length), and so is an efficient design. When the packaging demands a reduction in diameter by less than an inch to 260 mm (10.2"), the flywheel weight will increase non-linearly to 26,92 kg to maintain the same energy content at 60,000 rpm.

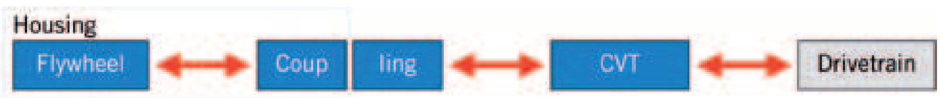

❶ System configuration of the mechanical hybrid drive – schematic

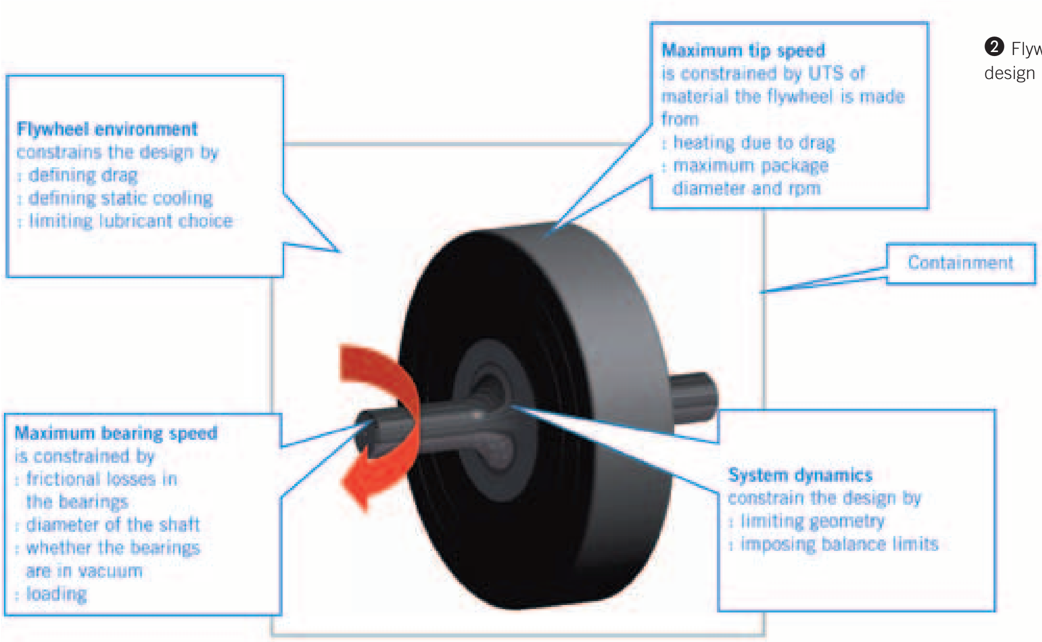

❷ Flywheel and its design parameters

High speed flywheels carry with them associated concerns over safety. A failure mode which is of particular concern is flywheel "burst". The burst event is where the strain on the inner diameter of the wheel exceeds that which the material can withstand, causing the wheel to fragment catastrophically.

Ricardo flywheels have a number of patented, safety design features that are test validated. These enshrine a three pronged approach to ensuring a burst firstly does not occur and then if it does the impact is contained. The three prongs are:

: deploy a fiber with a sufficient UTS such that the safety factor exceeds ten, which is in excess of that used by the aerospace industry when designing composite wings; as a result, a flywheel which has a maximum operating speed of 60,000 rpm might have a design maximum speed of 125,000 rpm
: built into the system are hard mechanical measures to prevent the operating speed being exceeded
: further, if by some combination of failures and events an over-speed does occur then benign failure mechanisms are designed in – i.e. non-burst failure mechanisms – at speed intervals between 60,000 rpm and 125,0000 rpm.

Ricardo has used its blast mitigation expertise used in other areas such as the Ocelot program to incorporate in the system weight a containment system that it will restrain any burst fragments created.

Looking forwards, Ricardo's research groups have patented novel high-speed flywheel design concepts that maximize energy storage and reduce flywheel weight. A comparison of Ricardo's future patented design (SlingShot) with the conventional flywheel technology that already gives a huge potential advantage is summarized in ❹. Ricardo's design will substantially increase the maximum speed rating of the flywheel and reduce the overall mass of the system while still retaining a high level of energy storage. As an enabler for increased system speed, Ricardo is also developing high-speed magnetic bearings. The net result of introducing these unique technologies into the current Kinergy suite will increased

mm													
360	0.86	1.27	1.70	2.12	2.55	2.97	3.40	3.82	4.25	4.67	5.10	5.61	6.12
340	0.99	1.39	1.75	2.18	2.62	3.06	3.49	3.93	4.37	4.80	5.24	5.76	6.29
320	1.23	2.46	3.18	2.53	3.04	5.31	6.07	6.86	7.59	8.35	5.91	6.50	7.09
300	1.18	1.75	2.62	4.79	5.53	6.31	7.17	8.06	8.96	9.85	6.72	7.39	8.06
280	2.02	2.50	2.65	4.60	5.41	7.59	5.14	5.78	6.42	7.07	7.71	8.48	12.88
260	2.99	3.57	4.76	5.93	6.30	8.03	5.95	8.51	7.44	9.41	13.90	15.13	26.92
240	2.81	4.70	6.68	7.02	8.39	9.78	11.22	12.58	13.98	24.67	14.28	15.13	15.94
220	3.26	5.02	6.66	8.98	9.51	11.09	12.67	21.83	12.79	13.73	27.08	25.37	25.50
200	3.72	5.59	7.31	8.68	10.41	12.15	21.19	13.00	20.17	25.71	24.06	26.23	28.18
180	3.70	5.55	7.40	9.25	11.10	17.42	19.45	23.57	23.15	24.80	27.08	28.11	29.79
160	4.34	6.33	8.23	9.98	17.12	19.06	20.85	22.52	24.09	25.59	29.40	28.67	30.25
kJ	250	375	500	625	750	875	1000	1125	1250	1375	1500	1650	1800

All carbon
Mostly carbon (bit of steel)
Mostly steel (bit of carbon)
All steel
Ip/It < 0.6

❸ Flywheel design space mapping for 60,000 rpm

DESIGN	ALL STEEL (EXISTING TECH)	CARBON (STATE OF THE ART)	SLINGSHOT (PATENTED)
Maximum speed (rpm)	42,500	75,000	145,000
Specific energy (kJ/kg)	6.25	200	1000
Axial thickness (mm)	55	85	75

❹ Flywheel material development

energy density and volumetric energy density at reduced cost.

MAGNETIC COUPLING

In its simplest motor sport incarnation the flywheel in the KERS was directly connected to the transmission via a CVT and step up gears. However, because of the flywheel tip speed it was required to be held in a vacuum to minimize losses. Whilst the rotating vacuum seal then deployed was adequate for a 2.5 h race, longer term usage would require the introduction of vacuum pumps and management systems. These vacuum management sub-systems would increase cost, weight and volume as well as adding to the service burden of the rotating seal.

As part of the hunt for an alternative to vacuum pumps, direct magnetic couplings were investigated. Such direct couplings provided a means of transferring the energy across a barrier. However, the separation required to fit the required vacuum barrier meant the torque density was severely compromised.

The natural next step was to deploy a complex magnetic gear in the role of energy transfer mechanism. Such gears can be seen as a magnetic analogue for an epicyclic gear. The difference is that rather than having rotating planet gears there are static pins between the rotating parts in which magnetic fields rotate, ❺. The pins being made from high permeability steel do not magnetically contribute to the air gap between the rotating magnets. As a result, the air gap between the drive shaft and the flywheel shaft can be set at an optimum for torque capacity. Consequently, a 60 kW unit can be fabricated for approximately 45 US$ of magnetic material. Serendipity also means that we have the ability to implement a ratio at the same time, enabling the final, high speed, mechanical epicyclic and its associated cost, volume and losses to be deleted.

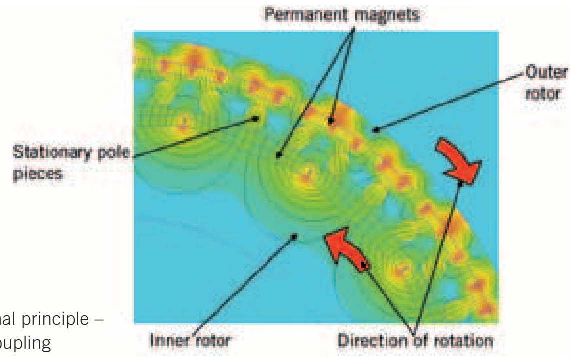

❺ Functional principle – magnetic coupling

CONTINUOUSLY VARIABLE TRANSMISSION

During operation the flywheel is accelerated using torque from the transmission either: as part of a deliberate charging cycle where the KES acts as a load on the engine to increase tailored to push the total load on the engine to a more efficient point on the engine map, or during braking in support; or in support of the foundation brakes. Similarly, when releasing energy the flywheel decelerates. This is done to deliver energy into the driveline to reduce load on the engine. Alternatively, it could also be used to supply energy to auxiliary systems in the vehicle.

A method of controlling the flow of torque either from the flywheel or to the flywheel is thus required. This is done through a CVT. The choice of CVT is dependent on the energy base being stored. For example, as shown in ❻ a mechanical CVT could be deployed if the

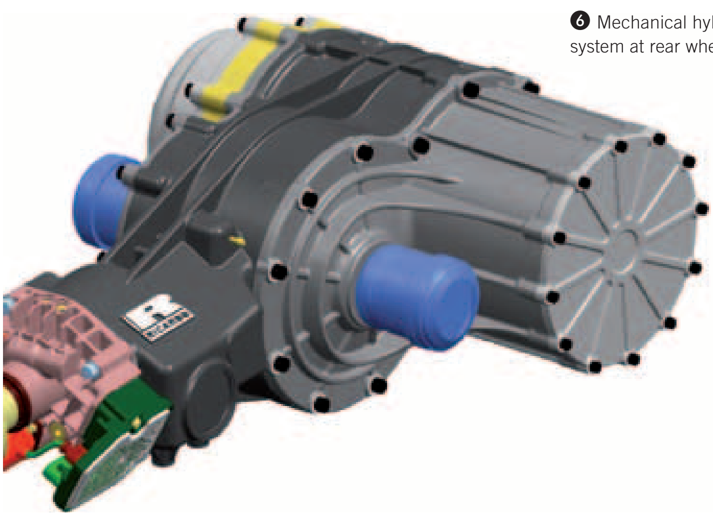

❻ Mechanical hybrid system at rear wheel drive connection were directly to the transmission. However, electrical, hydraulic, pneumatic, or hybrid thereof options are available. This technology is well known and so we will not review it any further depth in this paper other than to comment that system flexibility is increased with a hybrid CVT where a high efficiency mechanical path has an electrical take off in parallel to allow auxiliary systems to be powered whilst the primary engine is off (e.g. for a start-stop function).

APPLICATIONS

The Ricardo system can be utilized in a great number of applications enabling significant savings of fuel, reduction of CO_2 and other emissions and operational advantages. Depending on the particular requirements and conditions a system definition will need to be defined. In summary, the addition of a flywheel based system to the driveline will enable boost assist, regeneration, and potentially, engine off mobility.

The Ricardo system consists of a high speed flywheel, a magnetic coupling, an off-the-shelf continuously variable transmission, and a clutch. As such it would provide a robust, cost effective energy hub that could reduce fuel consumption by up to 25 % whilst increasing energy flexibility on board the vehicle in a small, light package. For example in ⑥, the hybrid drive system has an output of 60 kW and stores 1.4 MJ of energy. This reduces the fuel consumption in the NEDC (New European Driving Cycle) by 16 % and in urban traffic by 26 %, and the vehicle accelerates 2 s faster from 70 to 130 km/h. The system incurs costs of US$ 1,600.

CONCLUSION

Core powertrain efficiency improvement is currently the most effective way of improving fleet CO_2 emission but is limited in its maximum impact. In contrast electric hybridisation has greater impact on CO_2 emissions but at a higher cost. Kinetic hybridisation offers electrical hybrid CO_2 impact at core powertrain cost increment. Such flywheel system topologies are developed, a demonstrator programme is under work.

COATING FOR CYLINDER SURFACES IN ALUMINIUM ENGINE BLOCKS

With Alu-Thin-Fer, Honsel has developed a new coating method for cylinder surfaces such that it is ready for series production. The thin steel coating provides good thermo-mechanical properties, is wear-resistant and low-friction and thus creates good conditions for future low-consumption gasoline and diesel engines.

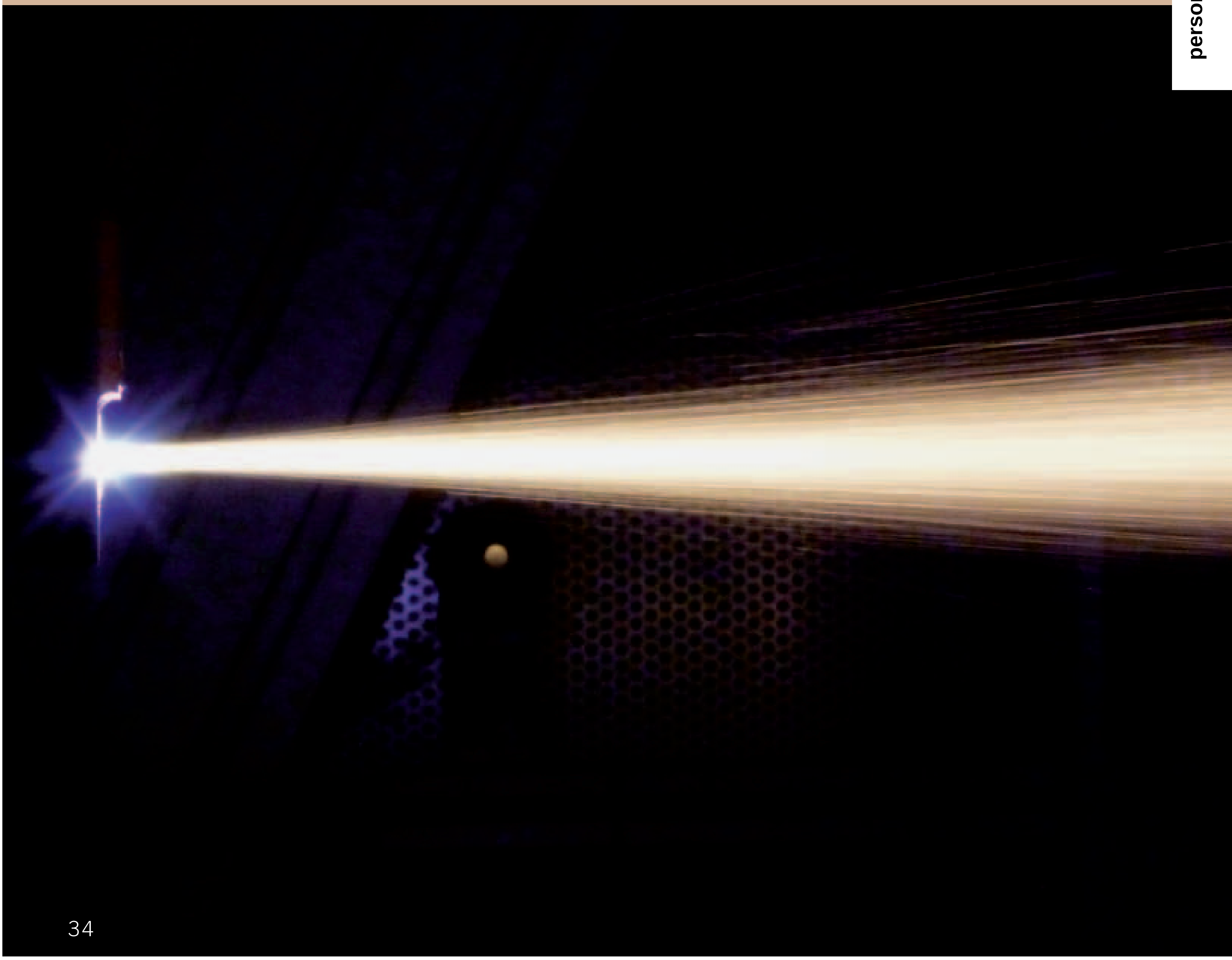

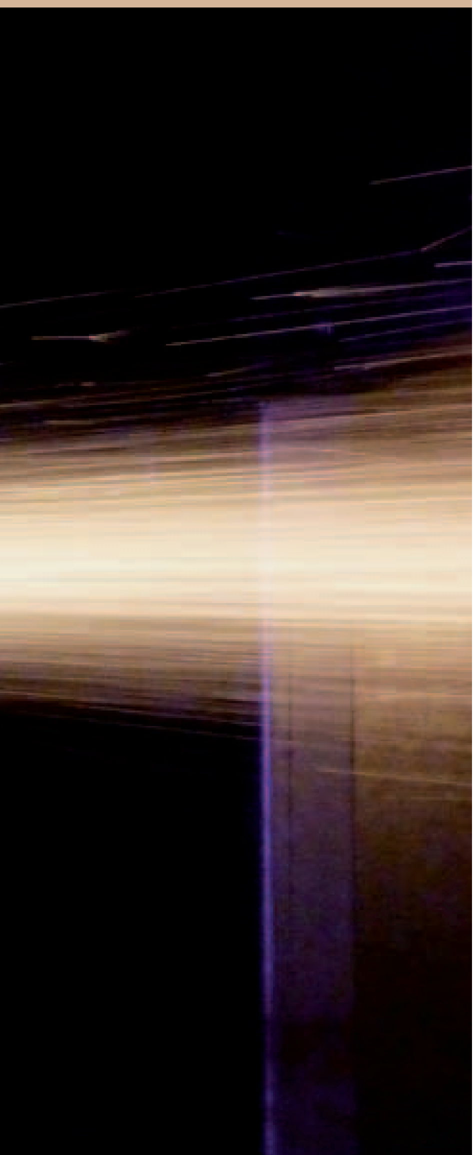

AUTHOR

DR.-ING. BERNHARD GAND
is Director of Engine Development at Honsel AG in Meschede (Germany).

ENGINE BLOCK

Because of the demands on modern gasoline and diesel engines, their engine blocks are being subjected to ever higher loads. Those loads are the result of an improvement of internal efficiency levels and thus of growing peak cylinder pressures, increased thermo-mechanical loading due to higher torque and power densities, through the obligation for light weight design and application of fuels of varying levels of aggressiveness.

In addition, the integration of secondary functions that need to be performed by the cast component for cost reasons are resulting in an increasingly complex architecture. Key secondary functions are integration of valve train drive housings, of clutch and flywheel, as well as media feeds (oil, water, blow-by, ventilation) etc. Reductions in the number of cylinders and/or engine displacement (downsizing) are leading directly to the obligation for a modular system of engine variants.

If one compares the diverse options for realising the engine block, ❶, and assesses them with a view to today's requirements, one arrives at the conclusion that the profile is best met by an aluminium engine block. The casting processes (low-pressure sand casting, low-pressure permanent mould casting, die casting etc.) have become so advanced that the dynamic strengths demanded can be achieved by reducing casting faults, improving the microstructure and by targeted application of heat treatment.

As the mechanical efficiency of a combustion engine is strongly influenced by the tribolocical situation between piston/piston ring and cylinder surface, the properties of the cylinder surface become particular significant.

CYLINDER SURFACES

The peripheral conditions at the cylinder surface thus play an important role. Cylinder surfaces with exposed silicon are used in many gasoline engines. These are either monolithic aluminium engine blocks or heterogeneous ones with aluminium-silicon cast-in liners. In application on modern gasoline direct injection engines in the tribology area and wear resistance, however, clear limits of this technology are becoming apparent. For that reason, the demands amongst engine developers for a robust, wear-resistant cyl-

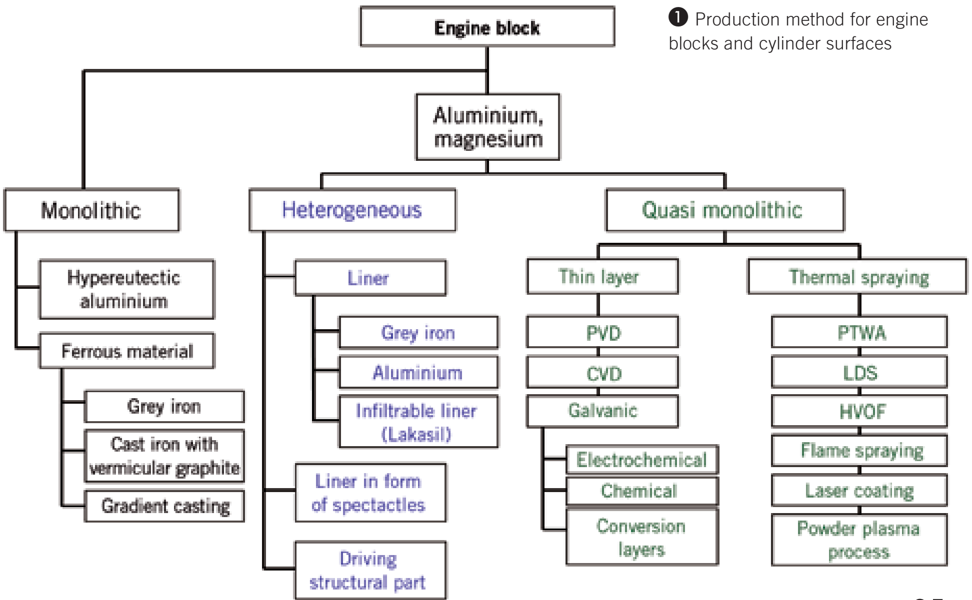

❶ Production method for engine blocks and cylinder surfaces inder surface with high levels of fuel compatibility are becoming ever stronger.

The verdict on cast-in grey iron liners in heterogeneous aluminium engine blocks, on the other hand, turns out to be very much milder. In large series production, the grey iron liner represents a cost-effective solution and, together with a modern honing method that produces a low-friction surface topology, creates favourable conditions in aluminium engine blocks for friction and wear when compared with cylinder surfaces of exposed silicon (monolithic or heterogeneous with AlSi liner).

The crux with cast-in grey iron liners is found in the mechanics of the aluminium surround casting. The shrinkage of the aluminium on cooling generates stresses in the surround casting and within the liner, which remain latent even after machining. In the worst case, delaminating of grey iron liner and aluminium surround casting or, for example, cracks in the aluminium or in the grey iron liner can occur – depending on the dimensioning of the parts. In any event, this basic deformation together with the additional deformations caused by the static and dynamic forces of the cylinder head/engine block assembly, as well as the force closure to the engine bearing, are highly undesirable. This can result in disadvantageous relations in terms of oil consumption, blow-by volumes, friction and wear and higher requirements for servicing intervals.

High residual stresses in the engine block structure also means lower potential for dynamic loading – another point in finding a better combination of monolithic aluminium structure and “intelligent” cylinder surface.

COATING METHOD FOR CYLINDER SURFACES

An investigation at Honsel of the existing thin layer method for suitability as an internal cylinder coating showed that application of the PVD (physical vapour deposition) and CVD (chemical vapour deposition) methods produced high substrate temperatures and can be ruled out because of excessive production costs.

Galvanic methods are interesting given the variant diversity and the low substrate temperatures, but are not favoured in terms of the costs, the cycle time and their environmental compatibility.

The thermal spraying methods for internal cylinder coatings are meanwhile so advanced that one can use certain methods in series production, particularly those that produce robust steel layers with certain properties. The Honsel Alu-Thin-Fer process has been developed based on the PTWA technology (Plasma Transferred Wire Arc). It was examined together with other manufacturing methods and subjected to a ranking, ❷.

Despite the fact that the microstructures of the layers are clearly different, it appears that both the Twin-Wire-Arc (DAG-LDS (Daimler)) and the Alu-Thin-Fer/PTWA method are of equal in the evaluation of quality in many areas. There are differences above all in development time, depth of experience and investment costs. With the PTWA method, the development time until series introduction lasted much longer than with DAG-LDS, and the depth of experience with DAG-LDS is significantly greater because of its longer application time in series production. In terms of the criterion of “coating process and environment” the high burner durability with DAG-LDS deserves a mention, and with Alu-Thin-Fer/PTWA the high spraying efficiency and the favourable conditions for extraction and filtering of the overspray.

As the Alu-Thin-Fer/ PTWA method can be controlled within wide limits via the current intensity, the plasma gases argon or helium, as well as hydrogen, and via the atomizer gas air or pure nitrogen, this results in very much more flexibility in the design of the microstructure of the layers versus the other thermal spraying methods.

As the GM – HVOF method (High Velocity Oxygen Fuel) is still in the pre-development phase and there is no series application, the depth of experience is relatively low. Characteristic in this process is that very high energy density is provided, which generates very high temperatures in the substrate. For that reason, water cooling is needed during the spraying. The high oxide content and the high hardness in the layer place certain demands on the piston ring technology.

The VW-Sulzer-Metco method has been in series production for a long time now – especially also in highly loaded diesel and gasoline engines. This method is strongly characterised by the roughening process

		GM – HVOF	DAG – LDS	VW – SULZER-METCO	ALUTHINFER®/PTWA
KNOW HOW CRITERIA	Time of development	--	+	++	++
	Depth of experience	--	++	++	+
PROCESS	Pre-treatment of cylinder surface	--	++	0	++
	Coating process and environment	--	++	+	+
	Cylce time	++	++	+	++
LAYER PROPERTIES	Adhesive pull strength	0	++	0	++
	Wear behaviour	+	++	++	++
	Tribology	++	++	++	++
COSTS	Investment	--	0	+	++
	Production cost	-	+	0	++

❷ Comparison of various thermam spraying methods

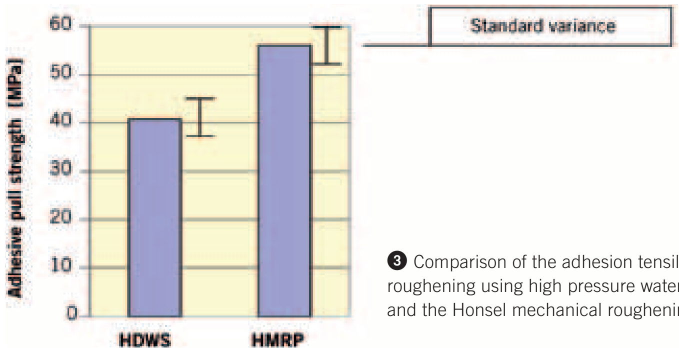

❸ Comparison of the adhesion tensile strenght on roughening using high pressure water jetting (HPWJ) and the Honsel mechanical roughening process (HMRP)

(blasting process) and the use of powder as coating medium. The roughening process serves to activate the aluminium cylinder surface. This pre-treatment is intended to ensure sufficient adhesion of coating layers and substrate, which is generally measured as adhesive tensile strength (cohesion of the layers and adhesion to the substrate). The roughening process used here produces adhesive tensile powers of a certain level and of a certain statistical distribution, which suffices. The use of powder lends the layer certain properties – among others a high pores share – and very much determines the costs of the method (powder manufacturing and powder feeding).

ALU-THIN-FER SPRAYING METHOD FOR CYLINDER SURFACES

Use of thermal spraying methods demands provision and availability of production processes ready for series production and assurance of certain qualities, and that quite regardless of the spraying method used. The development at Honsel comprises a complete package of casting, machining of the cylinder surface and the thermal spraying. This technology is called Alu-Thin-Fer at Honsel and consists of three individual methods that are highly geared to one another: the casting process, the preparation of the cylinder surface and the spraying process.

CASTING PROCESS

A prerequisite for thermal spraying of the cylinder surface is low-pore casting. Honsel has driven the developments in the processes LPSC (low-pressure sand casting), LPPMC (low-pressure permanent mould casting) and DC (die casting) so far forward that the specifications demanded in Europe, North America and Japan are met with all methods.

PRE-TREATMENT OF THE CYLINDER SURFACE

The cylinder surfaces must be pre-machined precisely to the position of the crankshaft axle and to the crankshaft bearing with high demands on cylindricity. This machining process must be coordinated with engine manufacturing, which does the final machining, such that the tolerances demanded can always be adhered to in the final machining. That can be ensured, for example, by means of indexation. In preparation for the coating process, the cylinder surface needs to be roughened to achieve a mechanical damping via macro- and micro-structuring of the substrate. In the development of this process, the fact that it had to be a fast method with high reliability and reproducibility was in the foreground. Under those boundary conditions, a machining process on a CNC machine and an associated tool was developed together with a well-known and worldwide operating tool manufacturer (Gühring). The process, which bears the name of HMRP (Honsel Mechanical Roughening Process), was introduced in series production at Honsel's Meschede plant in 2009. Depending on the bore diameter and length, a cylinder bore is roughened between 7 and 10 s. HMRP displays extremely high adhesion tensile strengths with only minor standard deviation, ❸. The adhesion tensile strengths through HPWJ (high-pressure water jetting) served as a reference for the development of HMRP. Whilst HPWJ guarantees a sufficiently high and stable adhesion to the substrate, however the method requires significant investments. Together with the substantial operating costs (water treatment, disposal of the aluminium sludge, H_2 formation etc.), among other things also by means of long cycle times and serious wear, this results in significantly higher total costs with HPWJ when compared with HMRP.

COATING PROCESS THROUGH MELTING OFF A SINGLE STEEL WIRE

The PTWA coating method was at the time developed and patented by the pioneers of Flame Spray Industries NY and was examined and further developed by many departments of Ford. Honsel has modified and further developed the method such that it could be introduced in series production in 2009. It creates a wafer-thin steel coating that provides the cylinder surface the robustness, wear resistance and friction-poverty demanded for future diesel and gasoline engine concepts.

Whilst in application of the classic PTWA method the adhesion of the sprayed steel layer is created by an adhesion agent – a so-called "NiAl Bond Coat", which achieves only relatively low adhesion tensile strength (~20 MPa) and makes the method extremely expensive (disposal of hydrofluoric acid) – with the Honsel variant with HMRP one took a

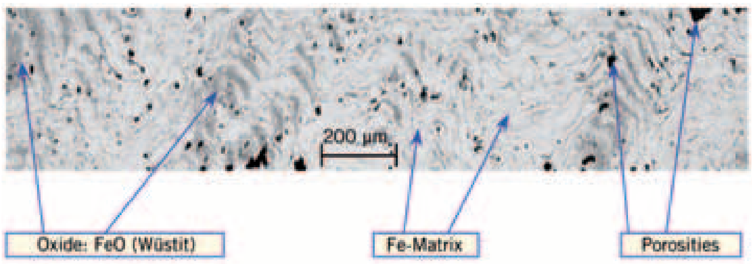

❹ Alu-Thin-Fer micro structure

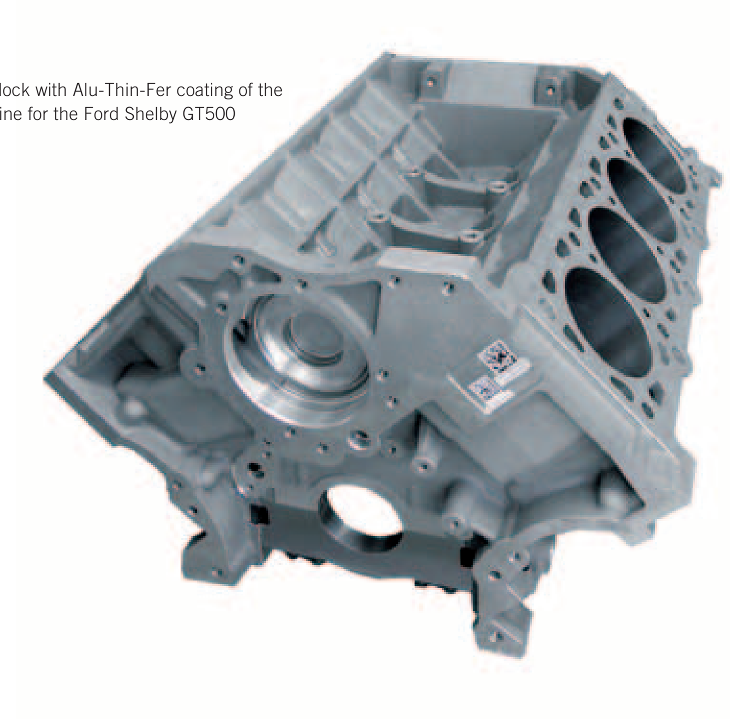

❺ Engine block with Alu-Thin-Fer coating of the 5.4-l V8 engine for the Ford Shelby GT500

new approach via the mechanical roughening and activation processes.

In the coating process, a single steel wire is melted electrically in a rotating burner. The droplets thus created of 20 to 40 µm in size are accelerated using an atomizer gas and thrown with high energy against the cylinder wall, on which they stick and solidify extremely quickly. A plasma gas adds additional thermal energy to the particle stream and facilitates the desired pore formation in the layer. Together with the plasma gas, the atomizer gas controls the shape of the particle beam and also causes oxide to form in the layer, which is wanted and serves as a hard material that minimises wear. Further development of the PTWA process at Honsel relates to the following areas:

- adjust of the coating parameters to the roughening profile used
- increase in burner performance (reduction of cycle time) and adjusting of the coating parameters
- increase of the burner and system durability and improved robustness with a view into mass production application
- development of block deck and crankcase space masking, as well as improved extraction, collection and filtering of the overspray
- realisation of wire barrel spool-out up to 500 kg.

The improvement of the burner and system durability and of the burner performance was carried out in a joint development programme between GTV, Flame Spray Industries and Honsel.

Starting from the "standard" coating parameters, the coating parameters need to be adjusted, developed and set individually for each engine block architecture. The different thermal conduction paths – open-deck and closed deck designs etc. – influence the development of the microstructure of the layers. ❹ shows a very densely sprayed layer with few, small and finely distributed pores. The higher the surface proportion of the pores, the smoother the honing should be. The exposed pores on the honed cylinder surface provide the oil reservoirs for lubricating the piston and piston rings in engine operation. The honing itself now serves more to represent the geometry and precision of the cylinder and less to realise the classic honing relief. The targeted distribution of the pores in the final cylinder surface represents a favourable boundary condition with regards to oil consumption and blow-by quantity.

SUCCESSFUL SERIES INTRODUCTION

The first series application of Alu-Thin-Fer is the V8 5.4-l engine for the Ford Shelby GT500. Honsel is producing the engine block in low-pressure sand casting, completely mechanically machined, coated and honed, ❺. Extensive quality control takes place thereby, ❻, [1]. The engine block is delivered directly to the Ford Romeo Engine Plant in Michigan USA for assembly of the engine ("two man – one engine").

The development of the engine, and thus also the validation of the thermal spraying system, took place at Ford SVT (Special Vehicle Team) in Allen Park, Michigan, USA. The engine has successfully passed the very different system, component and vehicle test series. In all tests – including endurance, piston scutting, hot and knock sensitivity tests, the cylinder and piston ring wear was hardly measurable (~ 1 µm).

The hardness of the cylinder surfaces, combined with sufficient oil being available thanks to the pores in the coating, produces significantly improved friction and wear patterns when compared to the

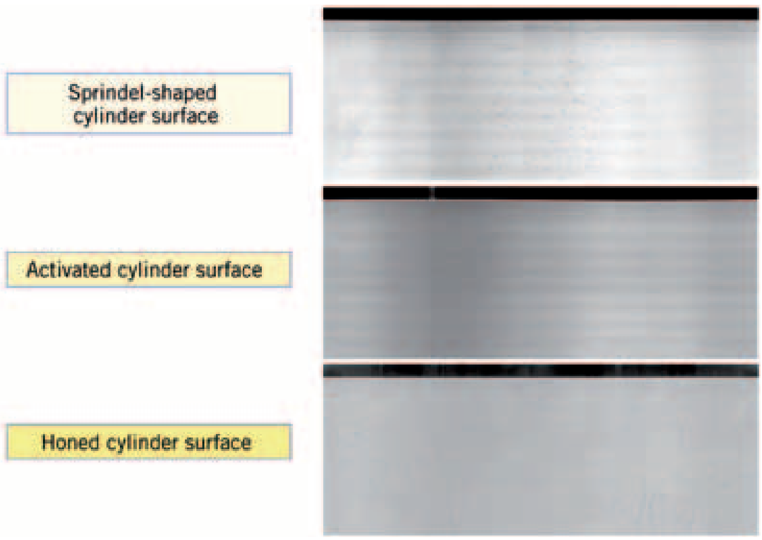

❻ Visual check of the cylinder surface and the coating in quality assurance predecessor engine. The latent cylinder deformations turned out to be much lower, because there are no cylinder liners cast-in or shrunk into the engine block.

That results in lower oil consumption and blow-by in engine operation, so the servicing intervals can be lengthened. Substitution of the pressed-in cylinder liners by in-cylinder thermal spraying creates a weight saving of 4.4 kg.

SUMMARY AND OUTLOOK

With Alu-Thin-Fer, Honsel has developed a new thermal spraying method for cylinder surfaces such that it is ready for mass production. The thin steel coating provides good thermo-mechanical properties, is wear-resistant and low-friction and thus creates good conditions for future low-consumption gasoline and diesel engines.

The coating was first used in series production in 2009 in the 5.4-l V8 engine for the Ford Shelby GT500. The success of that series application presupposed that certain manufacturing processes had been advanced to a high level of quality. For example, the casting process had to meet the demands on the cylinder surfaces in terms of size and number of pores after machining. In addition, an economical and robust roughening process had to be available.

The method has found great resonance by many leading auto manufacturers, so Honsel assumes based on the current developments that the Alu-Thin-Fer method will be introduced also in major mass production from the beginning of 2013.

REFERENCES

[1] Gand, B.; Salenbauch, H.: "Alu-Thin-Fer-Zylinderlaufflächen – Verbesserung des Kraftstoffverbrauchs und des Verschleißverhaltens für Motoren mit niedriger und hoher thermo-mechanischer Beanspruchung". 5th VDI Congress on Cylinder Surfaces, Pistons and Connecting Rods – Baden-Baden 2010

[2] Orlamünder F.: Optimization of the Coating Parameters for the Application of Low-Alloy C-Steel with the Plasma Transferred Wire Arc Thermal Spraying Process. Master Thesis, RWTH Aachen University, 2007

[3] Blume, W.; Verpoort, C.; Bobzin, K.; Ernst, F.; Richardt, K.; Schlaefer, T.; Schwenk, A.; Cook, D.; Flores, G.: Thermal Spraying of Nano-Crystalline Coatings for Al-Cylinder Bores. SAE 08M-271, 2008

[4] Cook, D.; Zaluzec, M.; Kowalsky, K.: Development of Thermal Spray for Automotive Cylinder Bores; Thermal Spray 2003, Advancing the Science & Applying the Technology. Dg.) C. Moreau and B. Marple, published by ASM International, Materials Park, Ohio, USA, 2003

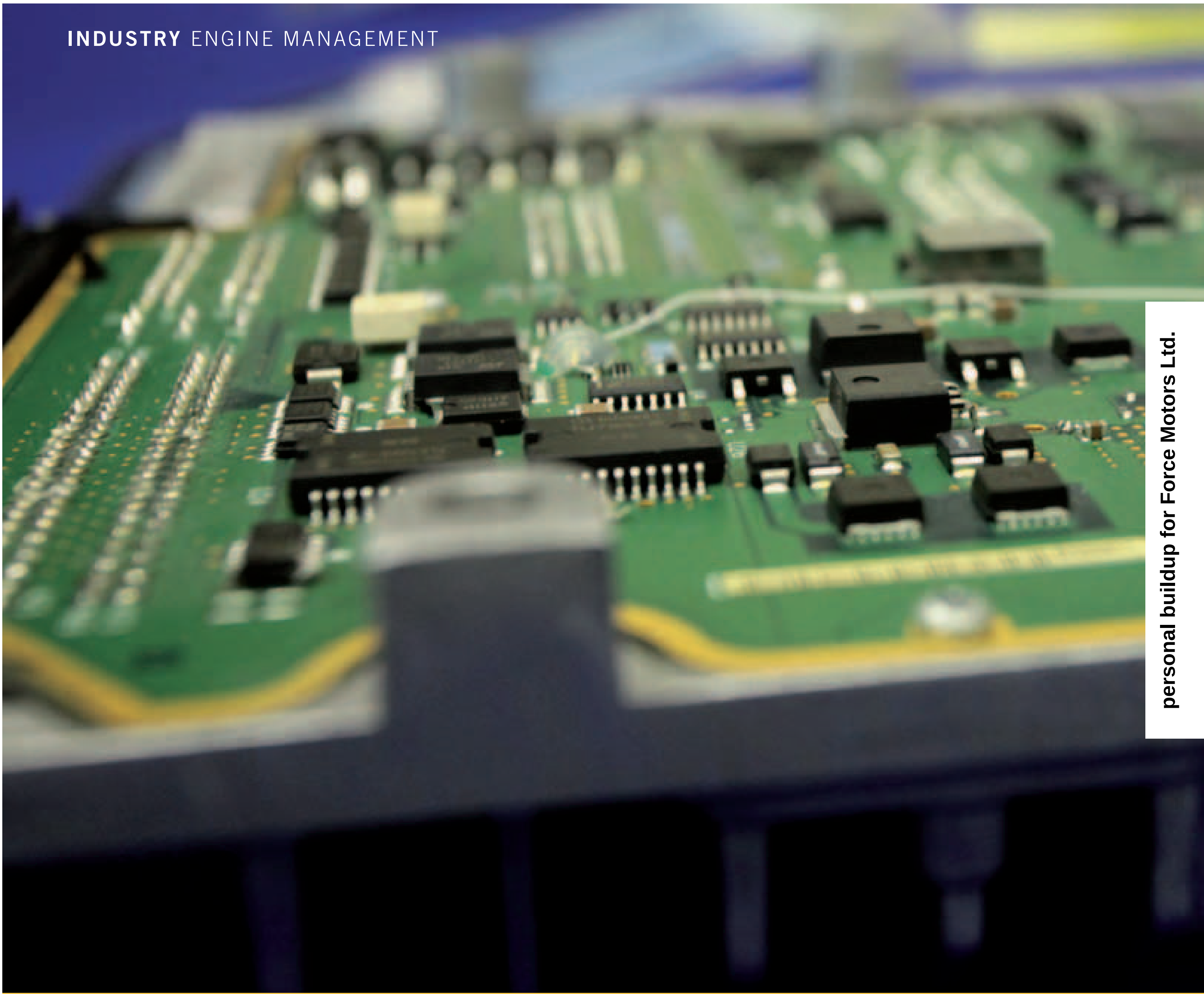

THE NEW GENERAL MOTORS DIESEL ENGINE MANAGEMENT SYSTEM

For more than ten years, General Motors has been developing ECUs for spark-ignition engines in-house. The company has now also developed an engine management system for diesel engines that offers such features as closed-loop injector control and integrated glow plug electronics.

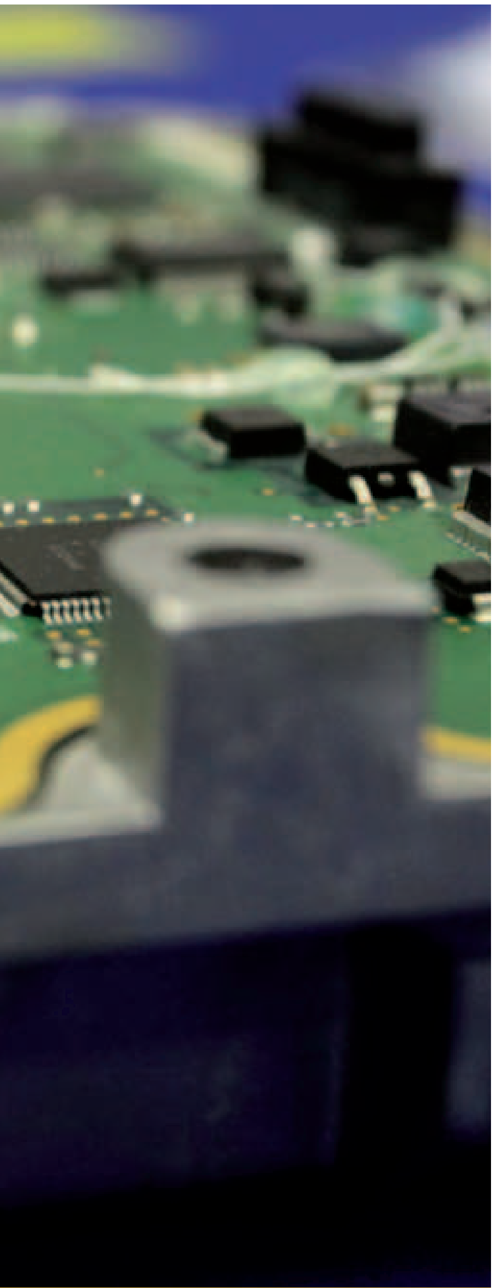

AUTHORS

DR. ING. RICCARDO GRAGLIA
is Global Diesel Controls Assistant Chief Engineer at General Motors Powertrain Europe S.r.L. in Torino (Italy).

PHD ALESSANDRO CATANESE
is Advanced Controls Regional Innovation Manager at General Motors Powertrain Europe S.r.L. in Torino (Italy).

DR. ING. FILIPPO PARISI
is Diesel Electronic Engineering and Software Integration Controls Engineering Group Manager at General Motors Powertrain Europe S.r.L. in Torino (Italy).

DR. ING. SIMONE BARBERO
is System Development and Base Calibration Engineering Group Manager at General Motors Powertrain Europe S.r.L. in Torino (Italy).

IN-HOUSE DEVELOPMENT OF POWERTRAIN CONTROL SYSTEM

It was the fall of 1989 when General Motors established an interdivisional project with the purpose to develop a specification for powertrain software. The result of this study was going to be used by powertrain developers, calibration engineers, software engineers and validation engineers as a base pattern for their specifications for specific powertrains, which would serve as technical requirements for the production of software. A specific target, taken in 1989, is still maintained today: to remain as common as possible and, while variations are expected in each specific powertrain system specification, the goal is to minimize the differences [1].

From the definition of a powertrain software specification to date, many other steps have been taken; that was just the first milestone which started the development of an all-new concept in General Motors and unique in the automotive world: the in-house development of the powertrain controls system.

Since the early nineties, GM invested in comprehensive capability in all aspects of controls engineering: the first internally developed software was in production in a gasoline engine in 1999, it was then applied across the engine portfolio and introduced also in transmission controls to create the first in-house generation estimated in 8 million parts sold in 2007. Today the second generation is in production controlling also hybrid systems and the first diesel: D1.

BUSINESS MODEL

Powertrain controls engineering requires rigorous system engineering on a complex, virtual product that can be described by a V-shape process, ❶, as many other software oriented developments. Generally, automotive OEMs depend on suppliers to cover much of this engineering process: system requirements and part of functional requirements are usually developed internally, while supplier goes to the lower levels of the V-shape taking responsibility of the general system development.

The “in house” concept of General Motors is moving the boundary between internal development and supplier activity to a deeper level of the V-shape,

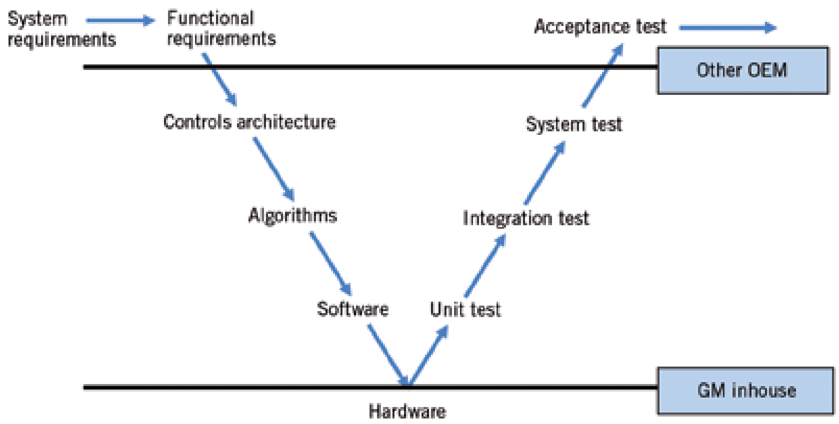

❶ The V-shape process as applied in General Motors

reducing the dependency from supplier to the minimum level. Today General Motors owns all the process steps as shown in ①.

CONTROLS ARCHITECTURE

The definition and optimization of the controls architecture is one of the relevant steps in the GM powertrain controls engineering process. The advantage of defining it internally gives to General Motors the freedom to break the link between the controller and the components, with two direct benefits, ❷: freedom to choose the best in the market part and enable the supplier competition during sourcing. In addition when the EMS (engine management system) architecture definition is done in parallel to the engine design, as a single team between controls and engine experts, the overall powertrain is brought to the highest level of optimization.

CONTROLLER HARDWARE DEFINITION

For a defined control system, the controller hardware is specified in terms of the so called BOM/BOD/BOP approach (bill of material, bill of design, bill of process) with detailed technical requirements selecting the proper electrical interfaces and software interfaces, also called HWIO software, from approved library templates. GM then selects a Tier 1 supplier that can meet the technical requirements, project timing, quality and cost targets.

As part of the "BOM" requirements, GM always selects also main processor, secondary processor and the related software tools development chain.

The split of the responsibilities between GM and the supplier is very simple, ❸: Tier 1 is mainly responsible of the HWIO software and hardware design and its validation according GM "BOD", GM is responsible of the integration with GM application software.

DIESEL ENGINE MANAGEMENT SYSTEM OVERVIEW

The D1 controller is a state of the art management system for Euro 5 engines with a low cost architecture and advanced performances. It's designed for four cylinder diesel common rail engine, including low voltage and high voltage solenoid injector drivers managing up to ten injection pulses per cylinder per engine cycle. For the first time on the market, the system offers four integrated low voltage glow plug drivers with high power dissipation and improved diagnostic capabilities. In this way a relevant reduction of system cost has been achieved by eliminating the need of an external glow plug controller.

Four combustion pressure sensors can be used for an advanced in-cylinder pressure closed loop control that allows emission reduction, CO_2 reduction and better combustion stability under every condition. Other supported features include two integrated DC-Motors drivers (used for throttle valve and EGR valve), one oxygen sensor interface, DPF management and advanced thermal management. Starting from Euro 5, the system is the basis for the new generation controllers, currently under development, which will be facing new challenges as Euro 6 emissions and North America standards.

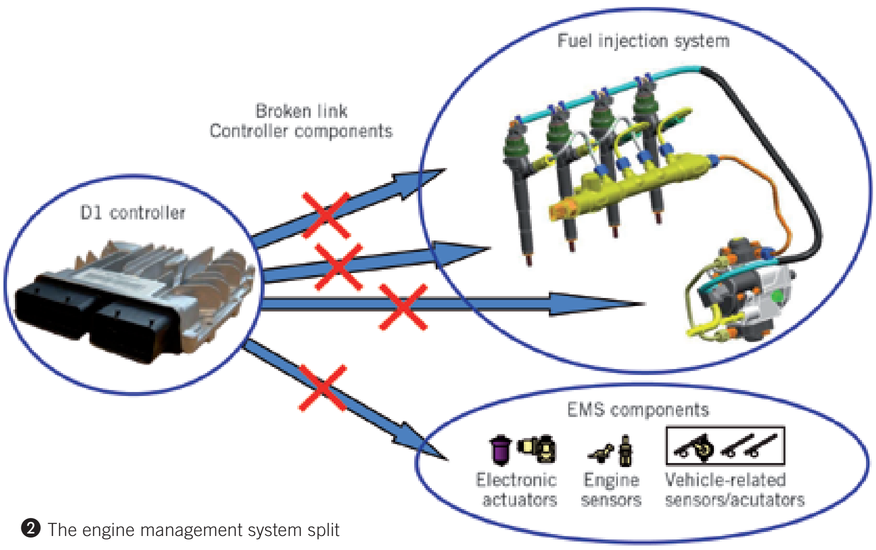

❷ The engine management system split

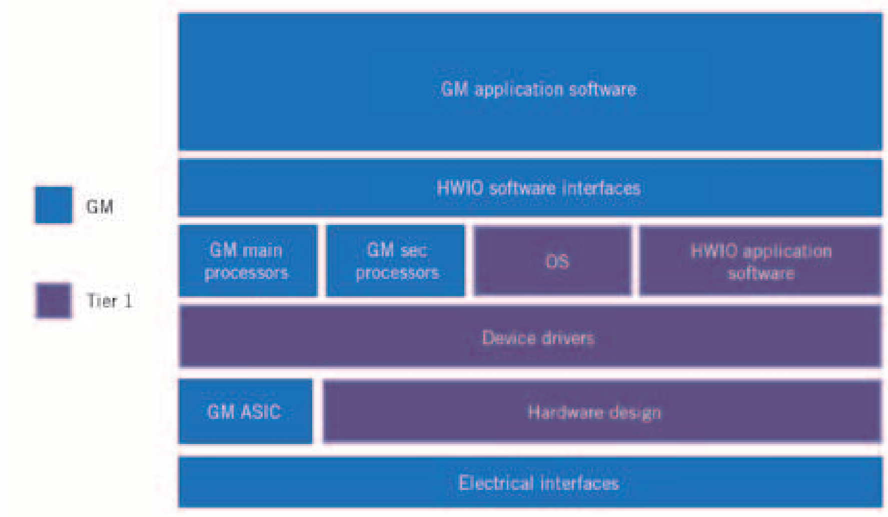

❸ ECM responsibilities partitioning between GM and Tier 1

INTEGRATED GLOW PLUGS DRIVERS

The integration of the glow plug drivers in the ECM (engine control module) design has driven several considerations, technical and economical, to make it feasible: availability of cheaper power devices, availability of a connection system capable to sustain the high current and power losses, system constraints and engineering norms.

The availability of cheaper power Mosfets with very low RDSON (drain to source resistance in on-state) in the market was, and still is a reality. Several sources are available for device with nominal R_{DSON} lower than 2.3 mΩ in a so called D^2PAK package, capable to sustain very high current and to dissipate the power losses if properly integrated in a printed circuit board (PCB) design.

The ECM glow plug driver provides a shared enable power switch with reverse battery protection that supplies an internal system voltage rail. The system voltage rail, properly conditioned and monitored for diagnostic, is then the supply source for the high-side drivers of each glow plug, also called selection Mosfets. A monitoring of the current for each selection Mosfet is provided for control and diagnostic purposes. The shared enable power switch has been introduced as redundant switch-off capability, in case of internal short circuit of a selection Mosfet, to protect the component since the external power supply feed is coming directly from the battery.

The necessity to partition the power transferred to each glow plug using a pulse width modulated technique, in combination with the pure "ohmic" nature of the glow plug, requested some measures to limit the ECM issues. A control of the turn-on and turn-off events has been introduced, making the complete switching event hundred times slower.

The control function has been developed and optimized performing several sub-system simulations. The so called Signal Delivery Sub System Analysis (SDSS) is the GM way to verify the robustness of the control including all subsystem parts: ECM hardware and software algorithms, wiring harness and external components, simulating also the spread of their production characteristics. An example of a simulation result, showing the control system reaction, in terms of glowing temperature variation, to the single components characteristics spread is reported in ❹.

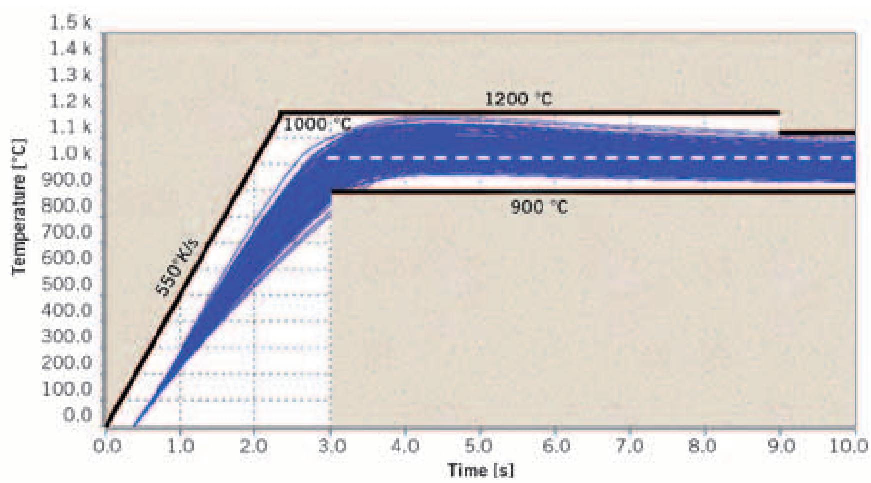

❹ Glowing temperature Monte Carlo simulation

COMBUSTION CONTROL

The D1 EMS from GM is one of the first controllers capable to monitor and control in real time the fuel combustion process, thanks to glow plug integrated cylinder pressure sensors. Combustion control is the key enabler for advanced strategies including highly premixed combustion and low air/fuel ratio combustion. These strategies provide the opportunity to reduce emissions, while maintaining or improving fuel consumption and combustion noise. Another important advantage is the improved long-term precision/stability of the complete injection system: the closed loop control compensates possible (mechanical) wear and tear and different fuel quality ensuring optimum fuel combustion and emission over the engine lifecycle.

In-cylinder pressure is sampled with a resolution of one crankshaft angle degree during the engine compression and expansion phases of each cylinder. This data is filtered, compensated for sensor drift, and processed in real time in order to calculate metrics characterizing the combustion process. In particular, for each injection event, the exact amount of energy released by the combustion and the phasing of the combustion are measured.

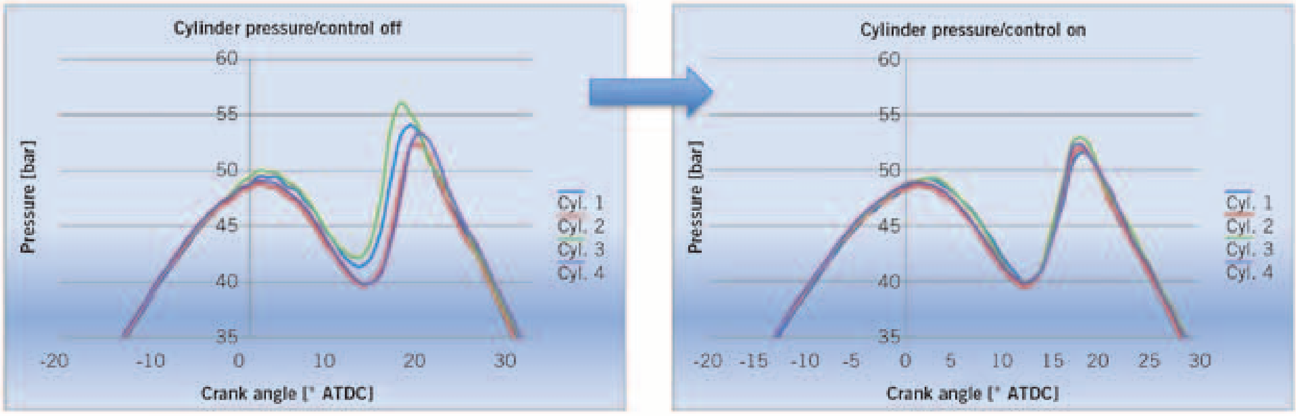

❺ Effect of combustion control on combustion robustness

The exact knowledge of the combustion characteristics allows the execution of a closed loop control acting on the fuel injection pulse. For example the start of injection can be adjusted cycle to cycle, in order to always achieve the requested combustion phasing with benefit to the overall combustion stability and robustness, ❺.

The availability of this technology at General Motors opens a number of control possibilities never explored before: apart from the obvious benefit in terms of robustness over engine production tolerance spread, aging compensation and adaptation to different environmental conditions [2], this control enables to explore engine operating conditions on the edge of combustion stability, gaining significant benefit in terms of emission and fuel consumption.

FUEL INJECTION ASIC DEVELOPMENT

A custom injection controller has been developed with the intent to manage all common rail diesel solenoid injector technologies available in the market. The necessary flexibility is mainly a translation of the various injector current profiles that must be supported in unique and common control architecture.

A generic injector current profile can be divided in different timing phases that can be mainly assumed in two categories: the transition phase and the regulation phase. Both phases are characterized by a set of control, monitoring parameters and an action to apply a selected switched voltage source to the injector. In the transition phase, the current is forced to change with a fast or slow transition. In the regulation phase, the average current is held constant.

The applied voltage sources are switched runtime selecting a value from the following list:

- high voltage: usually a boost voltage higher than the system voltage generated inside the ECM with the support of an electrolytic capacitor
- system voltage: the system voltage referred to ground
- 0 V: typically an approximation of the injector voltage when it is forced to recirculate the internal energy on itself. It's done with a diode or actively with a Mosfet
- negative high voltage: the residual energy inside the injector is recovered in a boost capacitor or dissipated on a clamp device to a negative voltage source.

❻ shows, as an example, three injector current profiles related to different components available today in the diesel market.

Supporting all possible combinations of the described parameters or a subset of them, the injection control provides the best driving flexibility. This is implemented via a finite state machine (FSM) that includes all the possible states and it is capable to evolve among them per timing parameters and comparison between current monitoring and current profile settings. Each state of the FSM has then

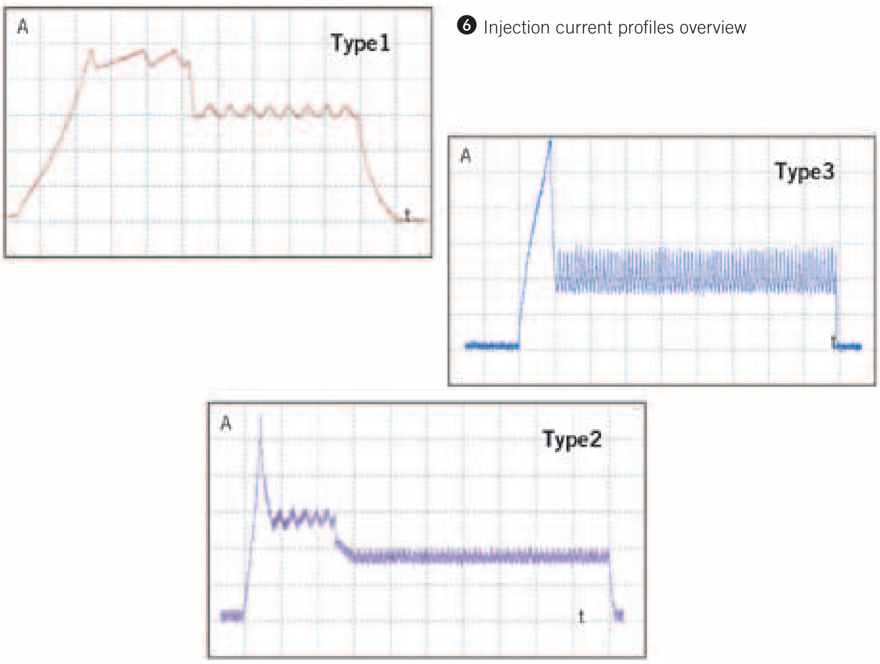

❻ Injection current profiles overview

to drive the power Mosfets of the electrical architecture, applying state-by-state the expected voltage to the injector.

The implementation of the FSM in the silicon technology could be done via a configurable FSM or a micro-coded FSM: this last option was chosen to grant the maximum flexibility of the injection controller.

This custom device also integrates all the pre-drivers of the power Mosfet part of the injection driver electrical architecture. This is the result of the compromise between the overall system cost optimization and the chosen device technology; it allows the designer to get full support from the device to manage all the external power Mosfets and current senses of a typical electrical architecture topology.

CONCLUSION

General Motors for more than a decade has been applying the unique strategy among other OEMs of developing "in house" the powertrain control systems. D1 is the first diesel EMS in production which has been taking this approach. GM becomes the owner of the architecture definition, algorithm and software development, integration and testing, reducing the dependency from suppliers and enabling a "component level competition" with direct benefits to the system cost.

The synergic development of controls system and engine hardware is the biggest advantage of the "in house" strategy which drives the overall system to the highest level of optimization making it unique among competition.

After having successfully launched D1 on Corsa and Meriva 1.7 CDTI, GM is already working to its successors which will become a relevant enabler of the powertrain controls strategy to address the growing demand of energy efficient systems with increased level of performance and stringent emission levels at a lower cost.

REFERENCES

[1] Elshoff, J. L.: Rationale for Powertrain software specification. General Motors research laboratories Warren, MI, 1990

[2] Beasley, M.; Cornwell, R.; Fussey, P.; King, R.; Noble, A.; Salamon, T.; Truscott, A.; Landsmann, G.: Reducing Diesel Emissions Dispersion by coordinated Combustion Feedback Control. SAE Paper 2006-01-0186

PEER REVIEW ATZ | MTZ

PEER REVIEW PROCESS FOR RESEARCH ARTICLES IN ATZ AND MTZ

STEERING COMMITTEE

Prof. Dr.-Ing. Lutz Eckstein	RWTH Aachen University	Institut für Kraftfahrzeuge Aachen
Prof. Dipl.-Des. Wolfgang Kraus	HAW Hamburg	Department Fahrzeugtechnik und Flugzeugbau
Prof. Dr.-Ing. Ferit Küçükay	Technische Universität Braunschweig	Institut für Fahrzeugtechnik
Prof. Dr.-Ing. Stefan Pischinger	RWTH Aachen University	Lehrstuhl für Verbrennungskraftmaschinen
Prof. Dr.-Ing. Hans-Christian Reuss	Universität Stuttgart	Institut für Verbrennungsmotoren und Kraftfahrwesen
Prof. Dr.-Ing. Ulrich Spicher	Universität Karlsruhe	Institut für Kolbenmaschinen
Prof. Dr.-Ing. Hans Zellbeck	Technische Universität Dresden	Lehrstuhl für Verbrennungsmotoren

ADVISORY BOARD

Prof. Dr.-Ing. Klaus Augsburg
Prof. Dr.-Ing. Bernard Bäker
Prof. Dr.-Ing. Michael Bargende
Prof. Dipl.-Ing. Dr. techn. Christian Beidl
Dr.-Ing. Christoph Bollig
Prof. Dr. sc. techn. Konstantinos Boulouchos
Prof. Dr.-Ing. Ralph Bruder
Dr. Gerhard Bruner
Prof. Dr. rer. nat. Heiner Bubb
Prof. Dr. rer. nat. habil. Olaf Deutschmann
Dr. techn. Arno Eichberger
Prof. Dr. techn. Helmut Eichlseder
Dr.-Ing. Gerald Eifler
Prof. Dr.-Ing. Wolfgang Eifler
Prof. Dr. rer. nat. Frank Gauterin
Prof. Dr. techn. Bernhard Geringer
Prof. Dr.-Ing. Uwe Grebe
Prof. Dr.-Ing. Horst Harndorf
Prof. Dr. techn. Wolfgang Hirschberg
Univ.-Doz. Dr. techn. Peter Hofmann
Prof. Dr.-Ing. Bernd-Robert Höhn
Prof. Dr. rer. nat. Peter Holstein
Dr. techn. Heidelinde Holzer
Prof. Dr.-Ing. habil. Werner Hufenbach
Prof. Dr.- Ing. Roland Kasper
Prof. Dr.-Ing. Tran Quoc Khanh
Dr. Philip Köhn
Prof. Dr.-Ing. Ulrich Konigorski
Dr. Oliver Kröcher
Dr. Christian Krüger
Univ.-Ass. Dr. techn. Thomas Lauer
Prof. Dr. rer. nat. Uli Lemmer
Dr. Malte Lewerenz
Prof. Dr.-Ing. Markus Lienkamp
Prof. Dr. rer. nat. habil. Ulrich Maas
Prof. Dr.-Ing. Martin Meywerk
Prof. Dr.-Ing. Klaus D. Müller-Glaser
Dr. techn. Reinhard Mundl
Prof. Dr. rer. nat. Cornelius Neumann
Dr.-Ing. Lothar Patberg
Prof. Dr.-Ing. Peter Pelz
Prof. Dr. techn. Ernst Pucher
Dr. Jochen Rauh
Prof. Dr.-Ing. Konrad Reif
Prof. Dr.-Ing. Stephan Rinderknecht
Dr.-Ing. Swen Schaub
Prof. Dr. sc. nat. Christoph Schierz
Prof. Dr. rer.-nat. Christof Schulz
Prof. Dr. rer. nat. Andy Schürr
Prof. Dr.-Ing. Ulrich Seiffert
Prof. Dr.-Ing. Hermann J. Stadtfeld
Prof. Dr. techn. Hermann Steffan
Prof. Dr.-Ing. Wolfgang Steiger
Prof. Dr.-Ing. Peter Steinberg
Prof. Dr.-Ing. Christoph Stiller
Dr.-Ing. Peter Stommel
Prof. Dr.-Ing. Wolfgang Thiemann
Prof. Dr.-Ing. Helmut Tschöke
Dr.-Ing. Pim van der Jagt
Prof. Dr.-Ing. Georg Wachtmeister
Prof. Dr.-Ing. Jochen Wiedemann
Prof. Dr. techn. Andreas Wimmer
Prof Dr. rer. nat. Hermann Winner
Prof. Dr. med. habil. Hartmut Witte

Scientific articles of universities in ATZ Automobiltechnische Zeitschrift and MTZ Motortechnische Zeitschrift are subject to a proofing method, the so-called peer review process. Articles accepted by the editors are reviewed by experts from research and industry before publication. For the reader, the peer review process further enhances the quality of the magazines' content on a national and international level. For authors in the institutes, it provides a scientifically recognised publication platform.

In the ATZ | MTZ Peer Review Process, once the editors has received an article, it is reviewed by two experts from the Advisory Board. If these experts do not reach a unanimous agreement, a member of the Steering Committee acts as an arbitrator. Following the experts' recommended corrections and subsequent editing by the author, the article is accepted.

In 2008, the peer review process utilized by ATZ and MTZ was presented by the WKM (Wissenschaftliche Gesellschaft für Kraftfahrzeug- und Motorentechnik e. V. / German Professional Association for Automotive and Motor Engineering) to the DFG (Deutsche Forschungsgemeinschaft / German Research Foundation) for official recognition.

IMPRINT

MTZ WORLDWIDE

www.MTZonline.com

Founded 1939 by Prof. Dr.-Ing. E. h. Heinrich Buschmann and Dr.-Ing. E. h. Prosper L'Orange

Organ of the Fachverband Motoren und Systeme im VDMA, Verband Deutscher Maschinen- und Anlagenbau e.V., Frankfurt/Main, for the areas combustion engines and gas turbines
Organ of the Forschungsvereinigung Verbrennungskraftmaschinen e.V. (FVV)
Organ of the Wissenschaftliche Gesellschaft für Kraftfahrzeug- und Motorentechnik e.V. (WKM)
Organ of the Österreichischer Verein für Kraftfahrzeugtechnik (ÖVK)
Cooperation with the STG, Schiffbautechnische Gesellschaft e.V., Hamburg, in the area of ship drives by combustion engine

02 I 2011 _ February 2011 _ Volume 72
Springer Automotive Media I Springer Fachmedien Wiesbaden GmbH
P. O. Box 15 46 · 65173 Wiesbaden · Germany I Abraham-Lincoln-Straße 46 · 65189 Wiesbaden · Germany
Amtsgericht Wiesbaden, HRB 9754, USt-IdNr. DE811148419

Managing Directors Dr. Ralf Birkelbach (Chairman), Armin Gross, Albrecht Schirmacher I **Senior Advertising** Armin Gross I **Senior Marketing** Rolf-Günther Hobbeling
Senior Production Christian Staral I **Sales Director** Gabriel Göttlinger

EDITOR-IN-CHARGE
Wolfgang Siebenpfeiffer

EDITORIAL STAFF

EDITOR-IN-CHIEF
Johannes Winterhagen (win)
phone +49 611 7878-342 · fax +49 611 7878-462
johannes.winterhagen@springer.com

VICE-EDITOR-IN-CHIEF
Ruben Danisch (rd)
phone +49 611 7878-393 · fax +49 611 7878-462
ruben.danisch@springer.com

CHIEF-ON-DUTY
Kirsten Beckmann M. A. (kb)
phone +49 611 7878-343 · fax +49 611 7878-462
kirsten.beckmann@springer.com

SECTIONS
Electrics, Electronics
Markus Schöttle (scho)
phone +49 611 7878-257 · fax +49 611 7878-462
markus.schoettle@springer.com
Engine
Ruben Danisch (rd)
phone +49 611 7878-393 · fax +49 611 7878-462
ruben.danisch@springer.com
Online
Katrin Pudenz M. A. (pu)
phone +49 6172 301-288 · fax +49 6172 301-299
redaktion@kpz-publishing.com
Production, Materials
Stefan Schlott (hlo)
phone +49 8191 70845 · fax +49 8191 66002
Redaktion_Schlott@gmx.net
Research
Dipl.-Ing. (FH) Moritz-York von Hohenthal (mvh)
phone +49 611 7878-278 · fax +49 611 7878-462
moritz.von.hohenthal@springer.com
Service, Event Calendar
Martina Schraad (mas)
phone +49 611 7878-276 · fax +49 611 7878-462
martina.schraad@springer.com
Transmission
Dipl.-Ing. Michael Reichenbach (rei)
phone +49 611 7878-341 · fax +49 611 7878-462
michael.reichenbach@springer.com

PERMANENT CONTRIBUTORS
Richard Backhaus (rb),
Dipl.-Reg.-Wiss. Caroline Behle (beh),
Prof. Dr.-Ing. Stefan Breuer (sb),
Jürgen Grandel (gl), Ulrich Knorra (kno),
Prof. Dr.-Ing. Fred Schäfer (fs),
Roland Schedel (rs)

ENGLISH LANGUAGE CONSULTANT
Paul Willin (pw)

ADDRESS
P. O. Box 15 46, 65173 Wiesbaden, Germany
redaktion@ATZonline.de

MARKETING I OFFPRINTS

PRODUCT MANAGEMENT AUTOMOTIVE MEDIA
Sabrina Brokopp
phone +49 611 7878-192 · fax +49 611 7878-407
sabrina.brokopp@springer.com

OFFPRINTS
Martin Leopold
phone +49 2642 9075-96 · fax +49 2642 9075-97
leopold@medien-kontor.de

ADVERTISING

HEAD OF SALES MANAGEMENT
Britta Dolch
phone +49 611 7878-323 · fax +49 611 7878-140
britta.dolch@best-ad-media.de

KEY ACCOUNT MANAGEMENT
Elisabeth Maßfeller
phone +49 611 7878-399 · fax +49 611 7878-140
elisabeth.massfeller@best-ad-media.de

SALES MANAGEMENT
Sabine Röck
phone +49 611 7878-269 · fax +49 611 7878-140
sabine.roeck@best-ad-media.de

MEDIA SALES
Frank Nagel
phone +49 611 7878-395 · fax +49 611 7878-140
frank.nagel@best-ad-media.de

DISPLAY AD MANAGER
Petra Steffen-Munsberg
tel +49 611 7878-164 · fax +49 611 7878-443
petra.steffen-munsberg@best-ad-media.de

AD PRICES
Price List No. 54 (10/2010)

PRODUCTION I LAYOUT
Heiko Köllner
phone +49 611 7878-177 · fax +49 611 7878-464
heiko.koellner@springer.com

SUBSCRIPTIONS
VVA-Zeitschriftenservice, Abt. D6 F6, MTZworldwide
P. O. Box 77 77, 33310 Gütersloh, Germany
Renate Vies
phone +49 5241 80-1692 · fax +49 5241 80-9620
SpringerAutomotive@abo-service.info

YOUR HOTLINE TO MTZ
Editorial Staff
☎ +49 611 7878-393
Reader's Service
☎ +49 611 7878-151
Advertising
☎ +49 611 7878-395

SUBSCRIPTION CONDITIONS
The eMagazine appears 11 times a year at an annual subscription rate 199 Euro for private persons and 299 Euro for companies. Special rate for students on proof of status in the form of current registration certificate 98 €. Special rate for VDI/ÖVK/VKS members on proof of status in the form of current member certificate 172 €. Special rate for studying VDI members on proof of status in the form of current registration and member certificate 71 €. Annual subscription rate for combination MTZworldwide (eMagazine) and MTZ (print) 398 €. The subscription can be cancelled in written form at any time with effect from the next available issue.

HINTS FOR AUTHORS
All manuscripts should be sent directly to the editors. By submitting photographs and drawings the sender releases the publishers from claims by third parties. Only works not yet published in Germany or abroad can generally be accepted for publication. The manuscripts must not be offered for publication to other journals simultaneously. In accepting the manuscript the publisher acquires the right to produce royalty-free offprints. The journal and all articles and figures are protected by copyright. Any utilisation beyond the strict limits of the copyright law without permission of the publisher is illegal. This applies particularly to duplications, translations, microfilming and storage and processing in electronic systems.

Springer Automotive Media is a brand of Springer Fachmedien. Springer Fachmedien is part of the specialist publishing group Springer Science+Business Media.

MODEL DEVELOPMENT FOR THE CONTACT PRESSURE DEPENDENT HEAT TRANSFER

The knowledge of the thermal contact resistance between two components adjacent to each other is of great relevance in many technical applications and also in the interpretation of thermally and mechanically loaded component connections. The example for this are the interfaces of cylinder head/gasket/engine block, cylinder liner/engine block, cylinder head/exhaust manifold and valve/ seat ring/cylinder head. An article by the RWTH Aachen University.

AUTHORS

DIPL.-ING. VICTOR USTINOV is a Research Associate at the Institute of Heat and Mass Transfer at RWTH Aachen (Germany).

DIPL.-ING. SEBASTIAN G. SCHULZ is a Research Associate at the Institute for Materials Applications in Mechanical Engineering, Department of Materials Science at the RWTH Aachen (Germany).

PROF. DR.-ING. REINHOLD KNEER is Director of the Institute of Heat and Mass Transfer at RWTH Aachen (Germany).

PROF. DR.-ING. ESSAM EL-MAGD is Director of the Institute for Materials Applications in Mechanical Engineering, Department of Materials Science at the RWTH Aachen (Germany).

THE SEAL OF APPROVAL FOR SCIENTIFIC ARTICLES IN MTZ.
MTZ
PEER REVIEW
RECEIVED 2010-06-10
REVIEWED 2010-06-30
ACCEPTED 2010-07-22
REVIEWED BY EXPERTS FROM RESEARCH AND INDUSTRY.

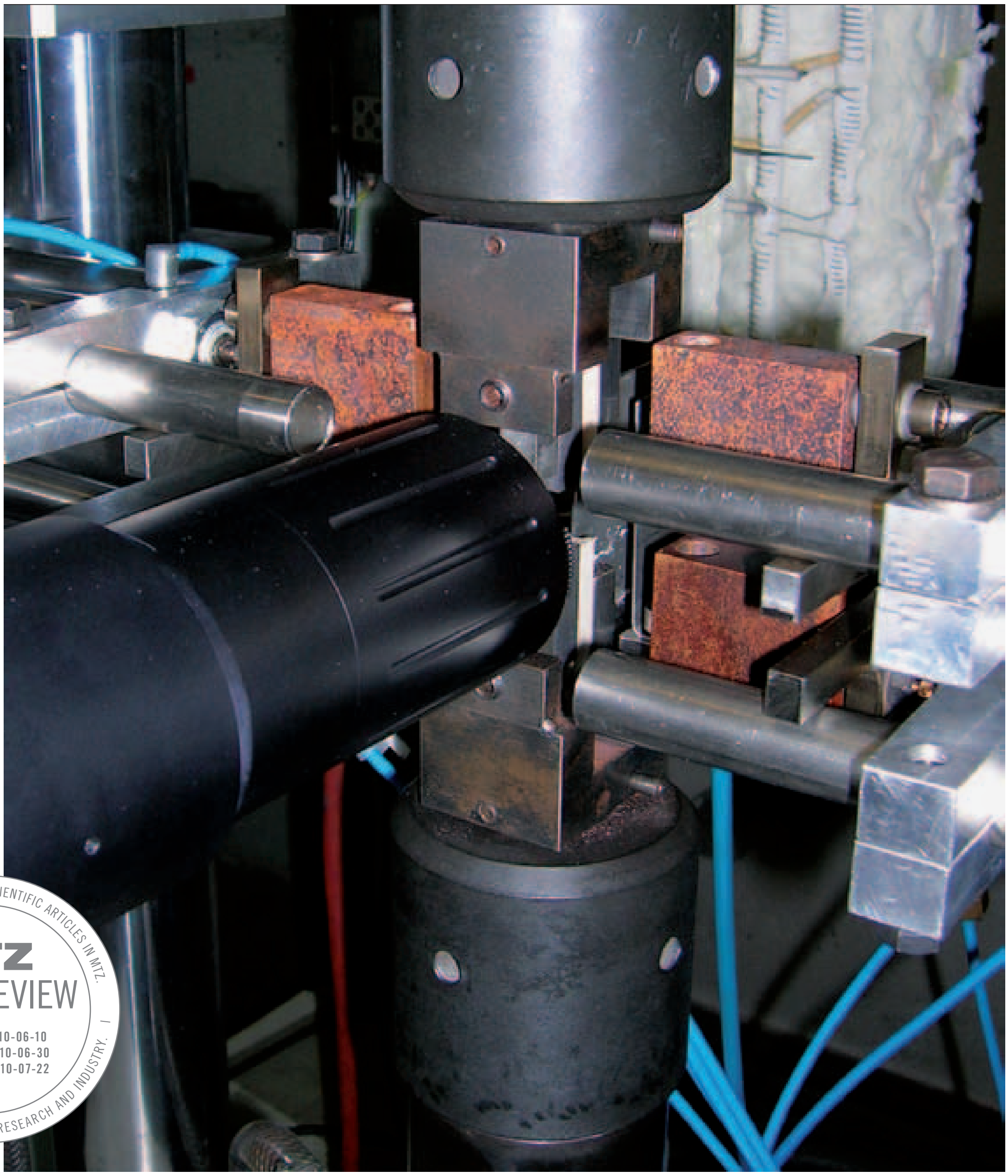

1 INTRODUCTION

The value of heat transfer coefficient for a specific material depends on the temperature, the contact pressure and the surface characteristics of the components which are in contact. Previous models for estimating the heat transfer coefficients are valid only up to low pressures of about 7 MPa [1, 2, 3, 4] and are not applicable at high pressures nearing 250 MPa, which are relevant and important to the design of components in internal combustion engines. In particular, the accuracy of Finite-Element (FEM) calculations for the mechanical and thermal design of composite components is dependent on the quality of input data.

The greatest difficulty in determining the contact resistance is the calculation of the actual contact area (only about 1 to 5 % of the nominal contact area [5]). This is only a fraction of the nominal cross-sectional area at the contact [6]. The heat flow occurs only through the contact spots thereby creating a contact thermal resistance ❶.

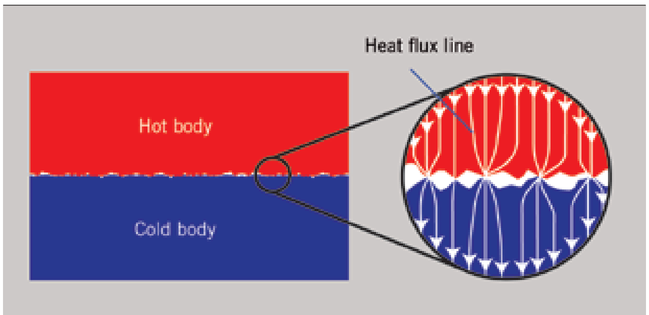

❶ Heat flow through the contact spots

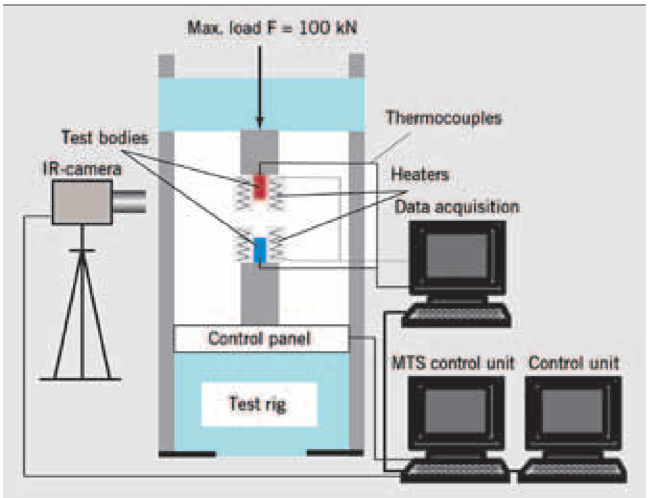

❷ Schema of experimental setup

Under applied pressure the actual contact is increased, thus the material properties, heat transfer conditions in the points of contact and in the cavities between are changing. Furthermore, at high temperature differences, the radiation heat transfer plays an important role in the gas-filled cavities. Additionally, the heat conduction of compressed gas in gaps also changes with pressure.

In the present work, it was attempted to develop a new approach for the calculation of heat transfer coefficient, based on results of experimental and numerical investigations, thermal and mechanical behaviors of materials under contact pressure, while taking into account the elastic and plastic deformations as a function of surface characteristics and the contact pressure.

2 EXPERIMENTAL AND ANALYTICAL INVESTIGATIONS

The investigations on the experimental determination of the contact heat transfer coefficients are limited to the influence of surface topography and the contact pressures in the range of 7 to 217 MPa. The method used for determining the contact heat transfer coefficient was developed and is described in details in [7]. According to this method, transient temperature measurements of the samples pressed against each other are carried out using a thermographic technique [7, 8, 9, 10]. The bodies are separately heated to different initial temperatures (upper sample 90 °C and lower sample 40 °C) and are then pressed together and filmed with an IR-camera. The schematic sketch of experimental setup is shown in ❷.

For the tests, different surface structures were tested against each other (polished – milled, polished – slotted and polished – polished) and classified by parameter R_z of roughness of 0,5 to 40 µm. ❸ present measured profiles for the three different surface qualities.

Experiments were conducted for three material combinations: 42CrMo4 – 42CrMo4, 42CrMo4 – X50CrMnNiNbN21-9 and 42CrMo4 – aluminum alloy.

❹ shows results of heat-treated steel (42CrMo4) – heat-treated steel (42CrMo4) case for different pressures and roughness. Points on the diagram are the results for the polished (R_z = 1 µm) – milled (R_z = 5 µm) and polished – slotted (R_z = 20 µm and R_z = 40 µm) case.

From the presented experimental results, general connection between the surface roughness, contact pressure and contact heat transfer coefficients cannot be seen. However, it has been shown that the deformation mechanisms occurring in the surface structures under increasing contact pressure significantly influences the global heat transfer. The characterization of surface topogra-

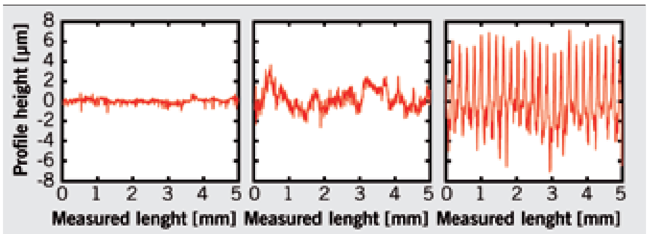

❸ Three different surface qualities; left: polished, center: milled, right: slotted (determined by a linear surface roughness tester)

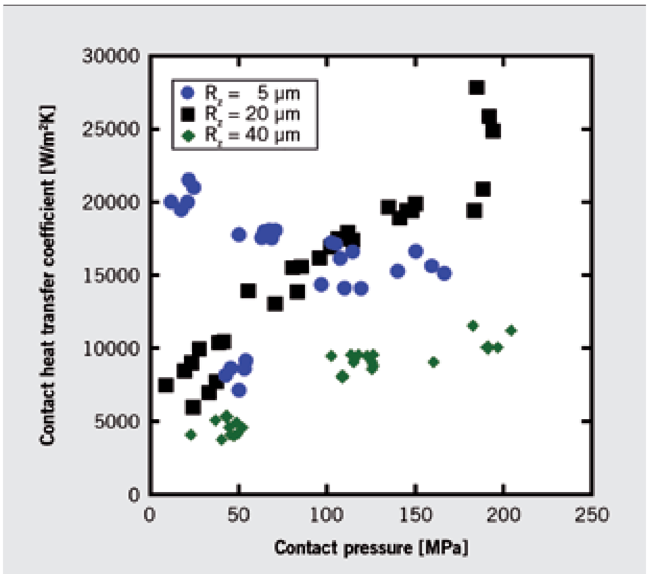

❹ Influence on pressures and roughness on the 42CrMo4 – 42CrMo4 combination on the contact heat transfer coefficient

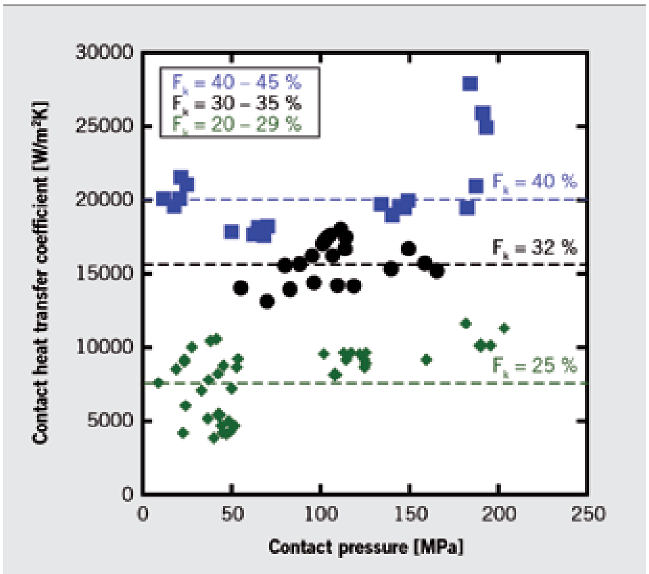

❺ Influence of pressures and F_k values for the 42CrMo4 – 42CrMo4 combination on the contact heat transfer coefficient

phy by means of the R_z value, particularly at low roughness, does not seem meaningful. Waviness in the surface structure with lower roughness is important and is described poorly by the R_z value. This knowledge was the starting points for the development of an appropriate a new method to describe the contact between two structured surfaces under the applied load. A new method (the F_k model) to determine the percentage share of Contact (F_k) was developed and presented in details in [11].

3 MODEL DEVELOPMENT

In the previously proposed models in literature the experimental results are conducted in vacuum conditions with contact pressures only up to 10 MPa. In these conditions there lies a good agreement of theoretical model with the measurement results. However, it is observed that highest accuracy of these theoretical models for the calculation of the contact heat transfer coefficient lies for the pressures not exceeding 7 MPa [9]. The previously known models usually consider only the elastic deformations of the contacting points between the surfaces of two bodies. Existing description of proposed approaches, which take into account plastic deformation currently cannot describe the heat transfer coefficients with reasonable accuracy as a function of surface characteristics and contact pressure. Obviously, this lacks the detailed mechanistic explanation of the involved heat transfer processes as a function of the prevailing conditions at the contact point. Primary motivation to develop a new model is based on the new knowledge of the behaviour of the contact heat transfer coefficient under high contact pressures. Here, an inversely proportional dependence of contact heat transfer coefficient at constant pressure under given circumstances with varying surface roughness can be established. This means that the value of the contact heat transfer coefficient depends only on the specific surface structure and thus also can be explained by determination of contact area.

In the following description, three different approaches or models for the determination of the contact heat transfer coefficients are presented, which differ mainly by operation and applications.

3.1 MODEL ON THE BASIS OF THE PERCENTAGE CONTACT AREA

The first model is based on the percentage share of contact (F_k model) and is used for the quantitative determination of the percentage area of contact F_k which takes into account both the surface profiles and the similarity between the two surfaces.

The parameters F_k is determined by equation (1) and is obtained according to the real surface profile.

EQ. 1

$$F_k = \cancel{F} \cdot k_D \cdot C_{AB} \cdot \frac{100\ \%}{\cancel{F}}$$

Where F is the line length (mm), k_D is a coefficient of dimension based on the Fractal theory of the measured profile [12] and C_{AB} is the cross-correlation coefficient [13] of the two profiles which was obtained from the actual surface measurements taken after the contact pressure is applied.

The percentage contact area obtained from the roughness profiles according to the experimental results shown in ④ were calculated and collected in the following ❺. The points on the diagram are the results obtained for polished (R_z = 1 µm) – milled (R_z = 5 µm) and polished (R_z = 1 µm) – slotted (R_z = 20 µm) surfaces, with the estimated percentage contact area of F_k = 40 % and F_k = 32 % respectively. For the case of polished (R_z = 1 µm) – milled (R_z = 5 µm) and polished – slotted (R_z = 20 µm and R_z = 40 µm) the percentage contact area is F_k = 25 %.

The influence of surface roughness and waviness are well described by the contact area according to results evaluated using the F_k model.

The influence of contact pressure plotted again by the percentage change in the contact can be described by the following proportionality:

α_c ~ (material properties, F_k)
and not, as before:
α_c ~ (material properties, R_z, contact pressure)
For better understanding of the proposed dependence, the observed proportionality approach made an attempt to develop a description regarding the new method for determination of actual contact area. Furthermore, the marginal cases "zero contact" and "maximal contact" were considered. The clear case of the zero contact was not investigated further. However, the maximal (100 %) contact was investigated experimentally.

For experimental implementation of maximum contact, two previously polished samples with an R_z value of 0,5 µm for a contact pressure tests were used. Maximum contact was expected using these polished surfaces. The samples used in tests (hardened and polished sample 42CrMo4 versus polished aluminium, 42CrMo4 and X50CrMnNiNbN21-9) have been pressed together at various contact pressures of up to about 200 MPa and their contact heat transfer coefficients were evaluated. The calculated heat transfer coefficients in dependence of the contact pressure are shown in the ❻.

The evolution of the calculated heat transfer coefficients reaches a constant level at high pressures. For aluminium, at a contact pressure of about 75 MPa saturation value of approximately 33.000 W/m²K is reached, and for X50CrMnNiNbN21-9 a saturation value of 5.500 W/m²K was observed at a pressure of nearly 120 MPa. The probable cause for the differences in the observed values of saturation levels can be the ability of different materials to adjust the dominating influence of the surface ripples under increasing contact pressures.

Therefore the experimental representation of the maximum contact is difficult to realize. Since the maximal contact could not be realized experimentally, linear extrapolation for the calculation of the theoretical value of contact heat transfer coefficient at the

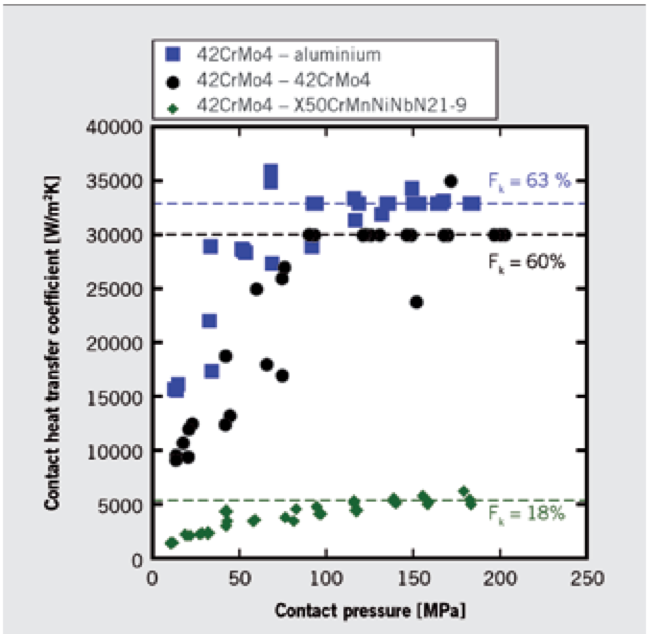

❻ Experimentally determined contact heat transfer coefficient as a function of the contact pressure for different material combinations

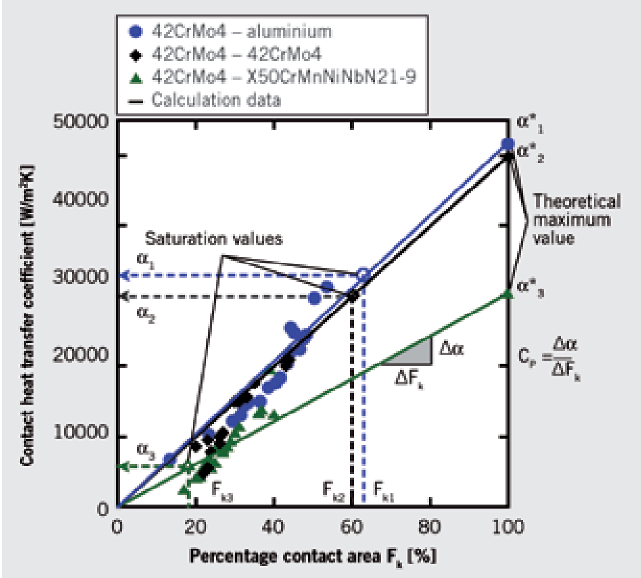

❼ Comparison of the experimentally determined values of the contact heat transfer coefficients (symbols) with the linear proportionality between heat transfer coefficients and percentage contact area (lines)

maximal contact area was attempted. In ❼, saturation values that are obtained from the experimental results, together with the theoretical maximum value of contact area by the extrapolation of the saturation values are connected by straight lines together with the previous experimental results (symbols).

The linear proportionality dependence between of the contact heat transfer coefficients and the percentage contact area along with the contact pressure is evident in ⑤ to ⑦. In theory it is suitable to represent the conservative description of the approach or the model for an upper limit of the contact heat transfer coefficients. For the investigated material combinations, the numerical model could be presented as follows:

EQ. 2
$$\alpha_c = C_p \cdot F_k$$

where C_p is the factor of proportionality from the ⑦ and can be determined from the experimental data. However, the transferability of this approach is a very limited since the actual research project was investigated for a limited number of materials having different surface structures. Also for determination of the actual contact area the profile scan measurement is necessary.

3.2 EMPIRICAL MODEL

For the determination of the contact heat transfer coefficient an empirical model was also developed [14]. Using a simple well known material, manufacturing and application parameters, without elaborate profile scans, the model is suitable for the approximate calculation of contact heat transfer coefficients and can be represented in equation 3:

EQ. 3
$$\alpha_c = C \cdot \frac{\bar{\lambda}_{av}}{\bar{\delta}_{av}} \left(\frac{P}{H_B} \cdot U \right)^{\sqrt{\frac{R_p}{P}}}$$

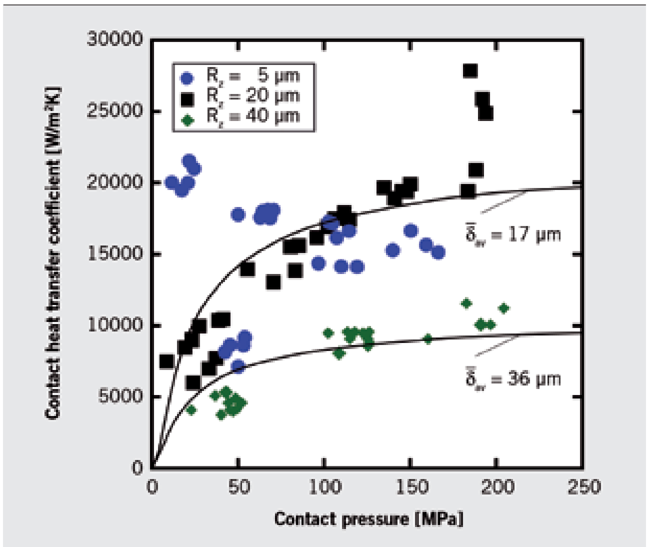

❽ Comparison of experimentally determined values of heat transfer coefficients (symbols) with the calculated values of heat transfer coefficients using empirical model (lines); material combination 42CrMo4 – 42CrMo4

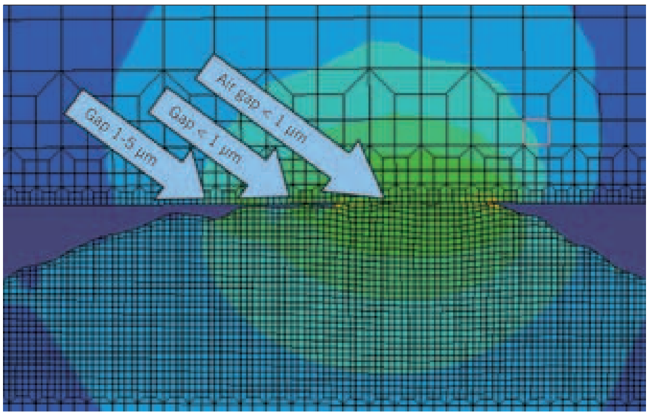

❾ Typical representation of a surface roughness peaks under load

The introduced equation consists of five physical values and two coefficients. One of coefficients is a constant value, and second is in correlation with the material hardness. The constant C (C = $8{\cdot}10^{-3}$) was selected by approximation of more than 1000 experimental results, $\bar{\lambda}_{av}$ – average thermal conductivity, $\bar{\delta}_{av}$ – average gap between two rough surfaces calculated using R_z values and an empirical relation, H_B is Brinell hardness which is correlated and can be represented as flow stress R_M, P – applied contact pressure, P_0 (P_0 = 1 MPa) is the nominal pressure. U (U = 0,6 ÷ 1,3) is empirical coefficient whose value depends on the hardness, derived by approximation of more than 1000 conducted experimental investigations [14].

To validate the empirical model, the experimentally determined heat transfer coefficients were plotted together with the calculated theoretical values of heat transfer coefficients as shown in ❽.

For the material combination of 42CrMo4 – 42CrMo4 and for the roughness R_z = 20 µm and 40 µm, the model can reproduce a good agreement of the pressure dependence on experimental values of the contact heat transfer coefficients. The dominant influence of surface waviness for the smooth surface roughness complicates the modeling of the pressure dependant heat transfer coefficient. The empirical model can be used to estimate the contact heat transfer coefficients within a wide range of the contact pressures (P = 1 to 230 MPa) and surface roughness (R_z = 2 to 40 µm) and can be used for different material combinations (H_B = 240 to 500 N/mm²). The empirical model is in good agreement with the results from the literature and the current measurements [14].

However, there are significant discrepancies when using an aluminium alloy [14]. Therefore additional experimental investigations for aluminium alloys are considered necessary for further understanding.

3.3 ANALYTICAL MODEL

The third model presented here is an analytical power model based on the basis of the results of previously conducted finite element simulations. To reconstruct the experimental tests, 2D FE-simulations is used along with the real surface topography for the lower and upper sample, the initial temperatures and the experimentally determined material parameters. The exact contact pressure was found for each simulation from the corresponding force curve of the testing machine which was also tabulated for all tests. The model, in particular the meshing, was modulated using an automated model generator which allows the input and definition of its boundary conditions on a user interface.

The values of the total contact heat transfer coefficients can be determined from the experimental investigations by extrapolation to maximum contact. This is determined from the relationship of the contact heat transfer coefficients values obtained in experiments and estimation of value of the contact area using proposed F_k-Model. The simulation model shows that only few elements are in direct mechanical contact with each other, and heat transfer also take place in the gaps areas filled with gas, some of which are smaller than 1 µm, ❾ [14].

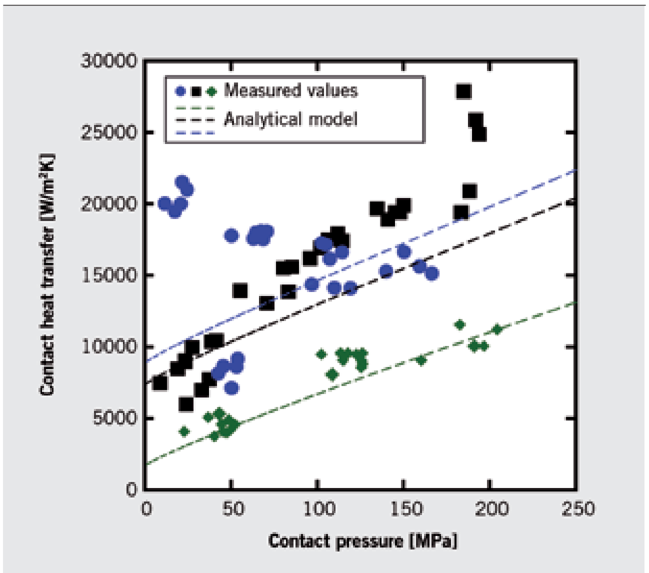

❿ Comparison of analytical model (line) and experiment (symbol) for the 42CrMo4 – 42CrMo4 material combination

The analytical model is independent of pressure and uses a combination of materials for specific heat transfer coefficient α^* (e.g. ⑦), which is multiplied by the effective contact area to the pressure-dependent contact heat transfer coefficients to describe α_c. The effective contact portion $F_{effective}$ is in turn based on the contact pressure p and the mechanical properties of the combined materials. Here k_f which is the yield stress of material and also takes into account the heat transfer passes through the air gaps between the specimens. The following equation gives the relationship as:

EQ. 4

$$\alpha_c = \alpha^* \cdot F_{effective}\,(P, k_f)$$

❿ shows the comparison of this model with the experimental results.

The analytical model and the data from the experiments show a relatively good agreement for a wide range of the investigated contact pressures. The power model uses mechanical material properties which can be derived once, either from literature characteristics or by the means of corresponding flow curves from tensile or compression tests. The model also uses a material-specific heat transfer coefficient, which is determined using a contact pressure test. This mechanical material property along with the material-specific heat transfer coefficient forms the input variables for the model. The development of the contact area with increasing pressure can be modeled. It also determines the heat transfer in small enclosures (gaps) with the consideration of elastic and plastic deformations for the calculation of the global heat transfer coefficient from the effective heat transfer coefficients.

4 SUMMARY AND OUTLOOK

In this work three different approaches or models for determining the contact heat transfer coefficients were presented, which differ essentially by operation and applications.

The comparison of three models with the experimental data shows that the magnitude of the experimentally determined contact heat transfer coefficients can be estimated and the quality of the assessment is pronounced differently, depending on the model.

A profound understanding of the present deformation mechanisms in the surface topography is a major milestone towards the development of a reliable thermal contact model which takes into account the crucial factors with extensive validation. The models presented in this paper are a first step towards a detailed mechanistic explanation of the involved heat transfer processes as a function of the prevailing conditions at the contact spots. Future projects can be built on these findings which can use the existing methods as a reference. However, the description of the real contact area as well as the determination of the prevailing conditions with greater accuracy by the means of new methods is needed. This requires experimental investigations of the connecting surfaces, in material properties such as thermal conductivity, hardness and micro structure, along with the necessary theoretical modeling approaches.

REFERENCES

[1] Fenech, H.; Rosenhow, W. M.: Prediction of the Thermal Contact Conductance of Metallic Surfaces in Contact, ASME Journal of Heat Transfer 15-24, 1963

[2] Cooper, M.; Mikic, B. B.; Yovanovich, M. M.: Thermal Contact Conductance, International Journal of Heat and Mass Transfer 12 279–300, 1969

[3] Mikic, B. B.: Thermal Contact Conductance, Theoretical Considerations, Int. Journal of Heat and Mass Transfer, Vol. 17, No. 1, pp. 205 – 214, 1974

[4] Bahrami, M.; Yovanovich, M. M.; Culham, J. R.: Thermal Joint Resistances of Conforming Rough Surfaces with Gas-Filled Gaps, Journal of Thermophysics and Heat Transfer, Vol. 18, No. 3, pp. 318 – 325, 2004

[5] Madhusudana, C. V.: Thermal Contact Conductance, Springer issue, New York, 1996

[6] Marotta, E. E.; LaFontant, S.; McClafferty, D.; Mazzuca, S.; Norley, J.: The Effect of Interface Pressure on Thermal Joint Conductance for Flexible Graphite Materials: Analytical and Experimental Study, 8th Intersociety Conferernce on Thermal and Thermomechanical Phenomena in Electronic Systems, 1-8, 2002

[7] Fieberg, C.; Korthäuer, M.; Kneer, R.; El-Magd, E.: Abschlussbericht zum Vorhaben Kontaktwärmeübertragung mit Zwischenmedien. Forschungsvereinigung Verbrennungskraftmaschinen e.V., Frankfurt am Main, Heft 847, 2008

[8] Fieberg, C.; Kneer, R.; Korthäuer, M.; El-Magd, E.: Transient Contact Heat Transfer Coefficients from Infrared Temperature Measurements, International Heat Transfer Conferences (IHTC), August 13 –18, Sydney, Australia [CD-ROM], 2006

[9] Fieberg, C.: Kontaktwärmeübertragung unter hohen Druck- und Temperaturrandbedingungen, Dissertation RWTH – Aachen, 2008

[10] Fieberg, C.; Kneer, R.: Determination of Thermal Contact Resistance from Transient Temperature Measurements, Int. J. of Heat and Mass Transfer, 51, 5-6, 1017/1023, 2008

[11] Ustinov, V.; Schulz, S. G.; Kneer, R.; El–Magd, E.: Zwischenbericht zum Vorhaben Modellentwicklung für den kontaktdruckabhängigen Wärmeübergang im motortechnischen Umfeld, Forschungsvereinigung Verbrennungskraftmaschinen e.V., Bremen, Heft R543, 2008

[12] Pietronero, L.; Tosatti, E.: Fractals in Physics Proceedings of the Sixth Trieste International Symposium on Fractals in Physics, ICTP, Trieste, Italy, July 9-12, 1985. Edited by Luciano Pietronero and Erio Tosatti. Amsterdam: North Holland Publishing (book), 1986

[13] Bendat, J. S.; Piersol, A. G.: Random Data: Analysis & Measurement Procedures, 2nd edition, 566 pages, John Wiley, New York, 1986

[14] Ustinov, V.; Schulz, S. G.; Kneer, R.; El–Magd, E.: Abschlussbericht zum Vorhaben Modellentwicklung für den kontaktdruckabhängigen Wärmeübergang im motortechnischen Umfeld, Forschungsvereinigung Verbrennungskraftmaschinen e.V., Bad Neuenahr, Heft R543, 2010

THANKS

The authors would like to thank the Research Association for Combustion Engines (FVV, Frankfurt), the Federal Ministry of Economics and Technology (BMWi) and the Association of Industrial Research Associations (AiF) for cooperation and financial support of the project.

AUTHOR

M.SC. MICHAEL BÜTIKOFER is an unaffiliated engineer which graduated recently at ETH Zurich (Switzerland).

HIGH-PERFORMANCE PNEUMATIC HYBRID ENGINE WITH COST-EFFECTIVE VALVETRAIN

The potential of the pneumatic hybrid engine has been demonstrated at the ETH Zurich by means of a fully functional prototype. The pneumatic hybrid technology improves the drivability of turbocharged engines and enables quick pneumatic engine starting as well as recuperation of braking energy. A novel valve train concept now implements these functions with components currently in use in many of today's engines. With minimal additional costs, output torque is increased by 20 % and fuel consumption is reduced by 27 % in comparison to a naturally aspirated engine.

1 INTRODUCTION

The development of electric and electric-hybrid powered vehicles is put forward. But the share of vehicles of this type in traffic is still below one percent [1], mainly because of high costs and extra weight of the complex power engine and the batteries. Hence, the majority of new cars will be equipped with petrol engines in the near future [2], even though these show low efficiency at part load operation. The pneumatic hybrid engine compensates for this shortcoming with low additional manufacturing costs and shows the potential to establish itself in the remaining segment of petrol engines.

1.1 FUNCTIONAL PRINCIPLE

In the pneumatic hybrid engine, each cylinder contains a compressed-air valve (A-valve), which connects the combustion chamber with the compressed-air reservoir, ❶. In the event of a braking manoeuvre, air is compressed within the cylinder (C-mode) and streams into the compressed-air reservoir via the A-valve. The stored, compressed air can be used in the following three ways:

- The engine is powered with compressed air only, which is called air motor mode (AM-mode)
- The engine is started very quickly by means of compressed air (special case of AM-mode)
- The compressed air is injected into the intake manifold in order to reduce the turbo lag (improvement of the engine response time).

The pneumatic engine start (within 0.2 s at 10 bar) allows for automatic start/stop operation of the engine. In combination with the recycling of braking energy (recuperation), this feature results in a remarkable reduction of the petrol consumption, especially in city traffic. Further reduction of the fuel consumption can be achieved by downsizing, which is at hand because of the possibility to reduce the turbo lag [3].

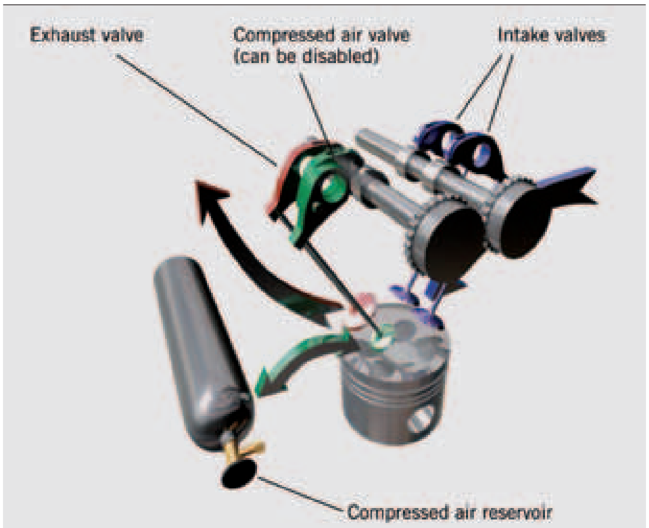

❶ Schematic illustration of a pneumatic hybrid engine

1.2 MAJOR SIMPLIFICATION OF THE VALVETRAIN

The prototype of a pneumatic hybrid engine developed at the ETH Zurich yielded proof that fuel savings between 25 and 35 % can be achieved in practice [4, 5, 6]. However, the prototype requires a fully variable valve for each cylinder, which leads to additional efforts and expenses in the development, production, maintenance and operation of the engine. Therefore, a new concept of a valve train has been developed which is based exclusively on components currently used in numerous engines. This patented concept will be explained more closely in the following sections [7].

2 METHOD

2.1 SIMULATION OF ENGINE CYCLES

Cylinder pressure and temperature during an engine cycle were calculated with mathematical models. During pneumatic operation, the cylinder contains pure air which is modelled as an ideal gas with a specific gas constant $R = 287$ J/kgK and an isentropic coefficient $\kappa = 1.35$. The temperature of the compressed air in the reservoir is estimated at 100 °C, as the hot air cools down quickly after compression [6, 8]. The mechanical friction is taken into account in the simulation of driving cycles, but not in the optimisation process of the gas-exchange.

2.2 QUASI-STATIC SIMULATION OF DRIVING CYCLES

Maps of engine characteristics for the pneumatic modes and the combustion operation are calculated with the mathematical model of the engine. Based on the drive cycle vehicle speed, the required torque at the crankshaft is calculated in steps of one second. The values of both the flow of compressed air and petrol consumption can be read from the respective maps.

3 ANALYSIS FOR SINGLE ENGINE CYCLES

Depending on the requirements, a pneumatic hybrid engine can be equipped with one or two camshafts (SOHC/DOHC) and with a total of three to five valves per cylinder. In the following, only a "standard" variant with two camshafts and four valves per cylinder will be discussed, but the method can easily be adapted to other configurations. Two of the four valves are used as intake valves, one as compressed-air valve (A-valve) and one as exhaust valve. The A-valve needs to remain closed during the combustion operation, which requires a mechanism for discrete or continuous variation of the valve lift. The calculations are based on the assumptions of having a valve with a fixed cam profile which can be deactivated. This can be brought about by means of a hydraulically operated locking pin, as used e.g. in Honda VTEC, which is in serial production since 1992 [9].

3.1 CHOICE OF OPERATION MODE

The pneumatic modes have the following characteristics:

- In the C-mode, as much fresh air as possible is compressed in the cylinder and transported to the compressed-air reservoir during the compression stroke

- In the AM-mode, the compression stroke is reduced to a minimum. During the power stroke, compressed air flows into the cylinder and exerts force on the piston.

In both modes, maximum efficiency is attained when opening the A-valve close to the top dead centre [6, 10]. This results in the valve lift profiles schematically depicted in ❷. The opening maxima are located shortly before and after the top dead centre (the modes also differ in the position of the throttle). Therefore, a cam phasing device can be used to toggle between C- and AM-mode (required range of phase shift: 60° crank angle, e.g. BMW Vanos, Toyota VVT-i). In order to optimise the gas exchange in both pneumatic and combustion operation, the intake camshaft is also equipped with a phase shift device.

The valve lift of the A-valve is 2 to 3 mm, therefore a collision with the piston is impossible.

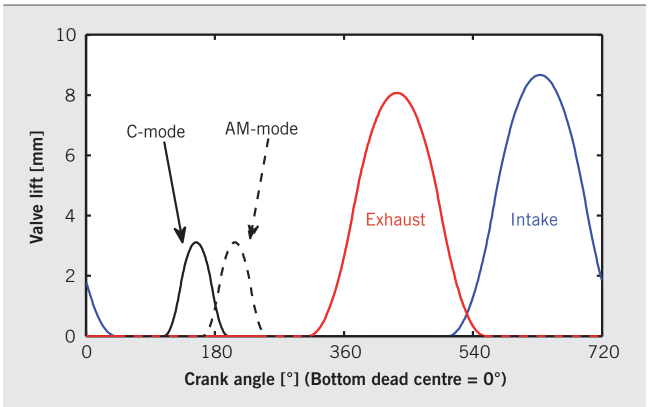

❷ Schematic depiction of the valve lift profiles in C- and AM- mode

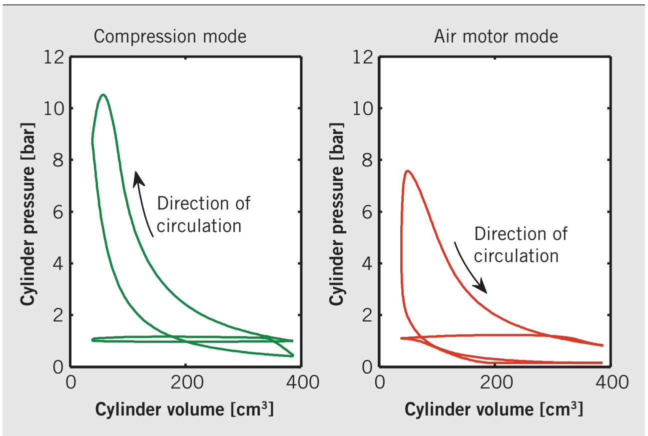

❸ Pneumatic modes with optimised cam profile and phase shift angles

COMPRESSION RATIO ε	10,0
BORE [mm]	76,5
STROKE [mm]	75,6
DISPLACEMENT VOLUME PER CYLINDER [cm³]	347
DIAMETER INTAKE VALVE [mm]	25,4
DIAMETER EXHAUST VALVE [mm]	29
DIAMETER COMPRESSED-AIR VALVE [mm]	20

❹ Engine data used for calculations

3.2 SHARED CAMSHAFT

In order to reduce complexity and costs of the engine, the A-valves are not operated by a separate camshaft but by the exhaust camshaft. This results in a modification of the exhaust valve timing in the event of toggling between C- and AM-mode. However, the phase shift angle imposed on the exhaust valve is almost equivalent to the one which optimises the gas exchange. Therefore, the simplification of the valve train leads to a better efficiency in the pneumatic operation modes. This is illustrated in the pV diagrams of both modes: in C-mode, ❸ on the left, the phase shift angle of the exhaust camshaft is close to the neutral position for a good charging of the cylinder with fresh air. The closure of the intake valve is slightly advanced in order to achieve an early rise in cylinder pressure. In AM-mode, ③ on the right, the opening times of all valves are delayed. The low intake pressure of 0.15 bar results in a minimal work consumption during the compression stroke. Very small pumping losses in AM-mode confirm that the phase shift imposed on the exhaust valve is very close to the optimum. This dependency of the valve timing only occurs in operation with pure air. The combustion operation is not affected by this, but profits from the possibility of adjusting both camshaft phase angles.

Output torque is varied via the throttle. In both pneumatic modes, torque decreases when opening the throttle and increases when closing it.

3.3 NUMERIC OPTIMISATION OF THE GAS EXCHANGE

The same cam profile, of which the design determines the engine properties, is used for both C- and AM-mode. Therefore, the development of the algorithms for the calculation of the ideal cam profile is a major part of this scientific investigation. In order to assess a cam profile, the ideal phase shift angles of both camshafts need to be chosen in both modes.

The indicated recuperation efficiency η_{rec} is the main criterion for the optimisation, see Eq.1. This variable expresses the ratio of the work W_{AM} which can be supplied in air motor mode using a certain air mass m to the work W_c which has to be invested to compress the same air mass m. For the calculations, the geometry and compression ratio of the 1.4-l TSI engine developed by VW have been used, ❹ (Twincharger, model CAVD). This is a state-of-the-art engine with direct injection, turbo charger and compressor. In our case of the pneumatic hybrid engine, there is no need for a compressor as the turbo lag can be reduced by means of the stored compressed-air.

EQ. 1

$$\eta_{rec} = \frac{m/W_C}{m/W_{AM}} = \frac{W_{AM}}{W_C} \qquad n,\ p_t = const$$

Eq. 1: Indicated recuperation efficiency η_{rec}

The valve lift profile of the A-valve is determined by three parameters which are presented in ❺. The valve acceleration is kept constant at a fairly high rate of +/- 80 mm/rad² in order to maximise the valve lift. Altogether, six parameters have to be optimised. The two parameters opening angle and opening duration define the geometry of the cam and are therefore equal for all operating points and for both modes. Because the recuperation efficiency η_{rec} is calculated based on two engine cycles (C- and AM-mode), anoth-

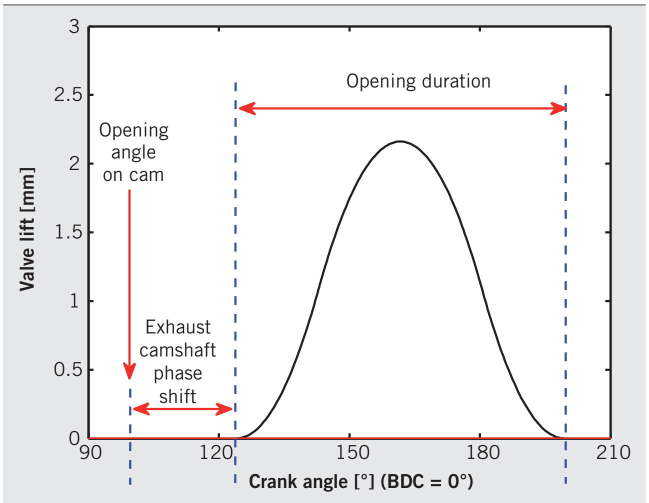

❺ The valve lift profile of the A-valve is defined by three parameters

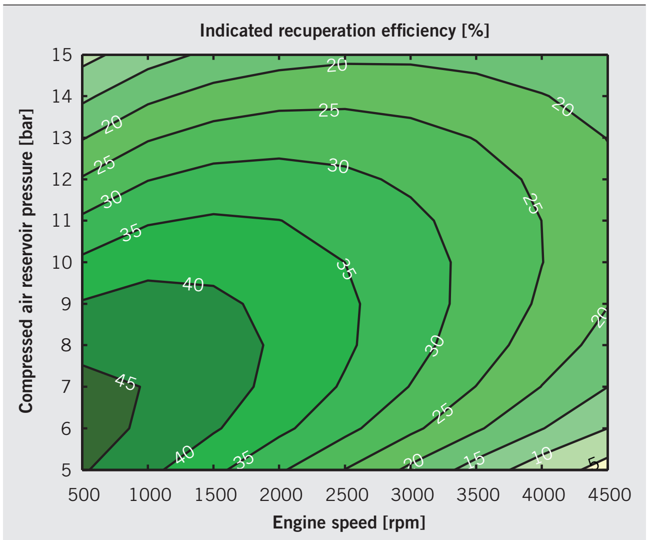

❻ The result of the optimisation is a characteristic diagram with good efficiency at all operating points

er four parameters need to be considered, namely the phase shift angles of both camshafts in both operation modes. These parameters will vary depending on the mode and operating point. An operating point is defined by the engine speed n and the air pressure in the compressed air reservoir p_r. For the optimisation, an arithmetic average operating point at $n = 1936$ rpm and $p_r = 9.11$ bar was determined (by means of an iterative approach and simulation of the FTP-75 drive cycle).

3.4 RESULTS

In order to conduct an analysis, the optimisation problem is looked at separately for the C- and the AM-mode and the cam geometry is assumed to be constant at fixed values. The phase shift angles of both camshafts are then optimised in each mode (with the criterion of air mass per work m/W). Both of these two-parameter subproblems behave convex and therefore they can be solved reliably with a numeric search algorithm. The superordinate problem in the optimisation of the two parameters of the cam geometry also proves to be convex if suitable initial conditions are chosen. Therefore, a numeric search algorithm can be used to look for solutions for all six parameters at once, which reduces the calculation time to a few minutes. In the next step, the phase shift angles are optimised for each operating point. ❻ depicts the resulting map of indicated recuperation efficiency with a maximum of 45 % at $n = 800$ rpm and $p_r = 7$ bar.

4 RESULTS FOR ENTIRE DRIVING CYCLES

The petrol consumption of a virtual vehicle on a simulated test track can be calculated by means of the method described in section 2. A modern middle-class car, the VW Passat Variant B6 Comfortline, was chosen as test vehicle. The above mentioned 1.4-l TSI engine is used as drive system, whereas the pneumatic hybrid version features a compressed-air reservoir with a volume of 42-l. This equals the volume of two cylinders with a diameter of 20 cm and a length of 70 cm, which could be positioned in the rear end of the vehicle (just as in natural-gas fuelled vehicles). The occurring pressure levels of up to 15 bar are comparatively low and require a wall thickness of only 1 mm steel (resulting weight: 7 kg). The total additional weight of the pneumatic hybridisation is estimated conservatively at 28 kg.

4.1 THE TEST ENGINES

Output torque of the 1.4-l TSI engine is limited to 200 Nm by VW in the version without compressor (model CAXA) in order to guarantee a good response behaviour despite the turbo lag [11]. In the case of the hybrid engine, output torque can be increased to the 240 Nm of the Twincharger version, whereas the turbo lag is reduced by the means of compressed air without additional costs for the compressor. The maximum of the mean effective pressure is increased from 18.1 to 21.7 bar, the maximum engine output reaches 118 kW.

In order to quantify the potential of the combined downsizing and pneumatic hybrid technology, a comparison to the calculated fuel consumption of a 2.0-l FSI naturally aspirated engine is made (output torque: 200 Nm, engine power: 110 kW, mean effective pressure: 12.7 bar). The combustion operation is modelled in the same way for all engine variants (same thermal efficiency), the mechanical friction and the pumping losses are scaled with the displacement volume.

4.2 THE TEST TRACK

The FTP-75 driving cycle (Federal Test Procedure) is used to officially ascertain the fuel consumption in the USA. It is based on measuring data, whereas the European counterpart, the New European Driving Cycle (NEDC), is of a purely synthetic kind. The FTP-75 driving cycle is preferable in our case because it features a broader range of different torque and engine speed values. The course of the vehicle speed can be seen in ❼, top. It consists of about 18 km urban and rural traffic and takes roughly 30 minutes (with an additional 10-minute-break before the last stage).

The forces which act on the vehicle and the engine during the simulated journey can be calculated using the parameters in ❽ [12].

4.3 RESULTS OF THE DRIVING CYCLE

It is stated that in these calculations, the end pressure in the compressed-air reservoir has to be equal or higher than the start pressure. The course of the air pressure in the reservoir can be seen in

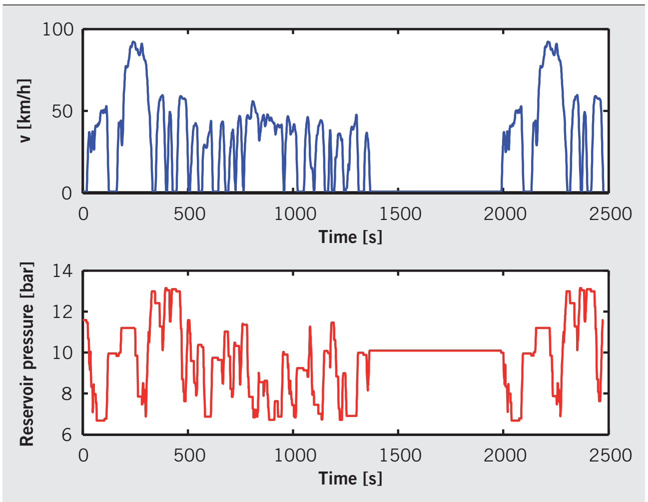

❼ Simulation data of the 1.4 l TSI hybrid engine in the FTP-75 driving cycle

VEHICLE WEIGHT 1.4 L TSI PNEUMATIC HYBRID [kg]	1532
VOLUME OF THE COMPRESSED-AIR RESERVOIR [l]	42
VEHICLE WEIGHT 1.4 L TSI TWINCHARGER [kg]	1504
VEHICLE WEIGHT 2.0 L FSI [kg]	1575
ALTERNATOR POWER OUTPUT (ONLY IN COMBUSTION OPERATION) [W]	400
ALTERNATOR EFFICIENCY [%]	55
GEARBOX EFFICIENCY [%]	97
ROLLING FRICTION COEFFICIENT c_r	0,01
FRONT SURFACE AREA A_f [m²]	2,27
AIR RESISTANCE COEFFICIENT c_w	0,32
WHEEL DIAMETER [m]	0,63
FINAL DRIVE RATIO	4,35
TRANSMISSION RATIO GEARS 1 – 6	3.62 1.96 1.28 0.97 0.78 0.65

❽ Parameter values for the driving cycle

⑦, bottom. A comparison with ⑥ shows that the range of pressures appears to remain within the region of highest recuperation efficiency between 7 and 12 bar, despite the usage of very simple control algorithms. ❾ depicts the calculated fuel consumption and the saving potential of the pneumatic hybrid engine.

The temporal share of the combustion operation is reduced by 33 % in the FTP-75 driving cycle. Firstly, the engine is turned off during 339 s of the vehicle standing still, which saves 5.9 % of fuel. Secondly, the engine is fuelled with pure air during 184 s, which saves another 7.2 % of petrol. An additional saving of 13.8 % results from downsizing.

5 DISCUSSION

A conceptual design of a pneumatic hybrid engine is presented where the valve train is based only on commonly available and tested technologies. The costs and the complexity of the engine have been reduced and the robustness of the system has been enhanced remarkably.

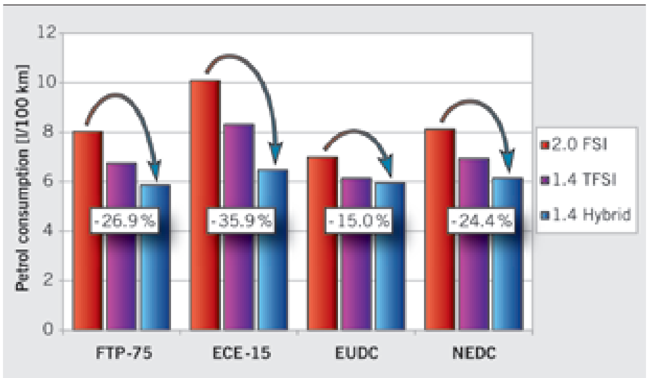

❾ Calculated petrol consumption and relative savings in various driving cycles

In combination with downsizing, this allows an increase in torque by 20 % and simultaneous fuel savings of 27 %. Due to the low additional cost of the pneumatic hybrid technology, its cost-benefit ratio is unreached by current electric hybrid engines.

REFERENCES
[1] Volken, T.: Faktenblatt zu elektrisch angetriebenen Personenwagen. Bern: Bundesamt für Energie BFE, 2010
[2] Dinger, A. et al.: Batteries for Electric Cars. Boston: Boston Consulting Group, 2010
[3] Dönitz, C.; Vasile, I.; Onder, C.; Guzzella, L.: Dynamic Programming for Hybrid Pneumatic Vehicles. In: Proceedings 28th American Control Conference (2009), pp. 3956 – 3963
[4] Dönitz, C.; Voser, C.; Vasile, I.; Onder, C.; Guzzella, L.: The pneumatic hybridization concept for downsizing and supercharging gasoline engines. In: MTZ 71 (2010), No. 01, S. 52-58
[5] Dönitz, C.; Vasile, I.; Onder, C.; Guzzella, L.: Realizing a Concept for High Efficiency and Excellent Driveability: The Downsized and Supercharged Hybrid Pneumatic Engine. SAE Technical Paper 2009-01-1326, USA, 2009
[6] Bütikofer, M.: Proof of Efficiency for a Pneumatic Hybrid Engine. Zürich, Swiss Federal Institute of Technology (ETH), Master Thesis, 2009
[7] Bütikofer, M.: Brennkraftmaschine. Patent application No. 00913/10, Switzerland, 2010
[8] Trajkovic, S.; Tunestål, P.; Johansson, B.: Investigation of Different Valve Geometries and Valve Timing Strategies and their Effect on Regenerative Efficiency for a Pneumatic Hybrid with Variable Valve Actuation. SAE Technical Paper 2008-01-1715, USA, 2008
[9] Hatch, Steve V.: Computerized engine controls. Delmar: Cengage Learning, 2009
[10] Dönitz, C.; Vasile, I.; Onder, C.; Guzzella, L.: Modelling and Optimizing Two- and Four-Stroke Hybrid Pneumatic Engines. In: Journal of Automobile Engineering, No. 223(2), 2009, pp. 255 – 280
[11] Der 1.4l TSI Motor mit Doppelaufladung. Wolfsburg: Volkswagen AG, 2006
[12] Grunder, S.: Verbrauchskatalog 2010 Fahrzeugliste mit Verbrauchsangaben. Bern: Touring Club Schweiz und Energie Schweiz, 2010

THANKS

Thanks go to ETH Zurich and the Institute for Dynamic Systems and Control for making possible a highly interesting master thesis. I want to thank especially Prof. Dr. Lino Guzzella and Mr. Christian Dönitz for the mentoring as well as Dr. Christopher Onder and Dr. Iulian Vasile for their technical assistance.